

Figure 1. Correlation of the expression profiles in 5 xenograft-derived human prostate carcinoma cell lines and 8 recurrent versus 13 non-recurrent human prostate tumors for 19 genes of the concordant class

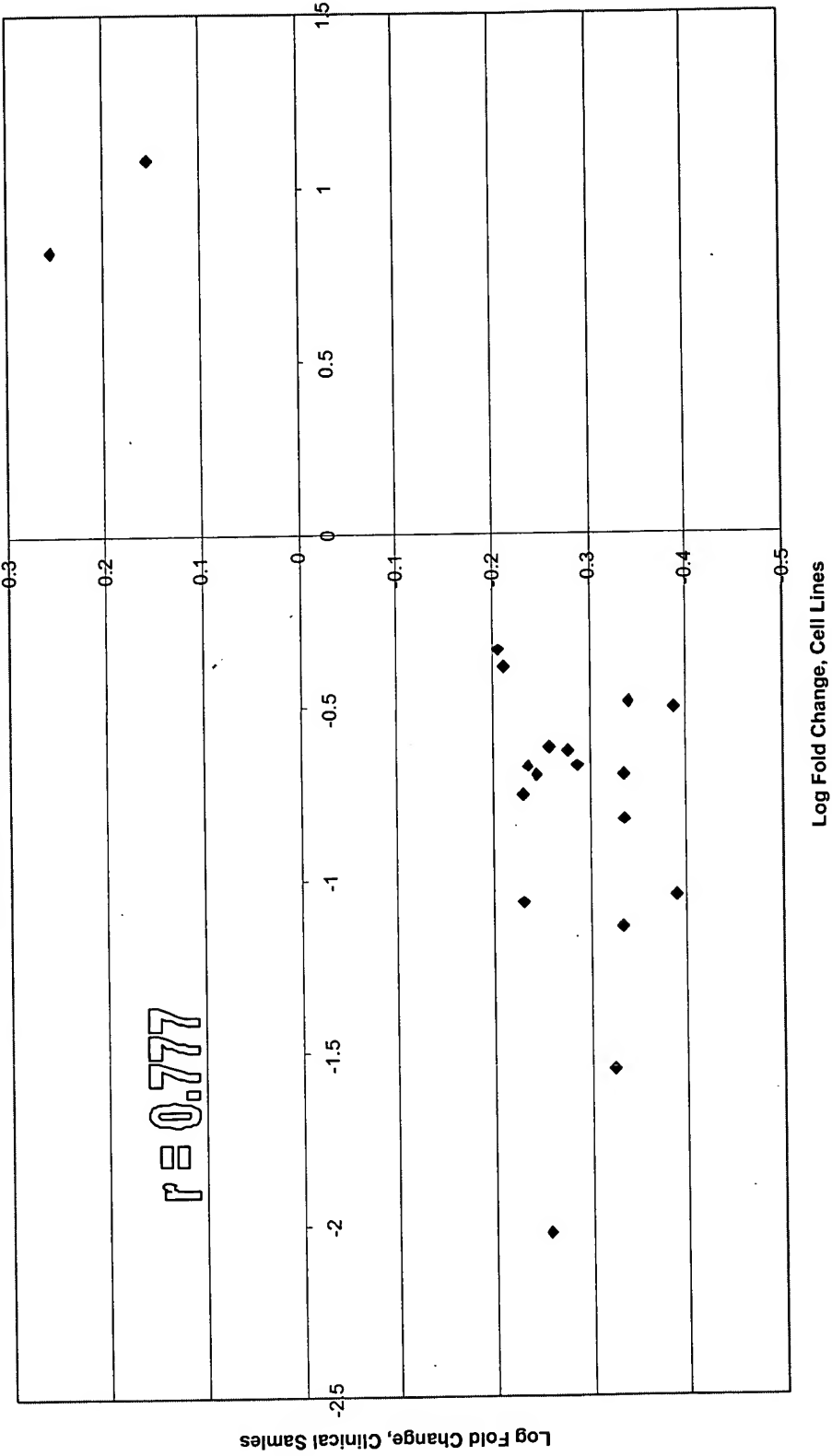


Figure 2. Correlation of the expression profiles in 5 xenograft-derived human prostate carcinoma cell lines and 8 recurrent versus 13 non-recurrent human prostate tumors for 9 genes of the PC3/LNCap consensus class (recurrence predictor class)

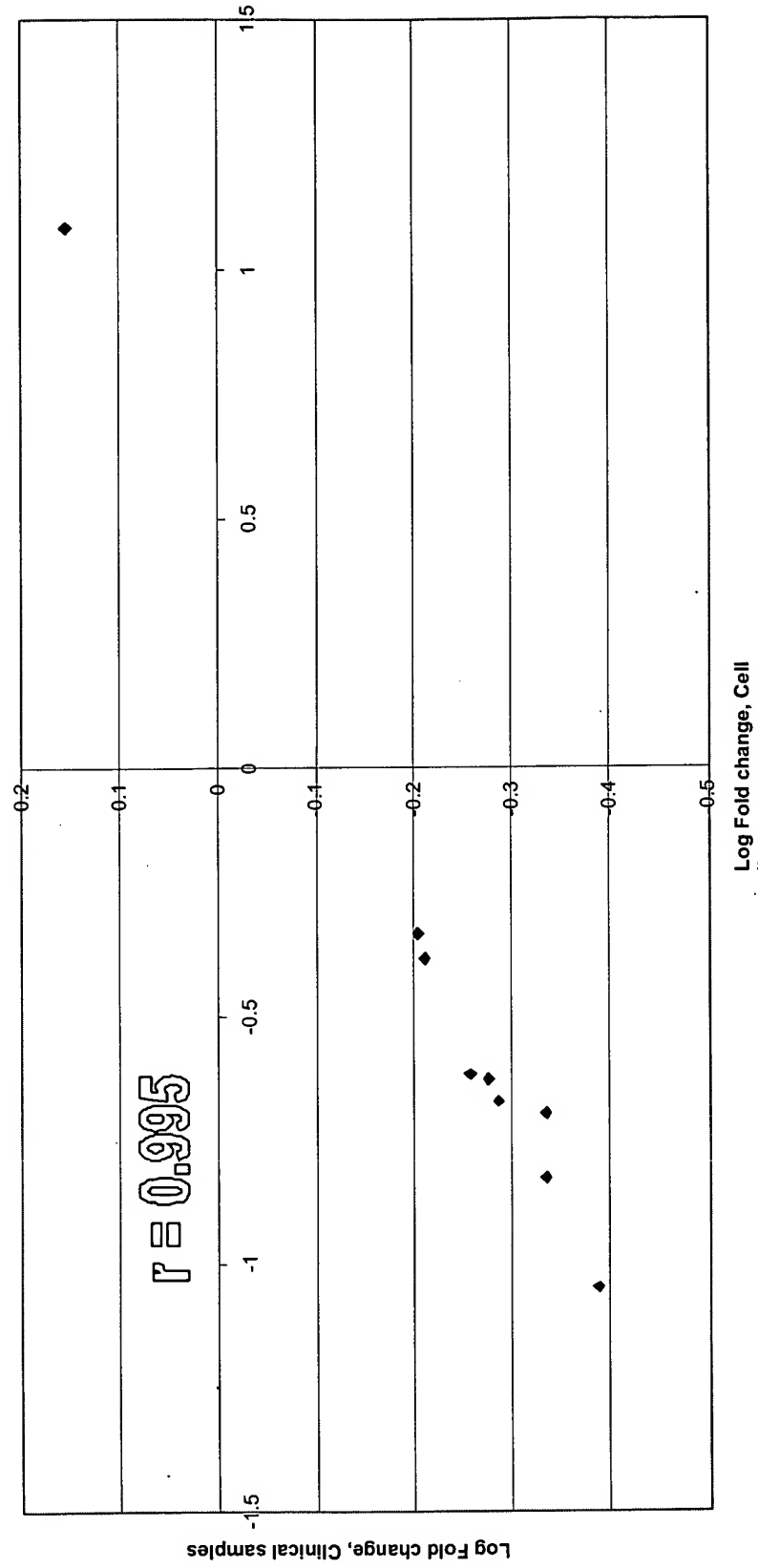


Figure 3. Association indexes for 9 genes of the recurrence predictor class in individual human prostate tumors exhibiting recurrent or non-recurrent clinical behavior

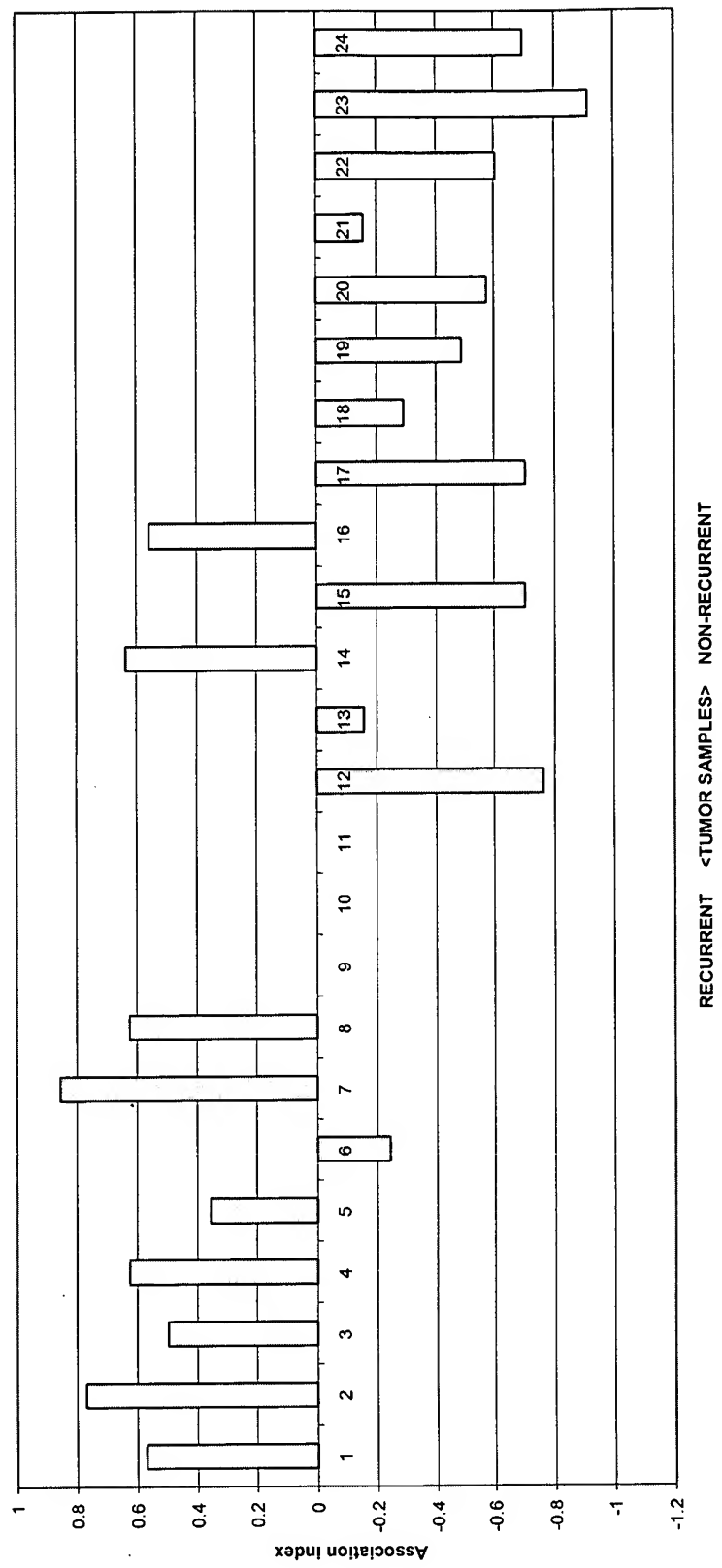


Figure 4. Phenotype association indexes for 54 genes of the prostate cancer/normal tissue discrimination class in 24 prostate tumors, 2 normal prostate stroma samples and 9 adjacent normal tissue samples

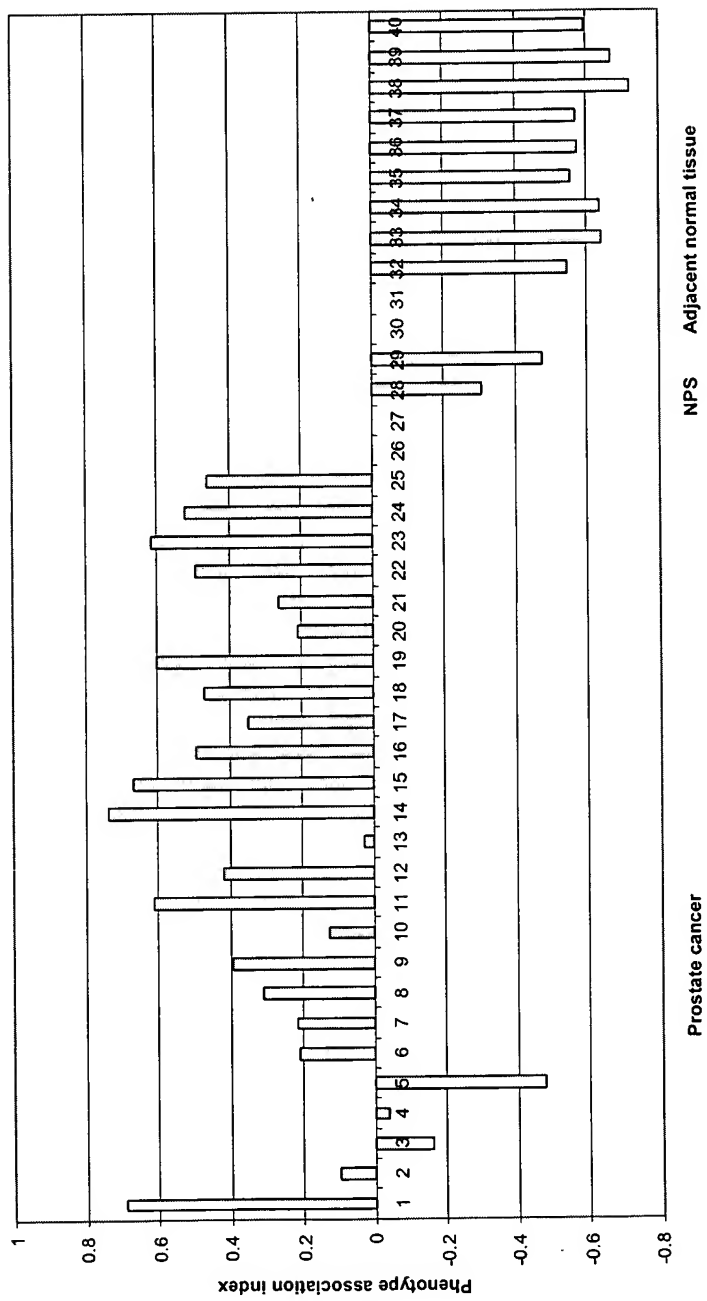


Figure 5. Correlation of the expression profiles in 5 xenograft-derived human prostate carcinoma cell lines and 24 prostate cancer tissue samples versus 9 adjacent normal prostate samples for 54 genes of the concordant class

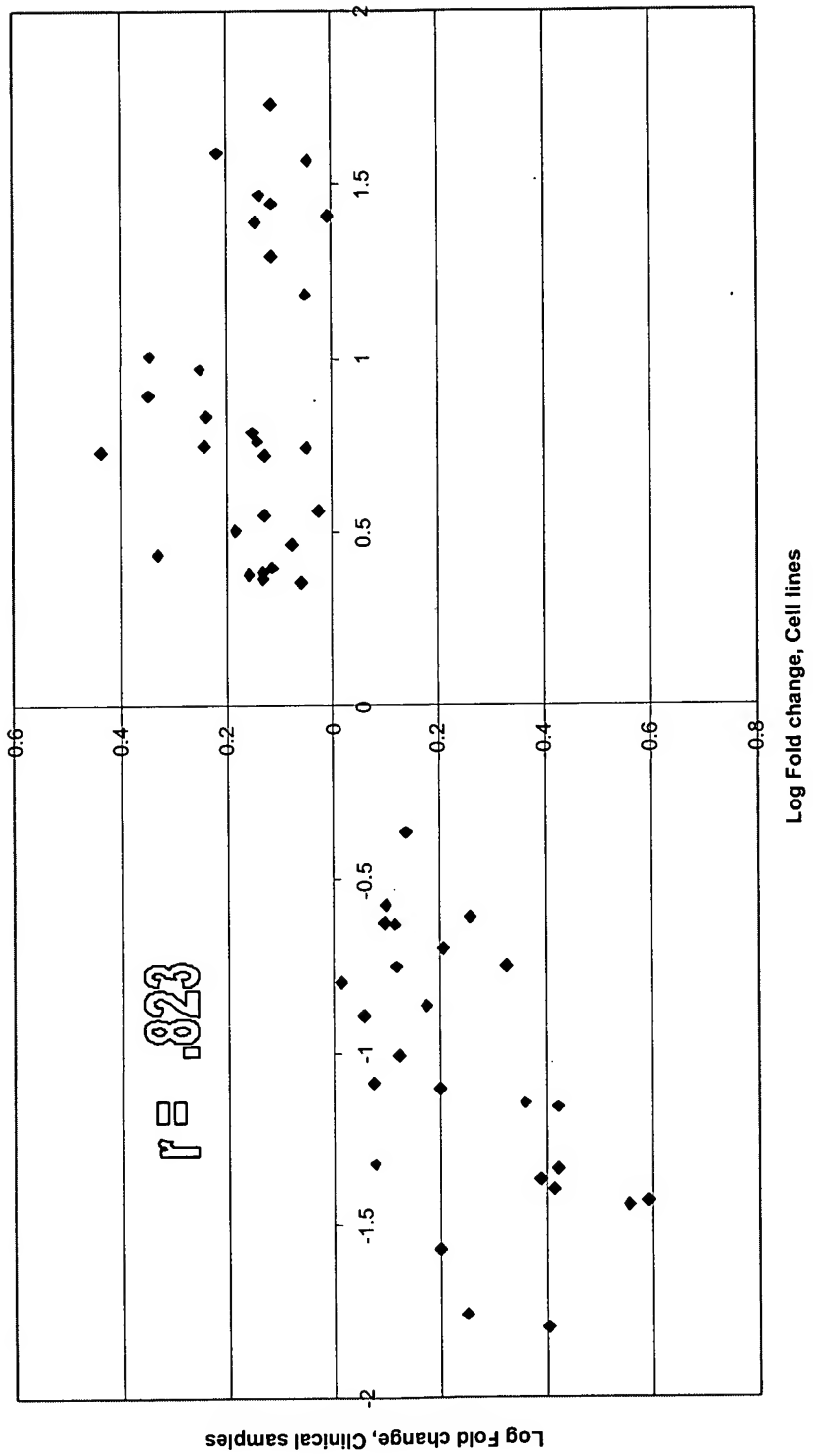


Figure 6. Phenotype association indexes for 10 genes of the prostate cancer/normal tissue discrimination class in 24 prostate tumors and 9 adjacent normal tissue samples

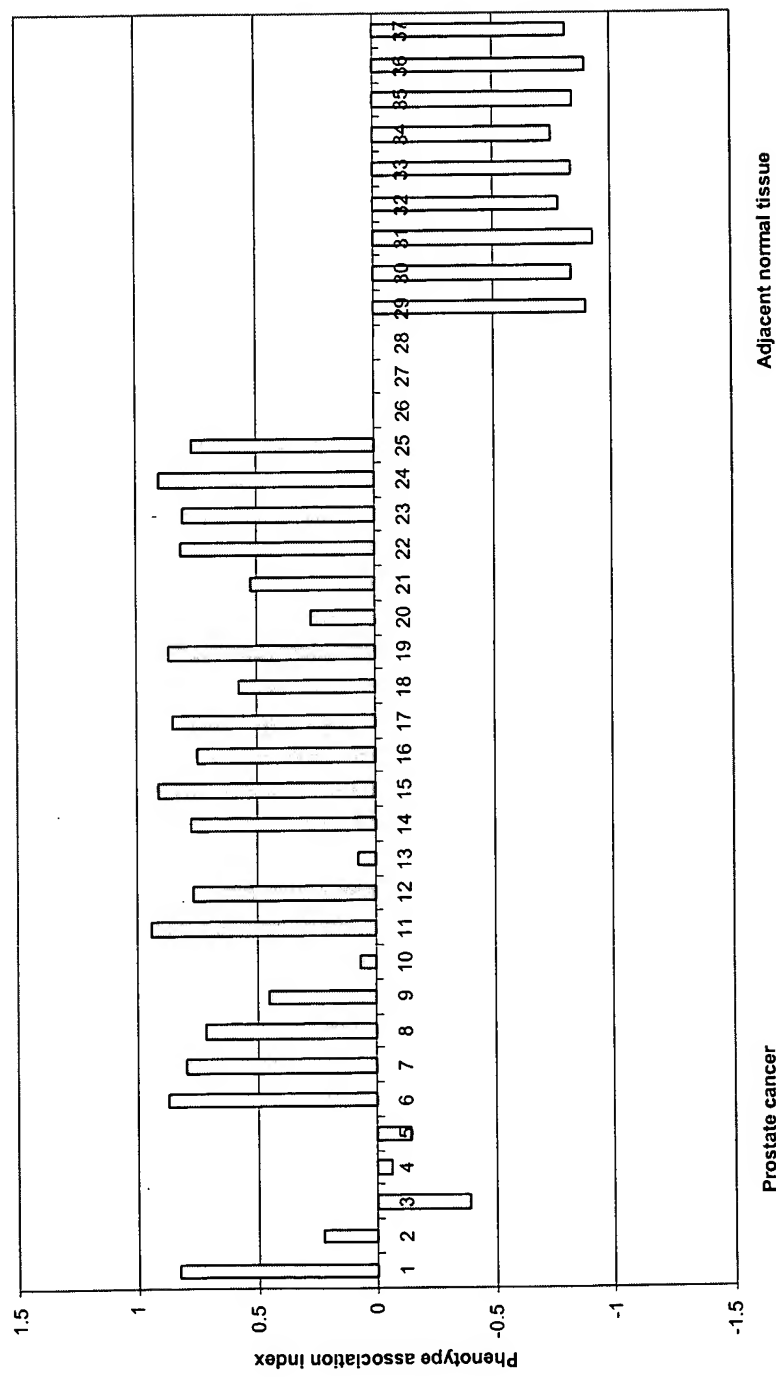


Figure 7. Phenotype association indexes for 5 genes of the prostate discrimination class in 24 prostate tumors and 9 adjacent normal

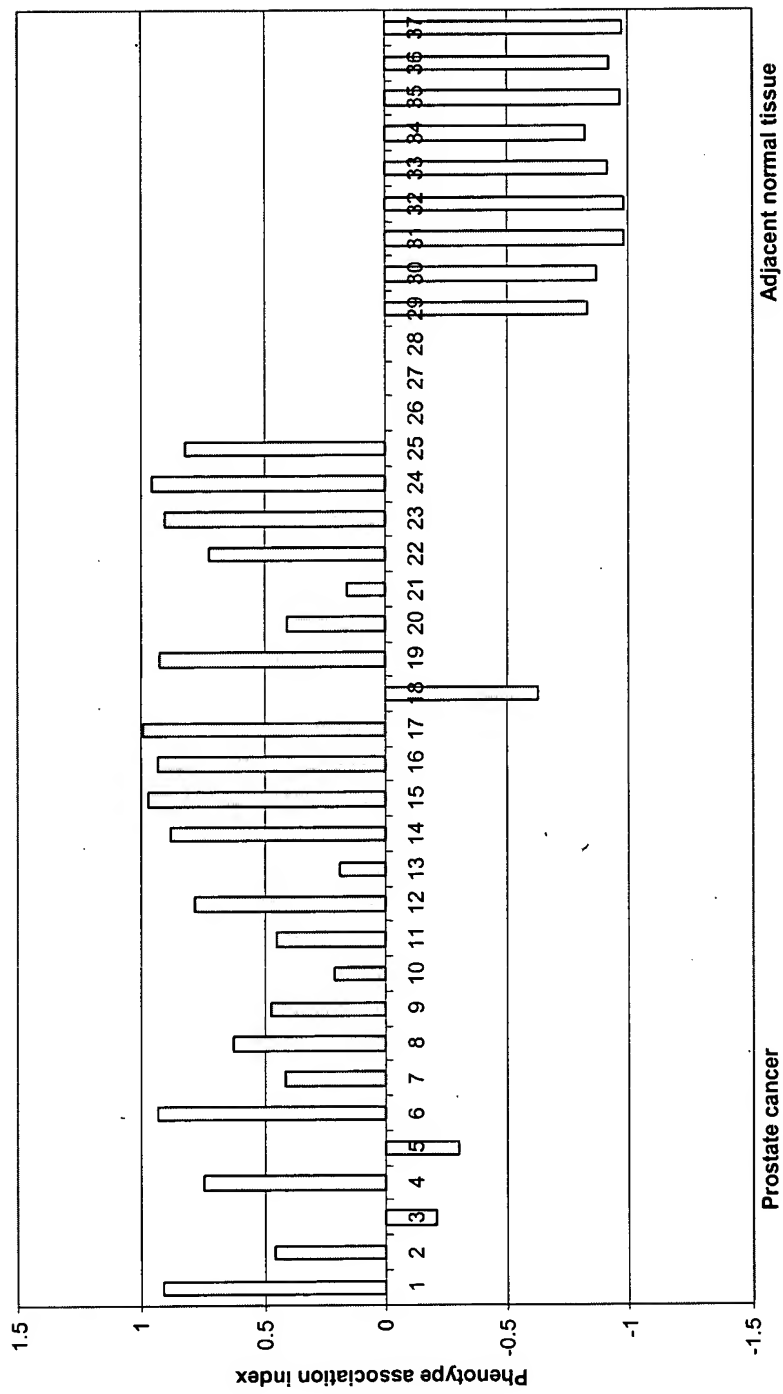


Figure 8. Phenotype association indexes for 10 genes of the prostate cancer/normal tissue discrimination class in 47 prostate tumors and 47 adjacent normal tissue samples

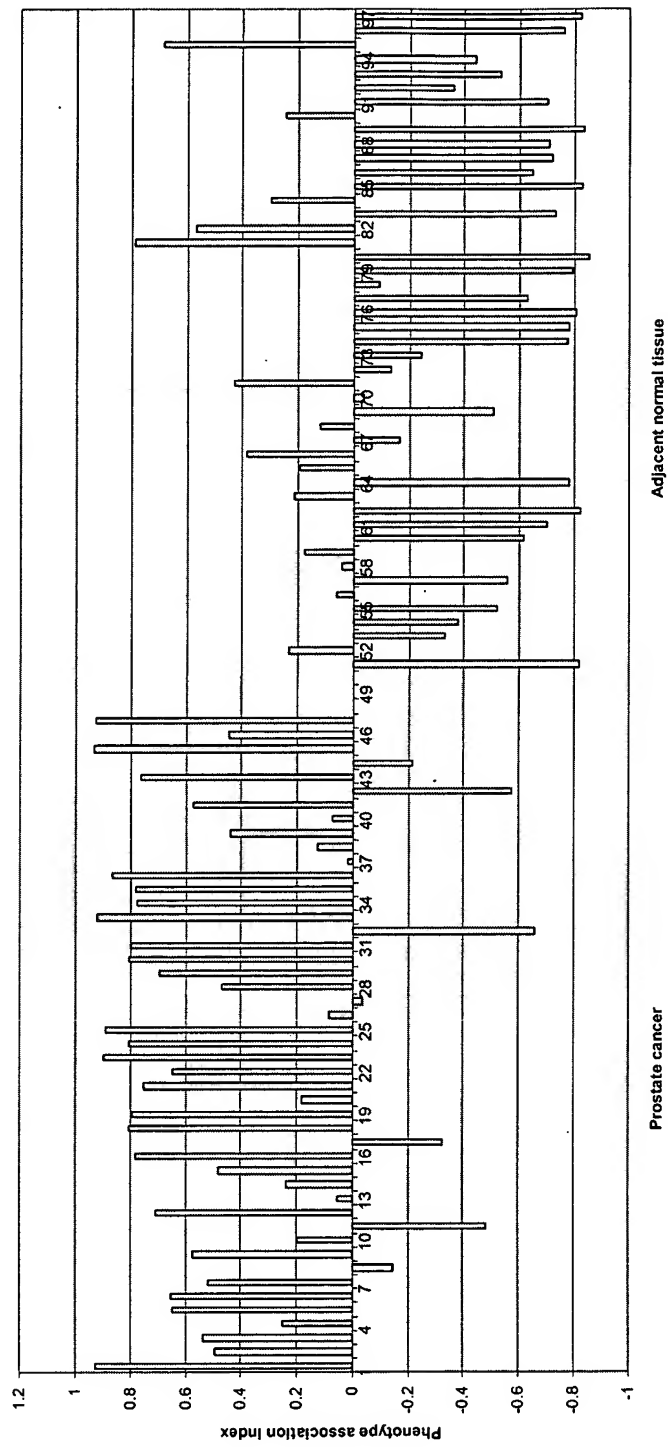


Figure 9. Phenotype association indexes for 5 genes of the prostate cancer/normal tissue discrimination class in 47 prostate tumors and 47 adjacent normal tissue samples

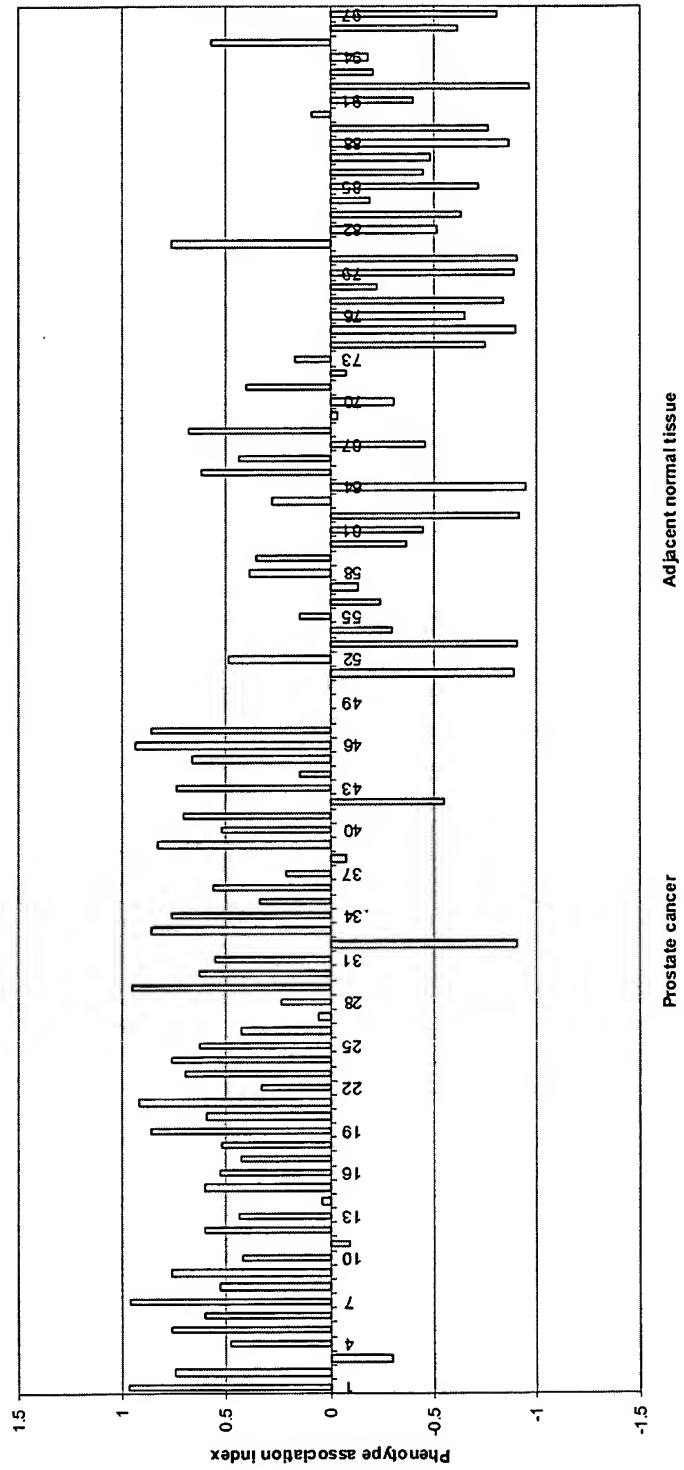


Figure 10. Correlation of the expression profiles in 5 xenograft-derived human prostate carcinoma cell lines and 14 invasive versus 38 non-invasive human prostate tumors for 104 genes of the concordant class

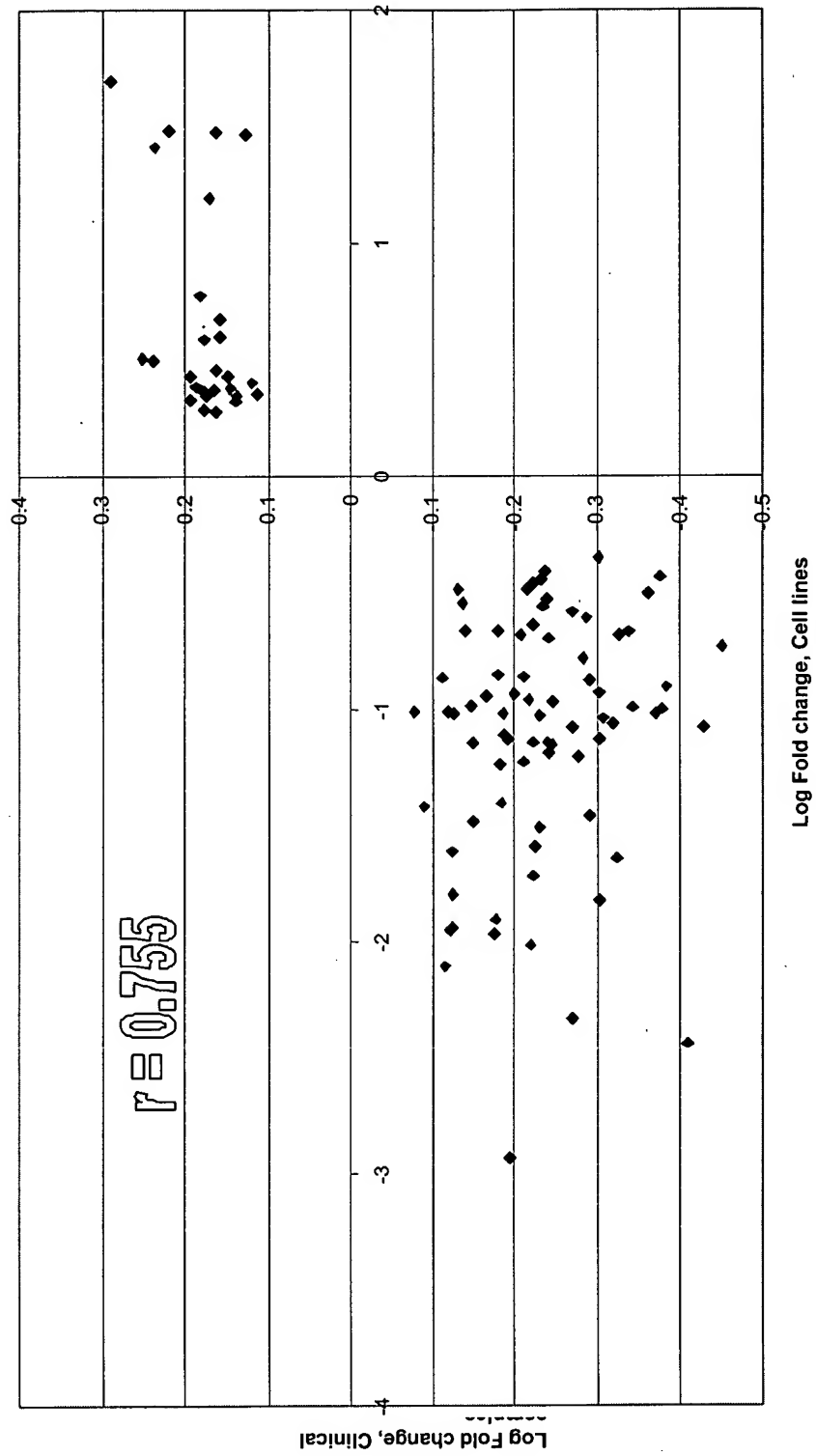


Figure 11. Correlation of the expression profiles in xenograft-derived human prostate carcinoma cell lines and 14 invasive versus 38 non-invasive human prostate tumors for 20 genes of the invasion minimum segregation class 1 (invasion cluster 1)

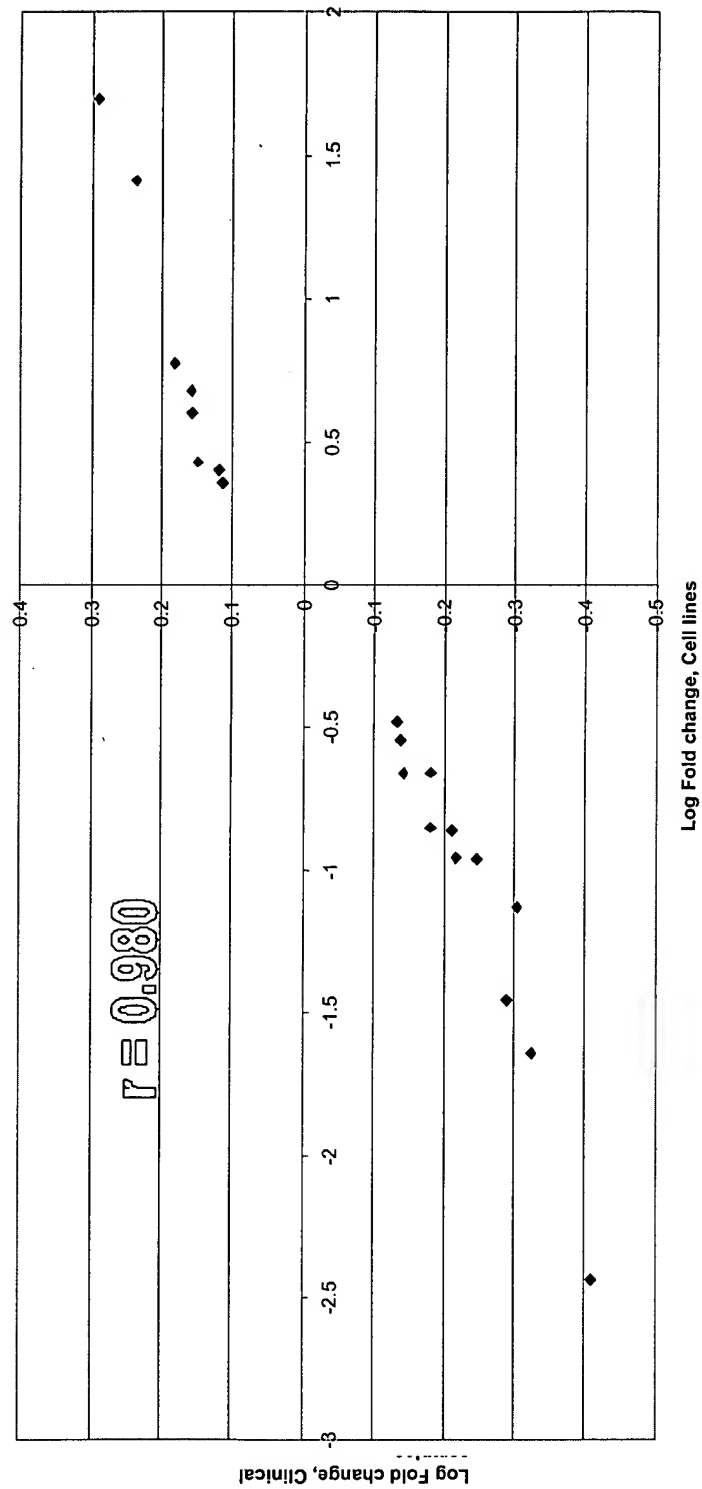


Figure 12. Phenotype association indexes in 14 invasive and 38 non-invasive human prostate tumors for 20 genes of the invasion cluster 1

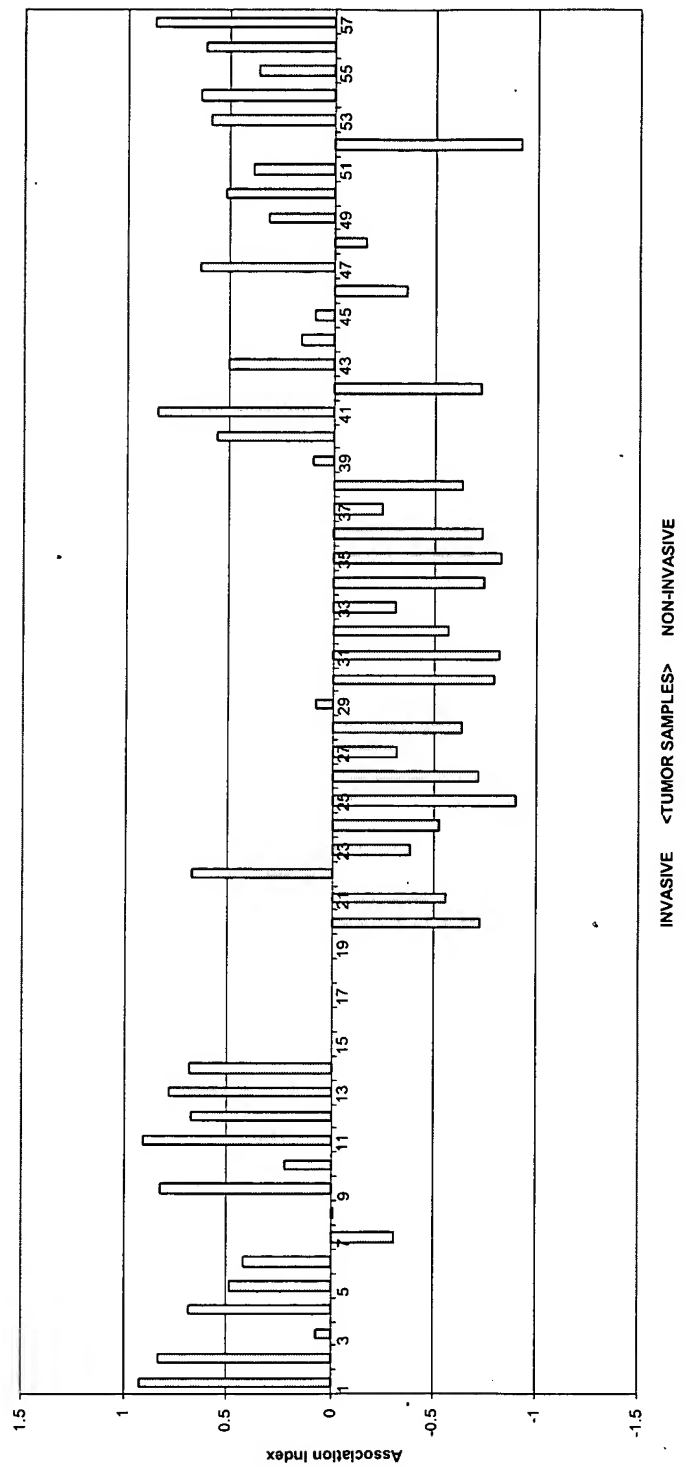


Figure 13. Correlation of the expression profiles in 5 xenograft-derived human prostate carcinoma cell lines and 12 invasive versus 17 non-invasive human prostate tumors (surgical margins 1+) for 12 genes of the invasion cluster 2

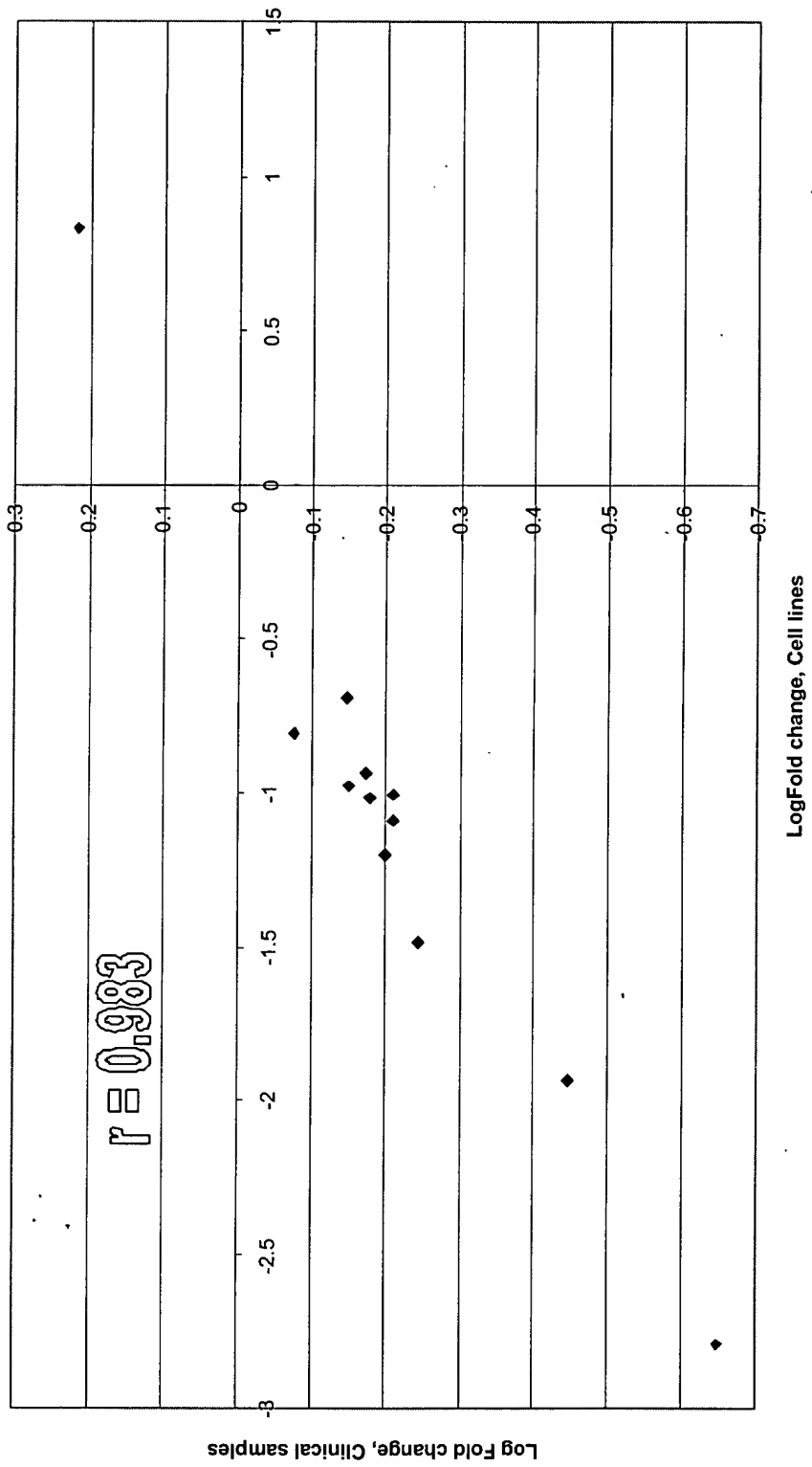


Figure 14. Phenotype association indexes in 12 invasive and 17 non-invasive human prostate tumors for 12 genes of the invasion cluster 2

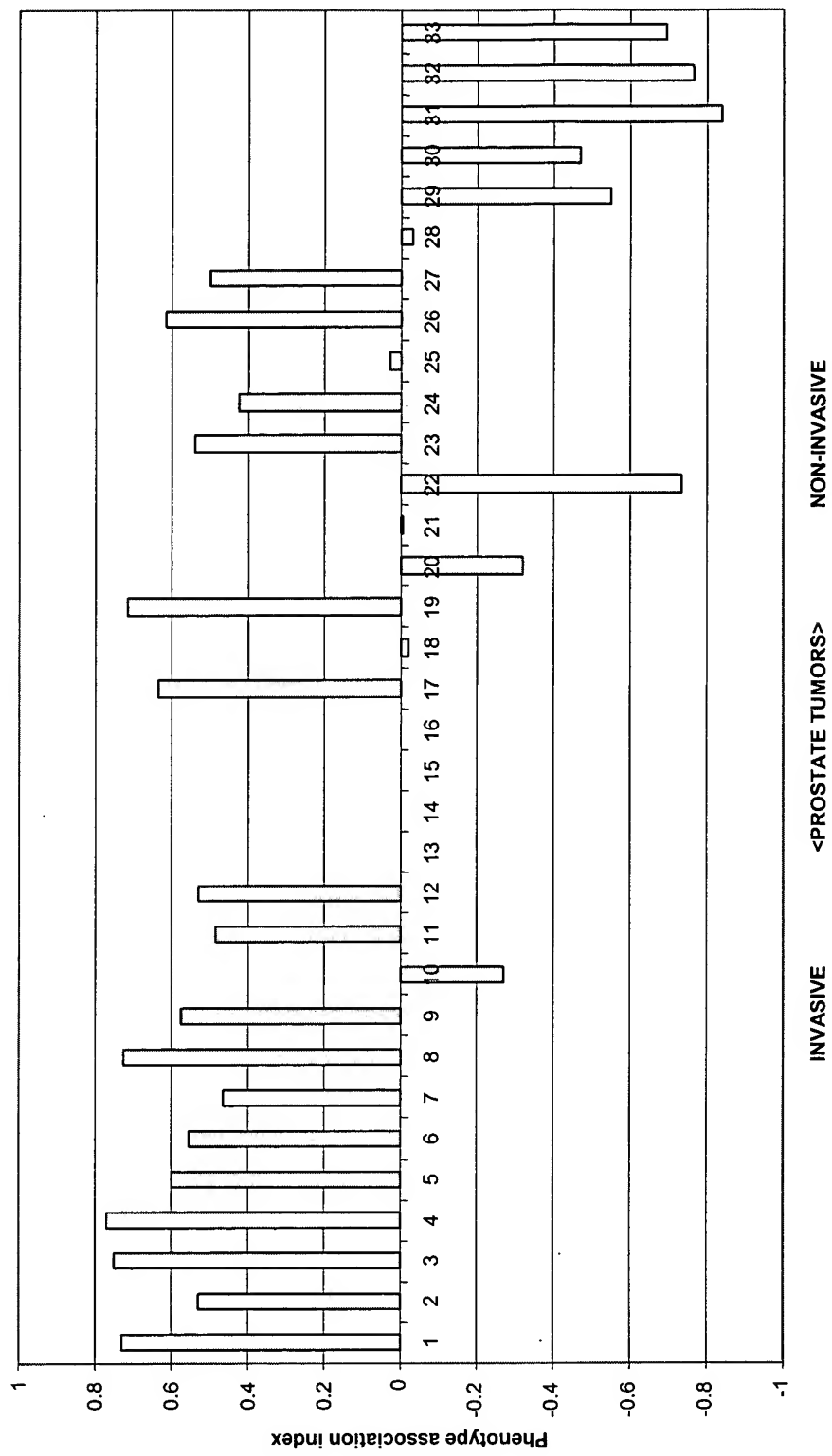


Figure 15. Correlation of the expression profiles in 5 xenograft-derived human prostate carcinoma cell lines and 11 invasive versus 7 non-invasive human prostate tumors (invasion clusters 1 & 2 +) for 10 genes of the invasion cluster 3

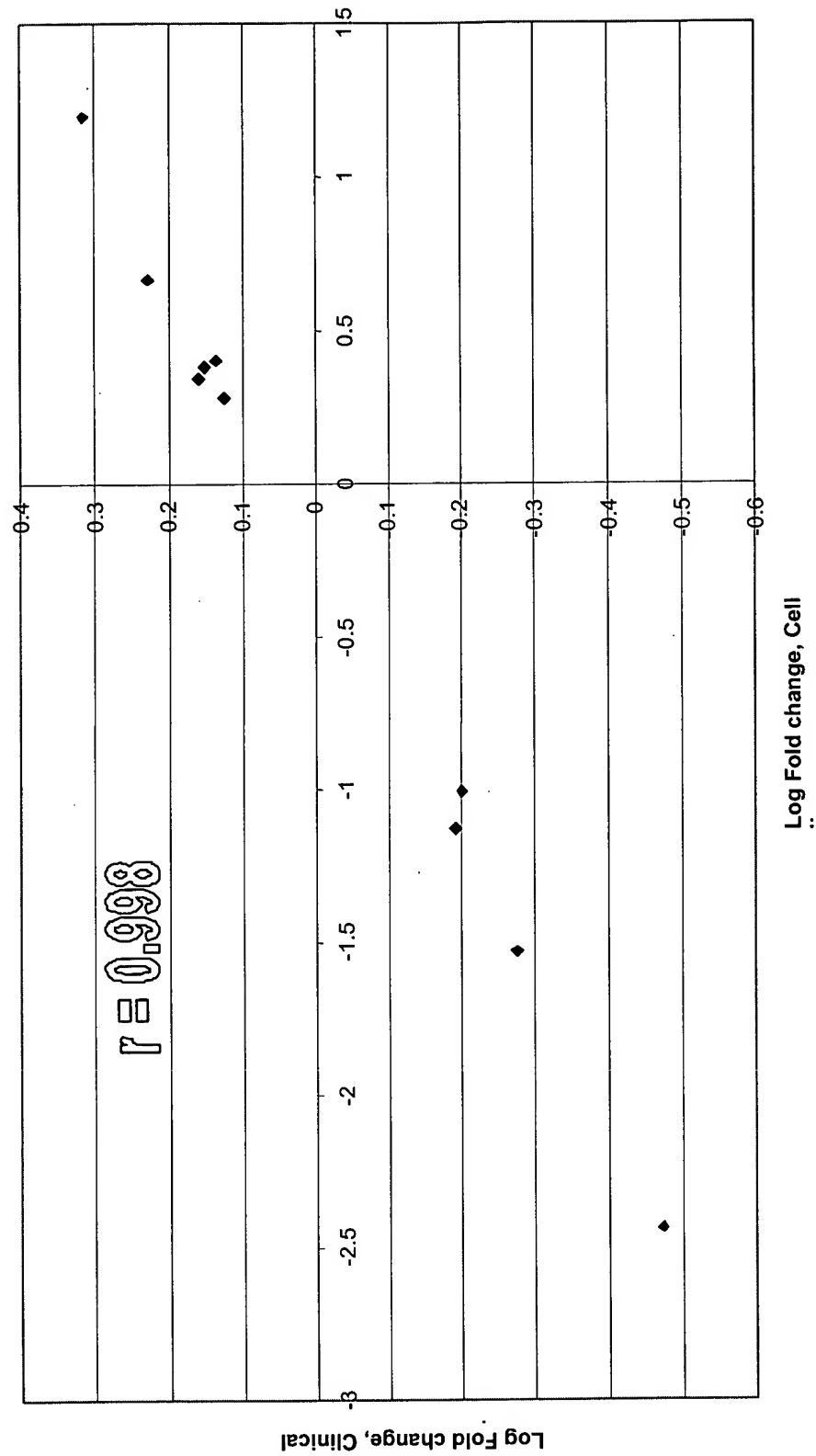


Figure 16. Phenotype association indexes in 11 invasive and 7 non-invasive human prostate tumors for 10 genes of the invasion cluster 3

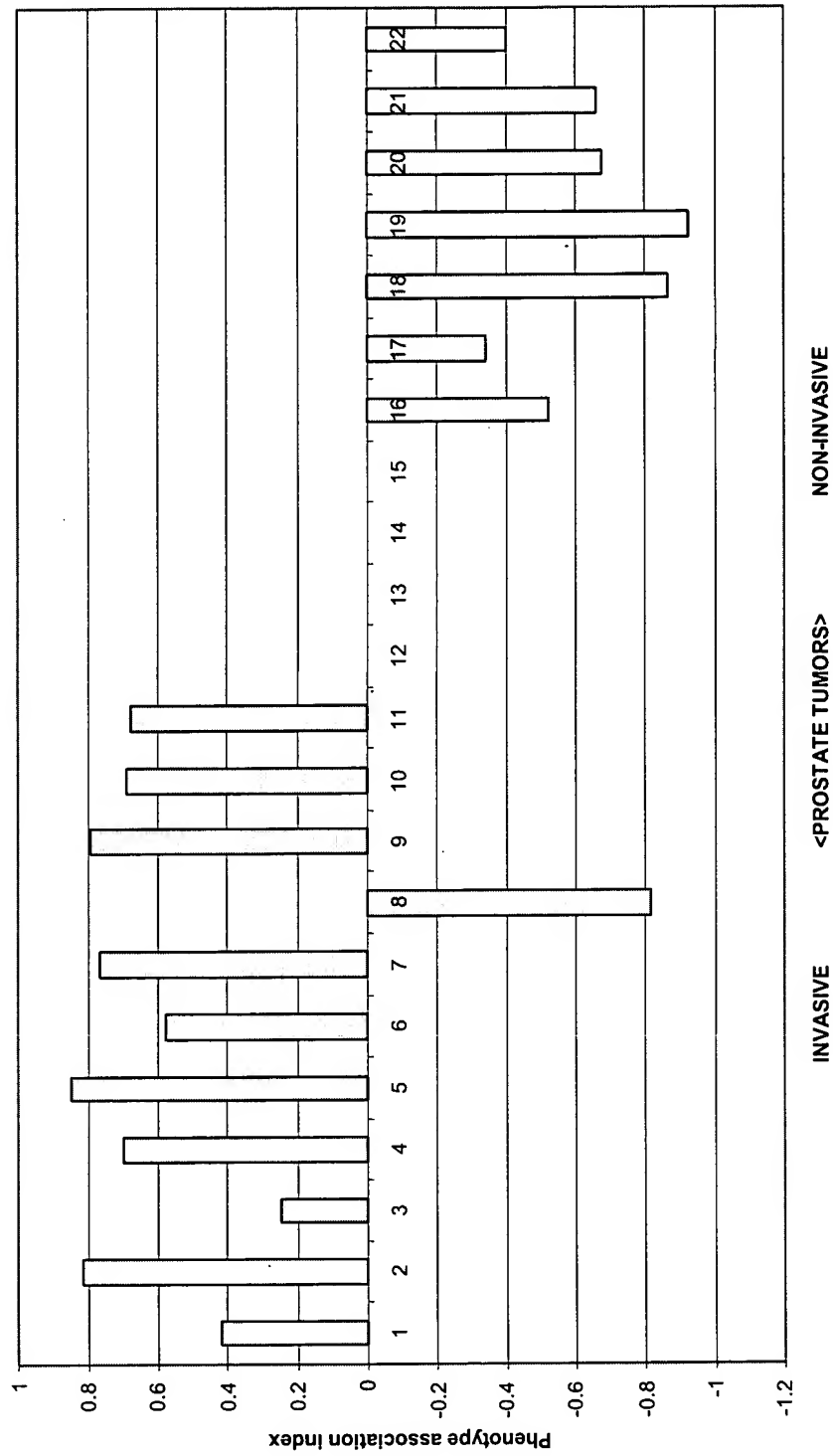


Figure 17. Correlation of the expression profiles in 5 xenograft-derived human prostate carcinoma cell lines and 3 invasive versus 21 non-invasive human prostate tumors for 13 genes of the invasion cluster 4.

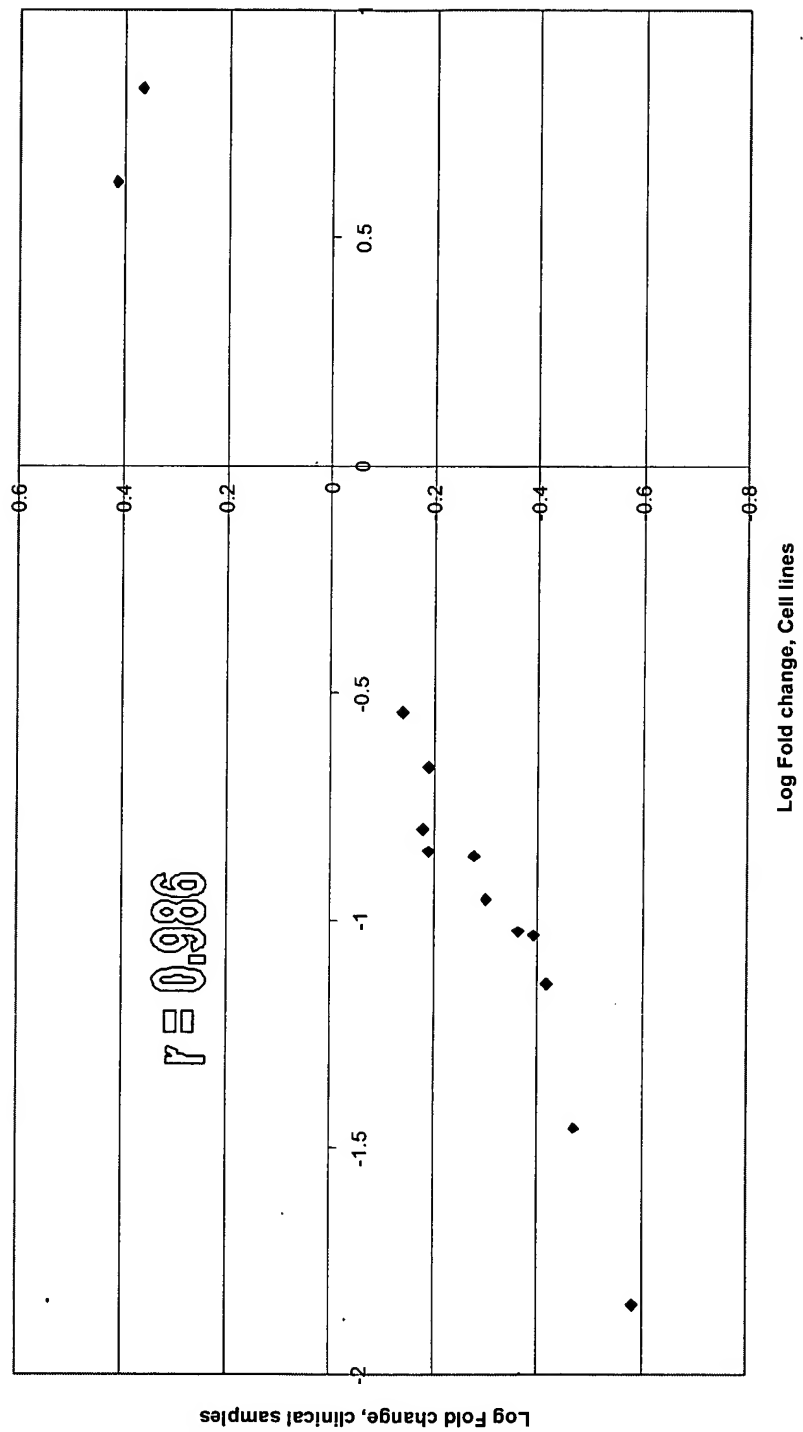


Figure 18. Phenotype association indexes in 3 invasive and 21 non-invasive human prostate tumors for 13 genes of the invasion cluster 4

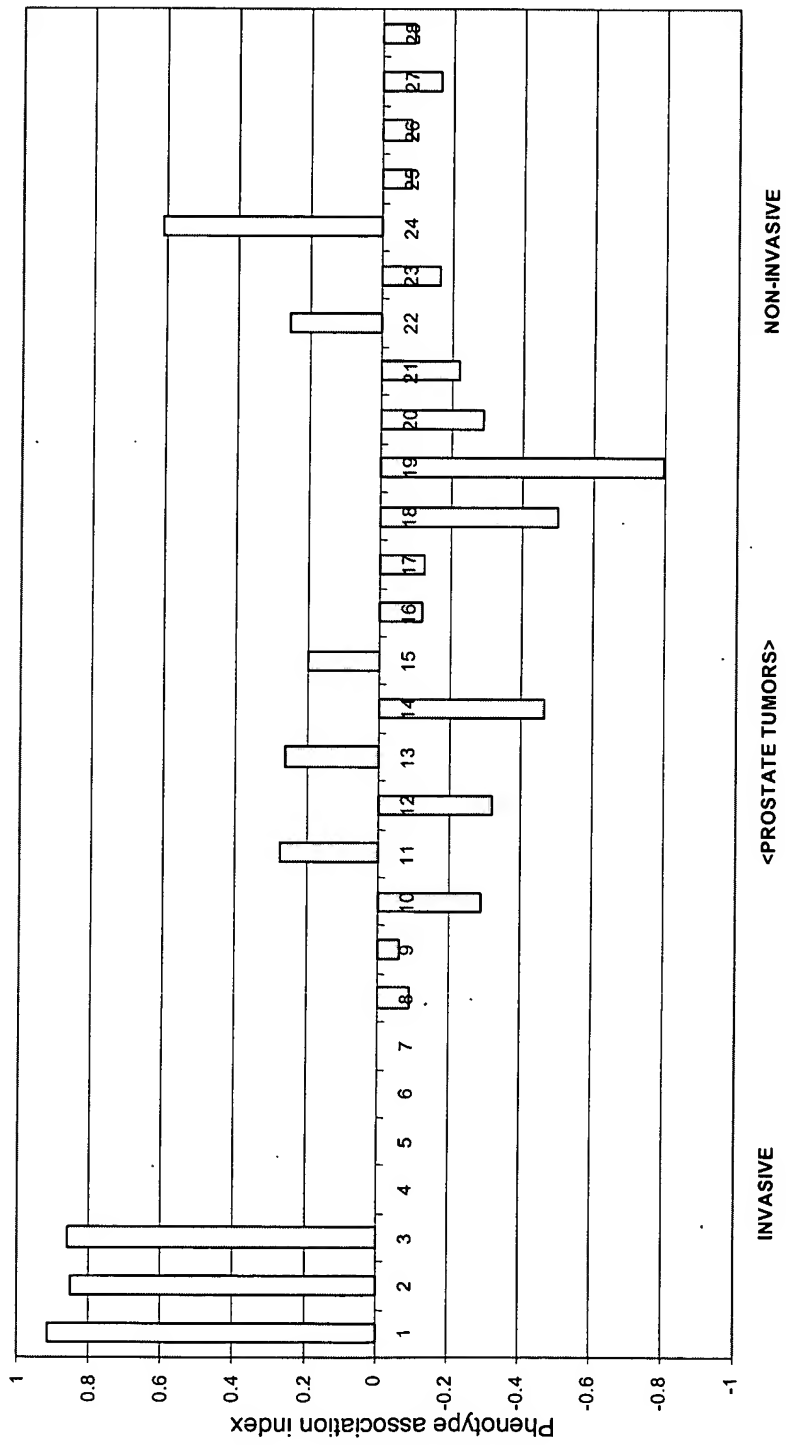


Figure 19. Correlation of the expression profiles in 5 xenograft-derived human prostate carcinoma cell lines and 6 high Gleason grade versus 46 low Gleason grade prostate tumors for 58 genes of the concordant class

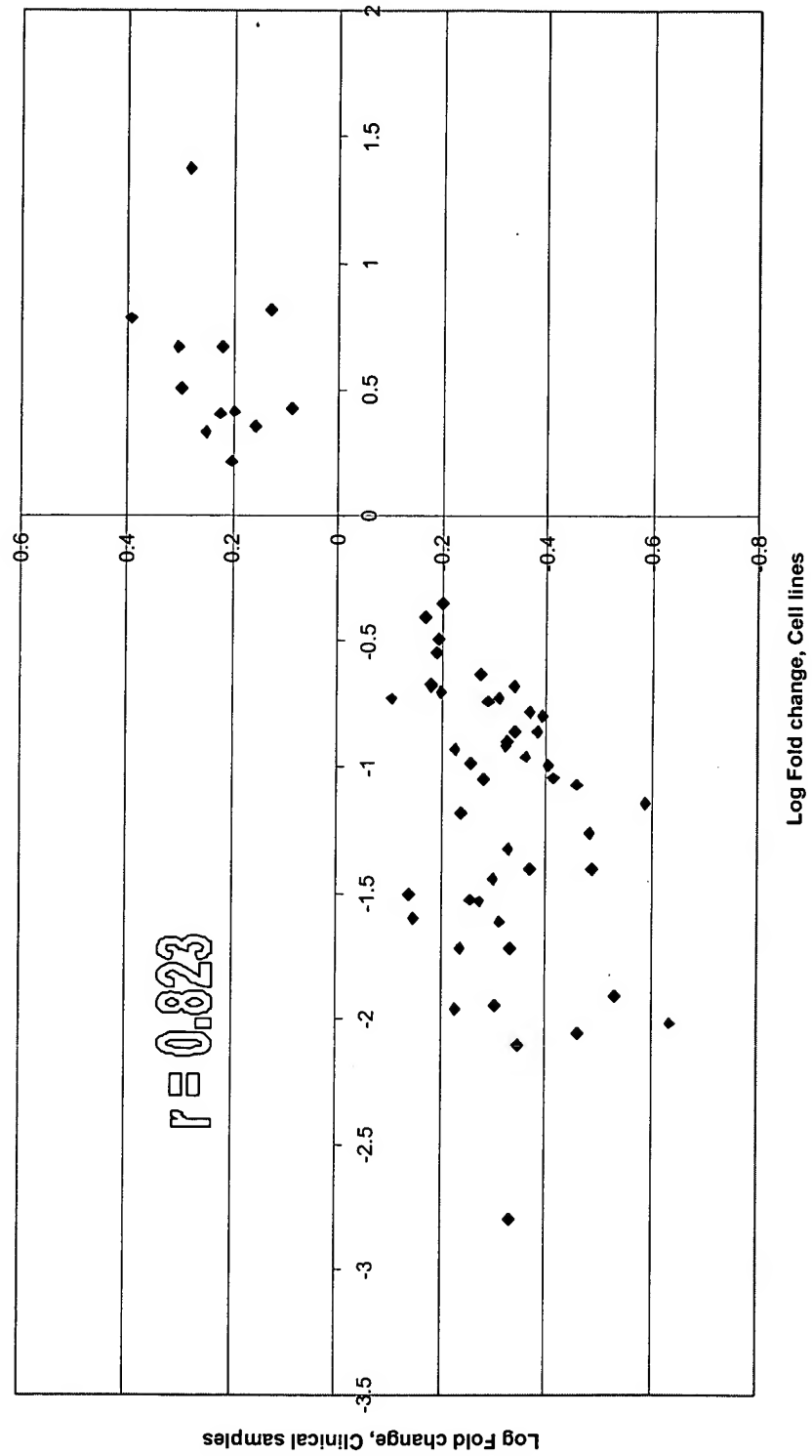


Figure 20. Correlation of the expression profiles in 5 xenograft-derived human prostate carcinoma cell lines and 6 high Gleason grade versus 46 low Gleason grade prostate tumors for 17 genes high grade cluster 1

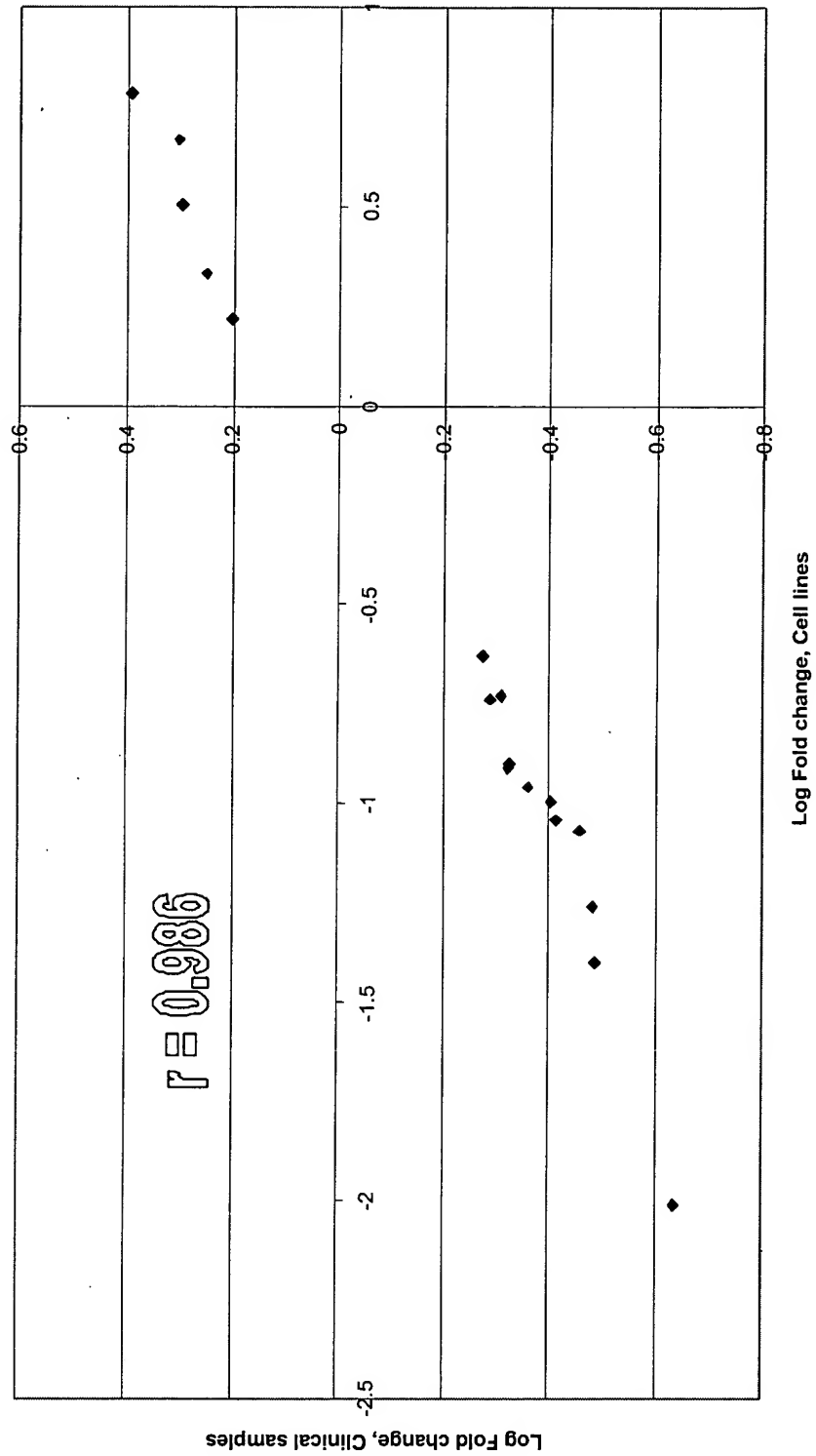


Figure 21. Correlation of the expression profiles in 5 xenograft-derived human prostate carcinoma cell lines and 6 high Gleason grade versus 20 low Gleason grade prostate tumors for 12 genes high grade cluster 2

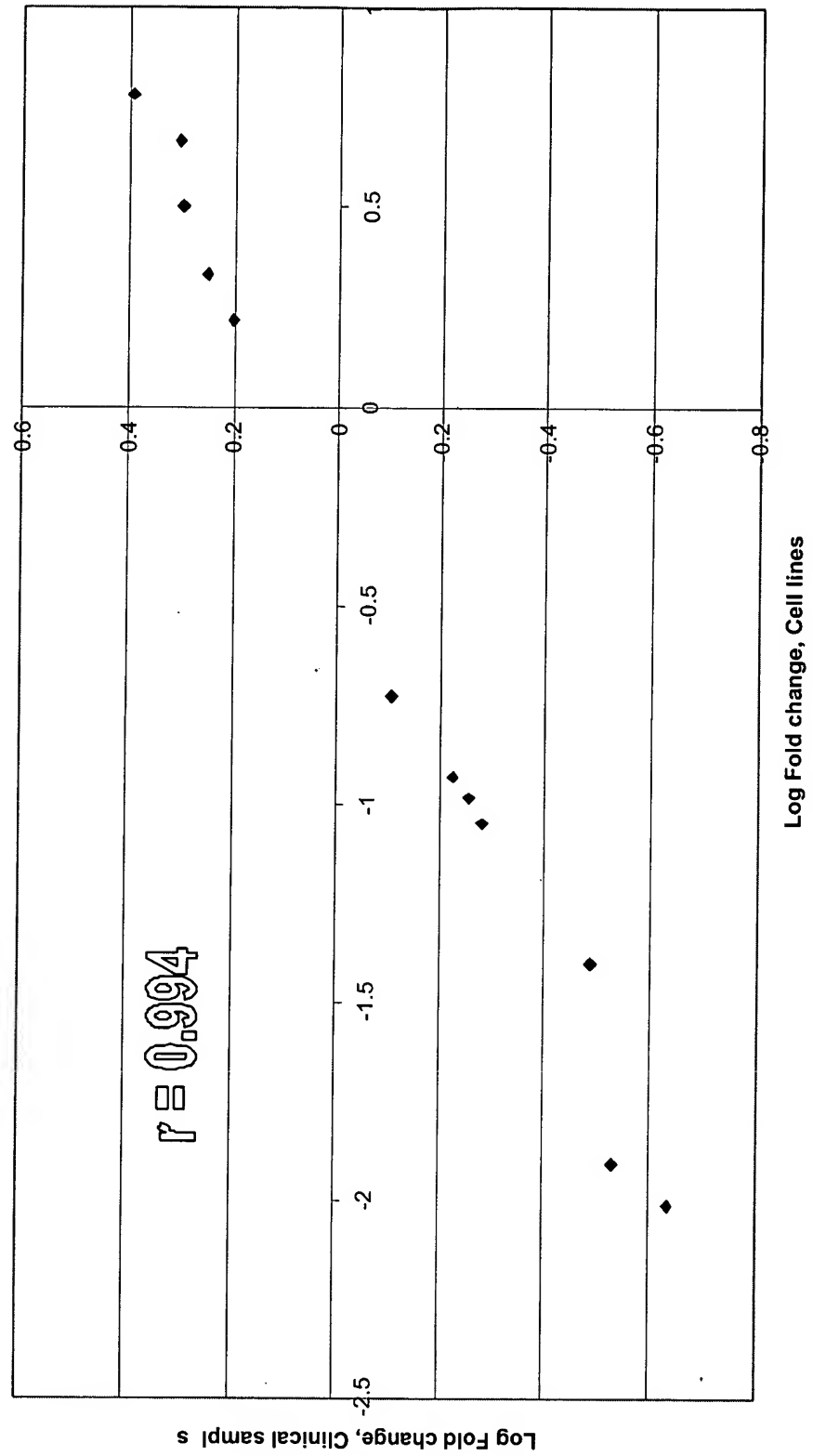


Figure 22. Correlation of the expression profiles in 5 xenograft-derived human prostate carcinoma cell lines and 6 high Gleason grade versus 16 low Gleason grade prostate tumors for 7 genes high grade cluster 3

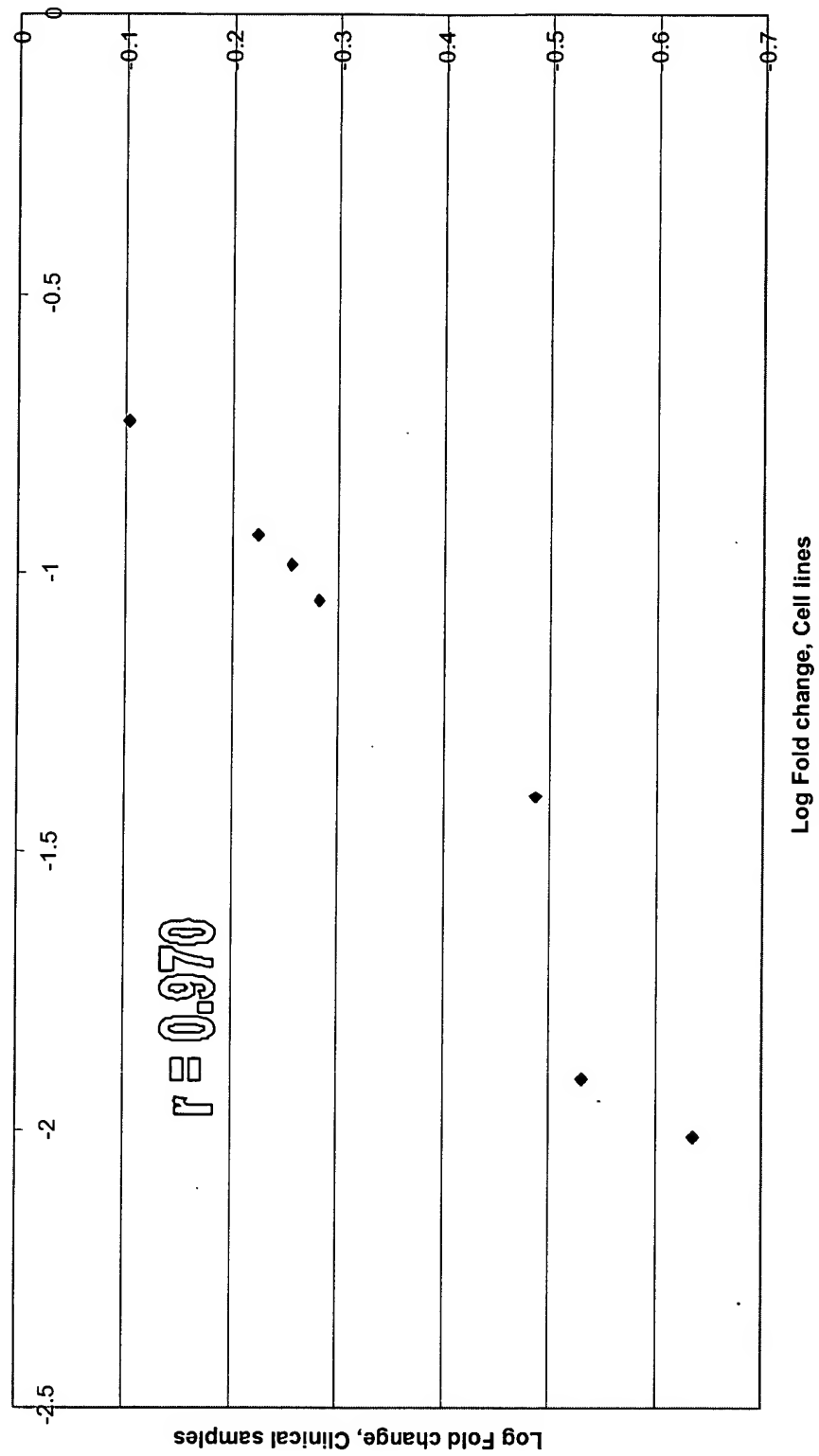


Figure 23. Correlation of the expression profiles in 5 xenograft-derived human prostate carcinoma cell lines and 6 high Gleason grade versus 46 low Gleason grade prostate tumors for 38 genes of the ALT high grade cluster

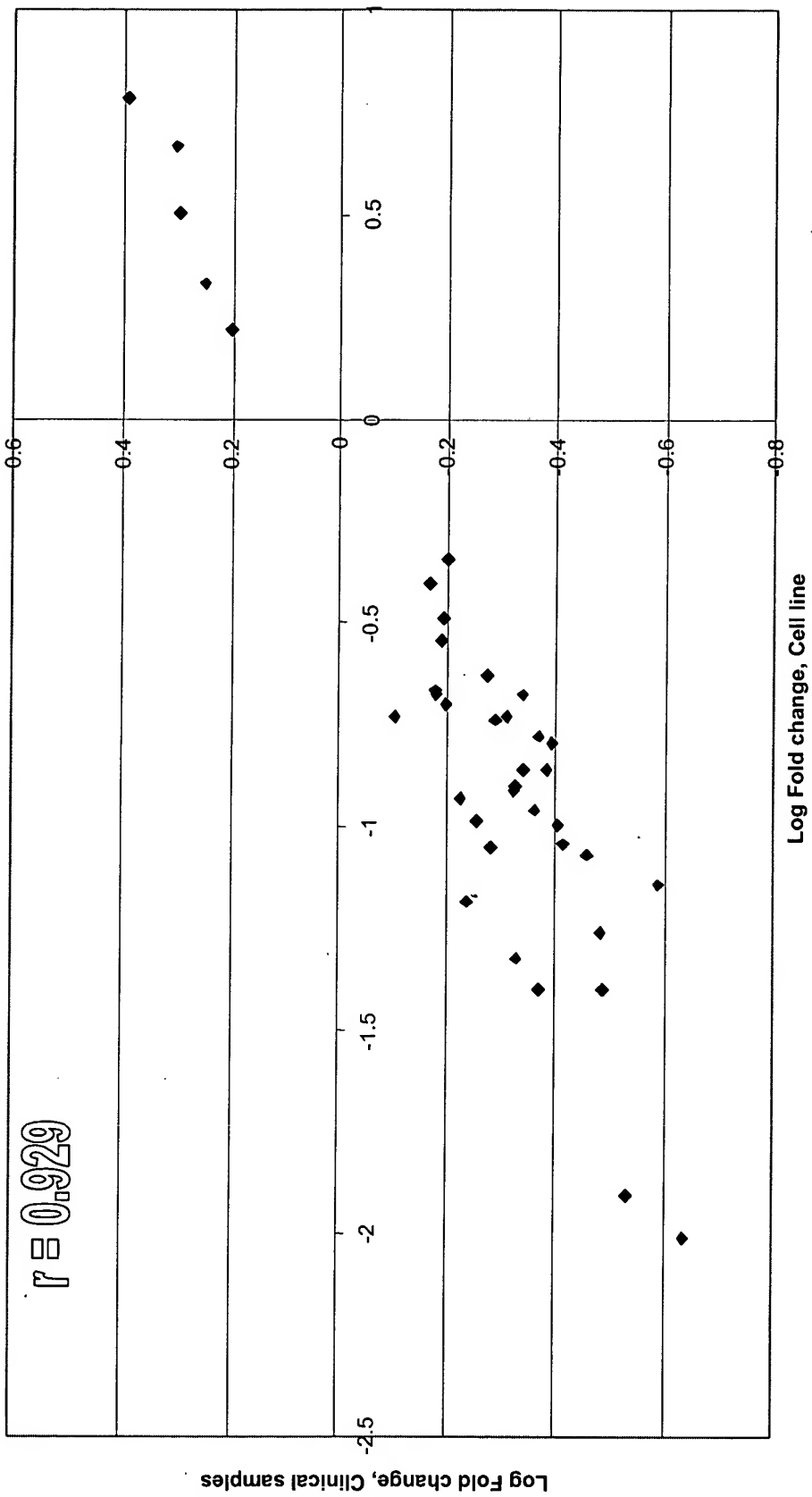


Figure 24. Correlation of the expression profiles in 5 xenograft-derived carcinoma cell lines and 6 high Gleason grade versus 17 low Gleason grade for 5 genes high grade cluster 4

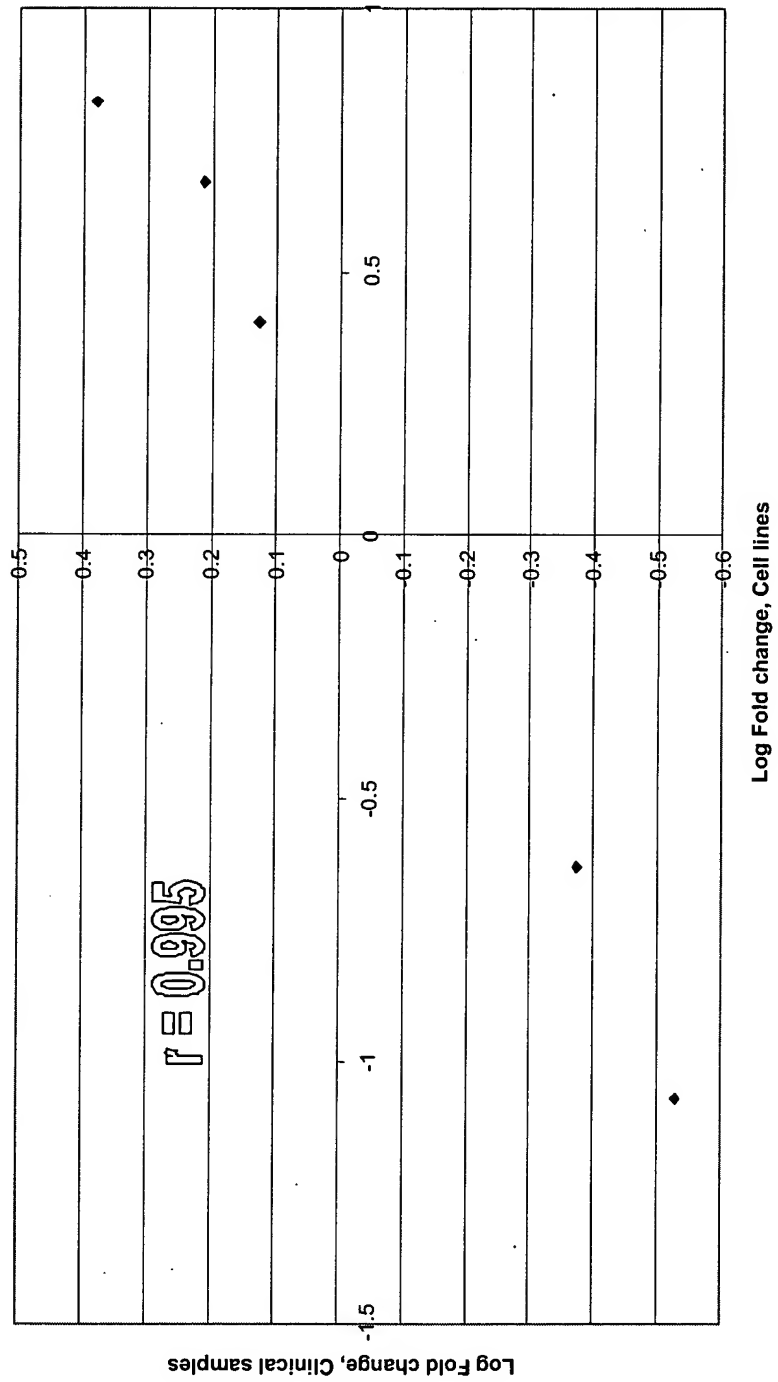


Figure 25. Correlation of the expression profiles in 5 xenograft-derived human carcinoma cell lines and 6 high Gleason grade versus 17 low Gleason grade prostate for 4 genes high grade cluster 5

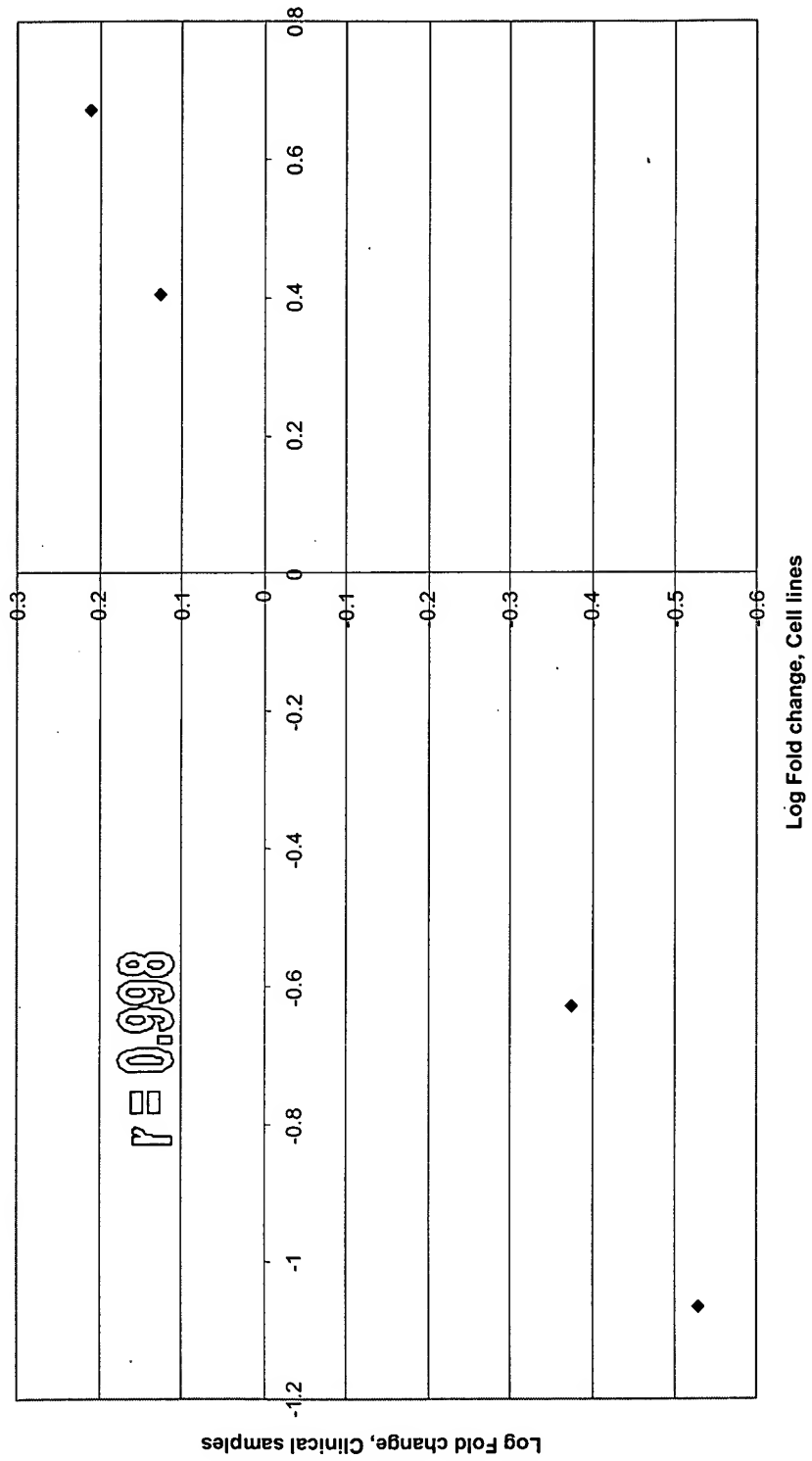


Figure 26. Correlation of the expression profiles in 5 xenograft-derived human carcinoma cell lines and 6 high Gleason grade versus 17 low Gleason grade prostate for 7 genes high grade cluster 6

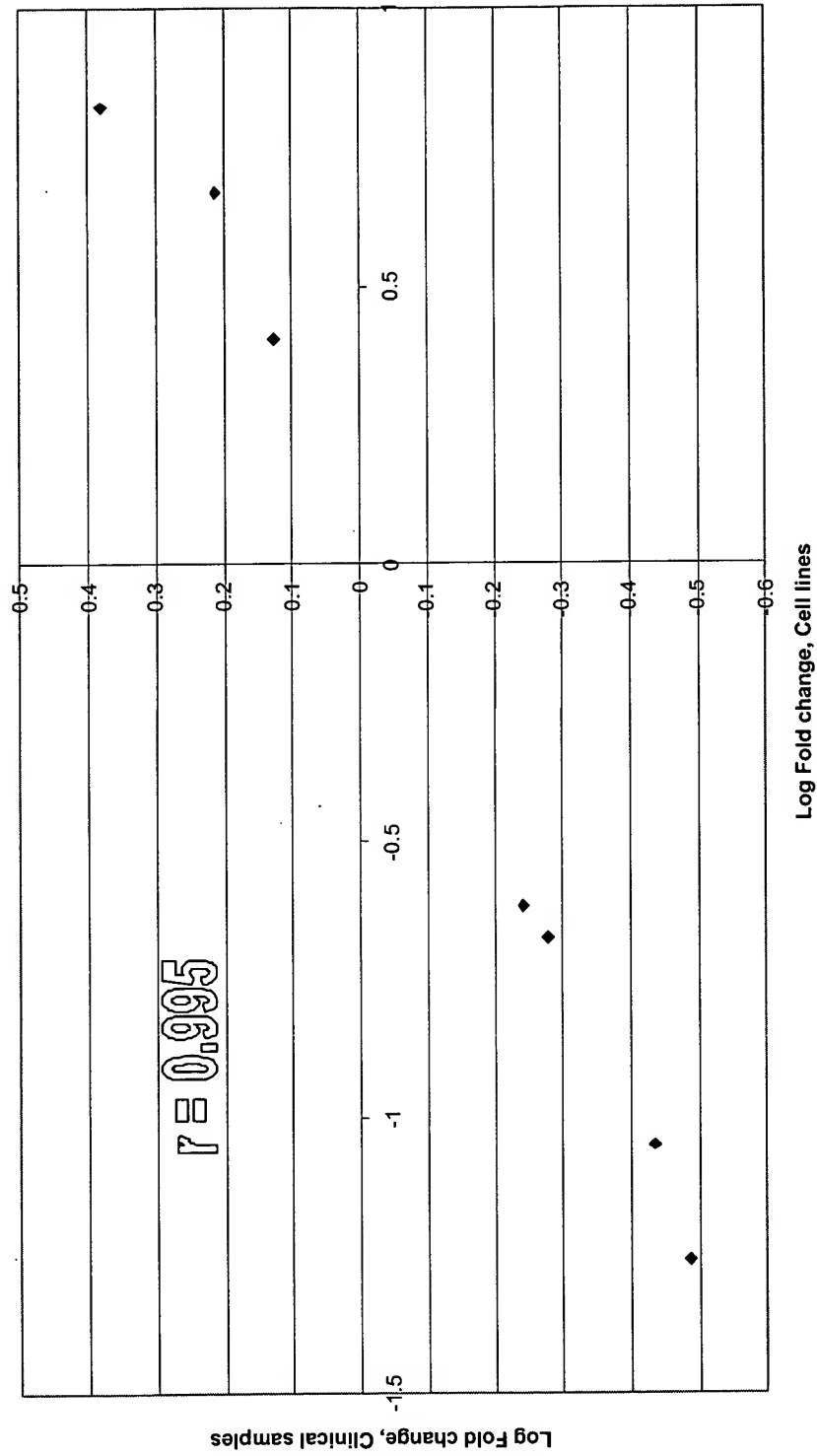


Figure 27. Correlation of the expression profiles in 5 xenograft-derived human prostate carcinoma cell lines and 6 high Gleason grade versus 17 low Gleason grade prostate tumors for 13 genes high grade cluster 7

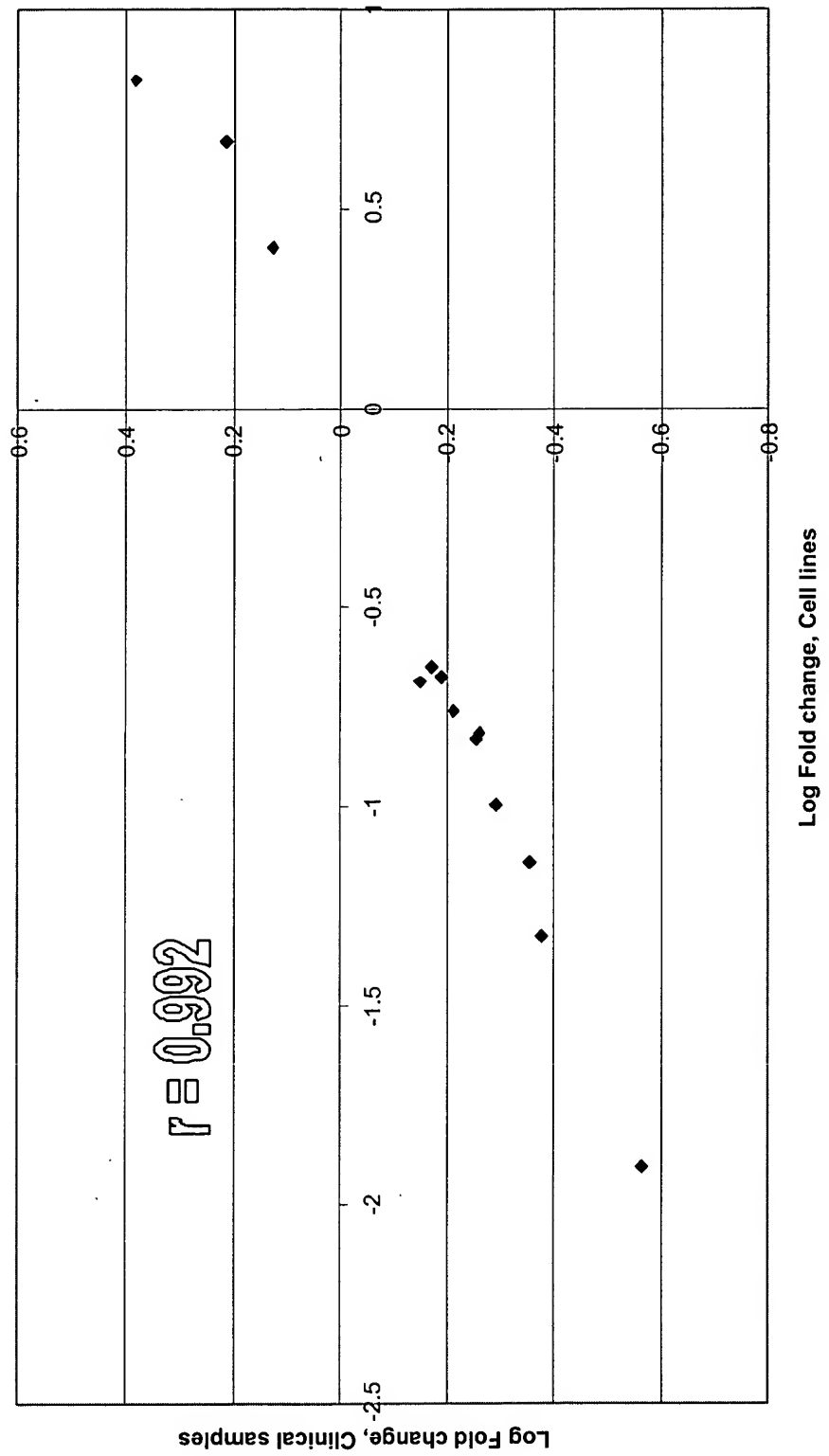


Figure 28. Phenotype association indexes for 54 genes of the BPH segregation cluster in 8 patients with BPH and 9 patients with prostate cancer

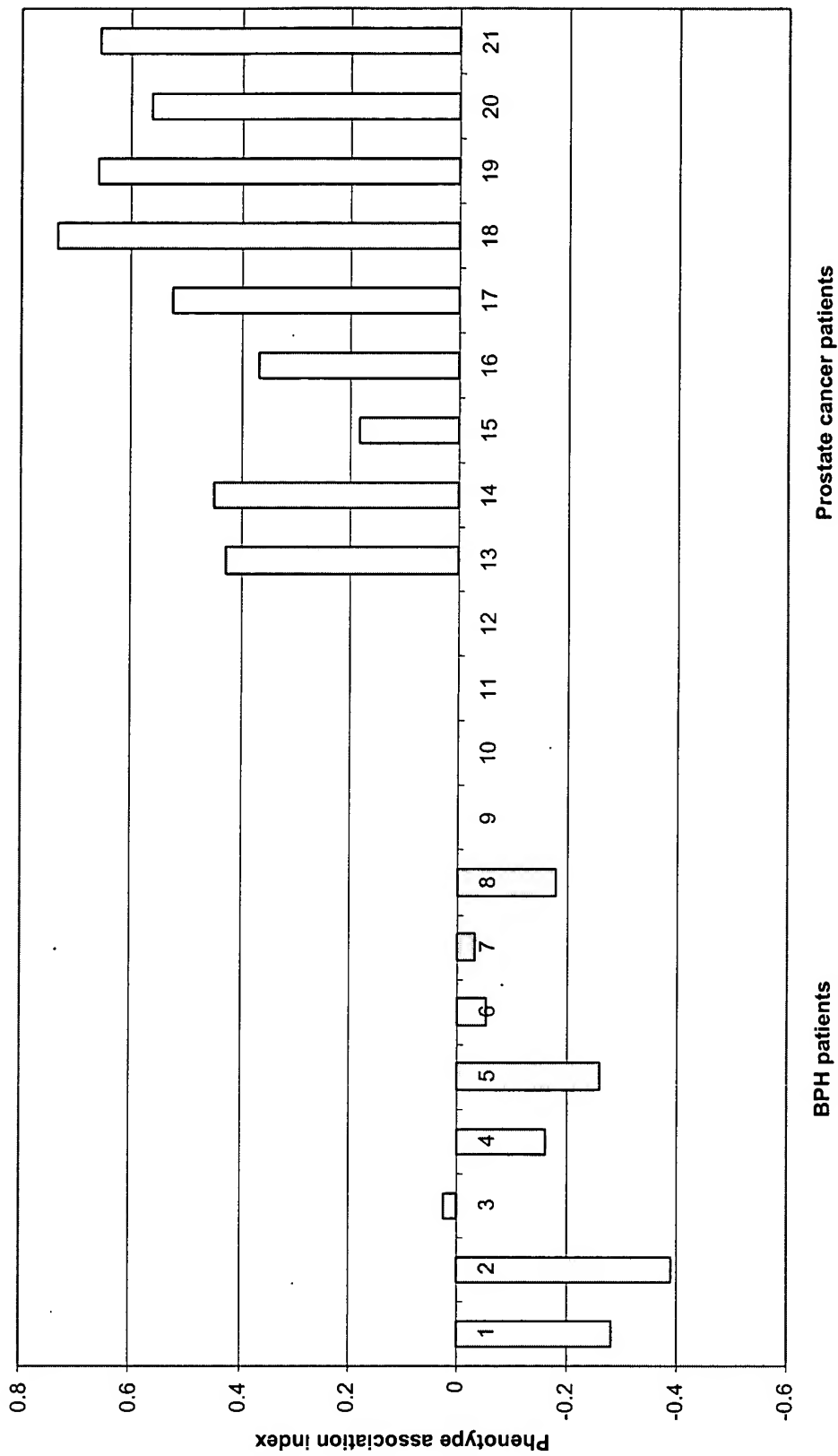


Figure 29. Phenotype association indexes for 14 genes of the BPH segregation cluster MAGEA1 in 8 patients with BPH and 9 patients with prostate cancer

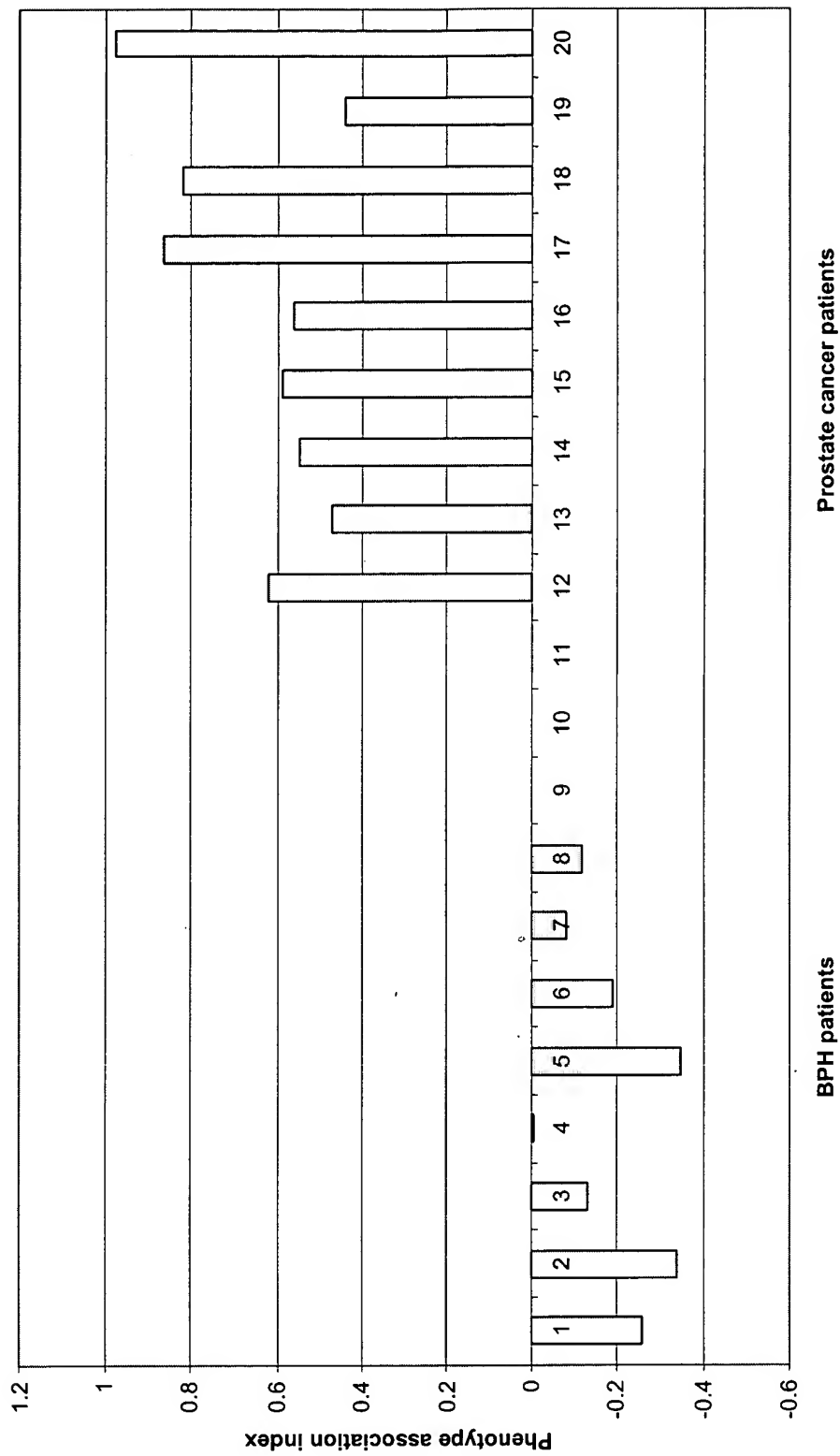


Figure 30. Phenotype association indices for 17 genes of metastasis segregation class 1 in 5 BPH samples, 3 ANP samples, prostatitis, 10 samples of localized prostate cancer (LPC), and 7 samples of metastatic prostate cancer (MPC)

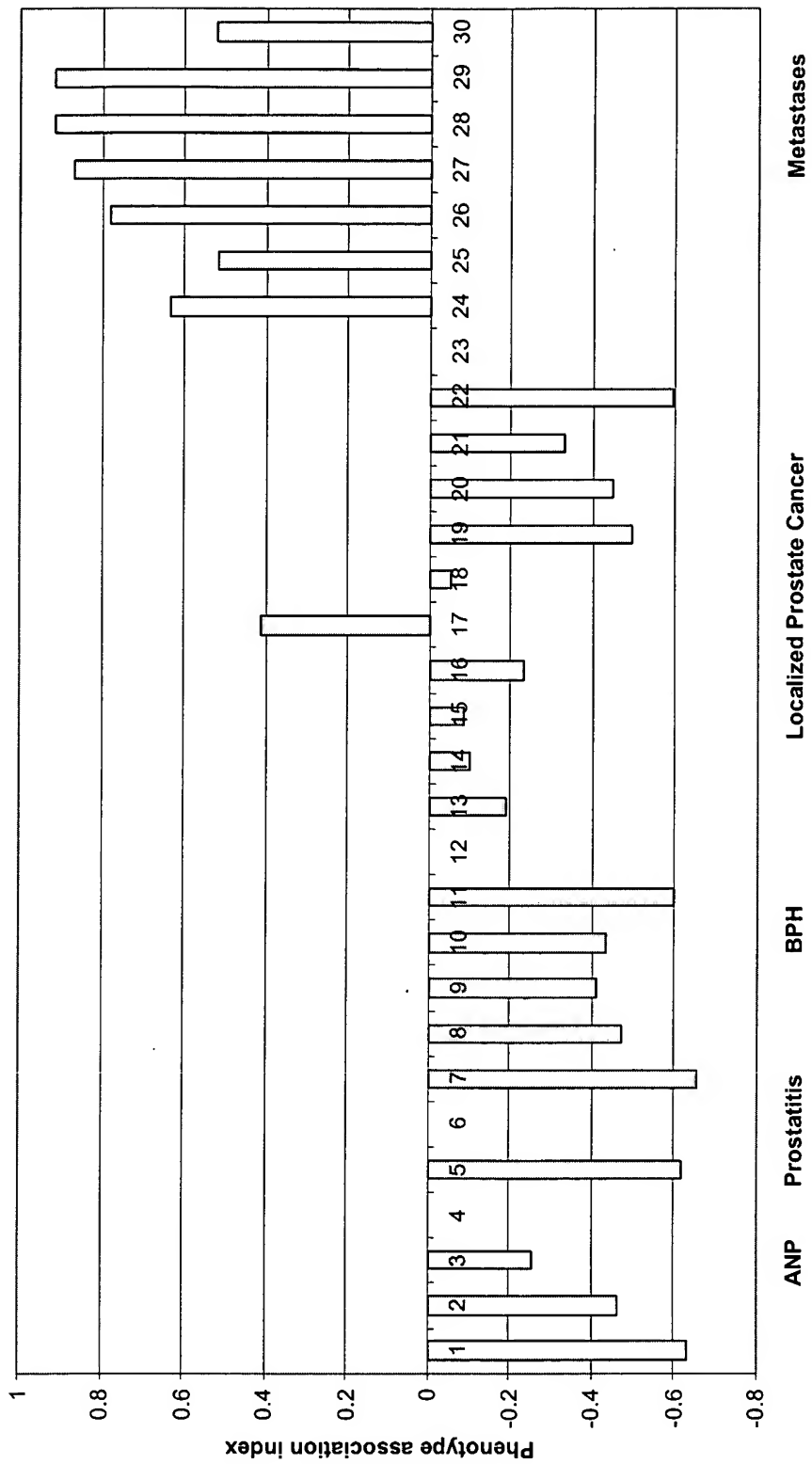


Figure 31. Phenotype association indices for 19 genes of metastasis segregation class 2 in 5 BPH samples, 3 ANP samples, prostatitis, 10 samples of localized prostate cancer (LPC), and 7 samples of metastatic prostate cancer (MPC)

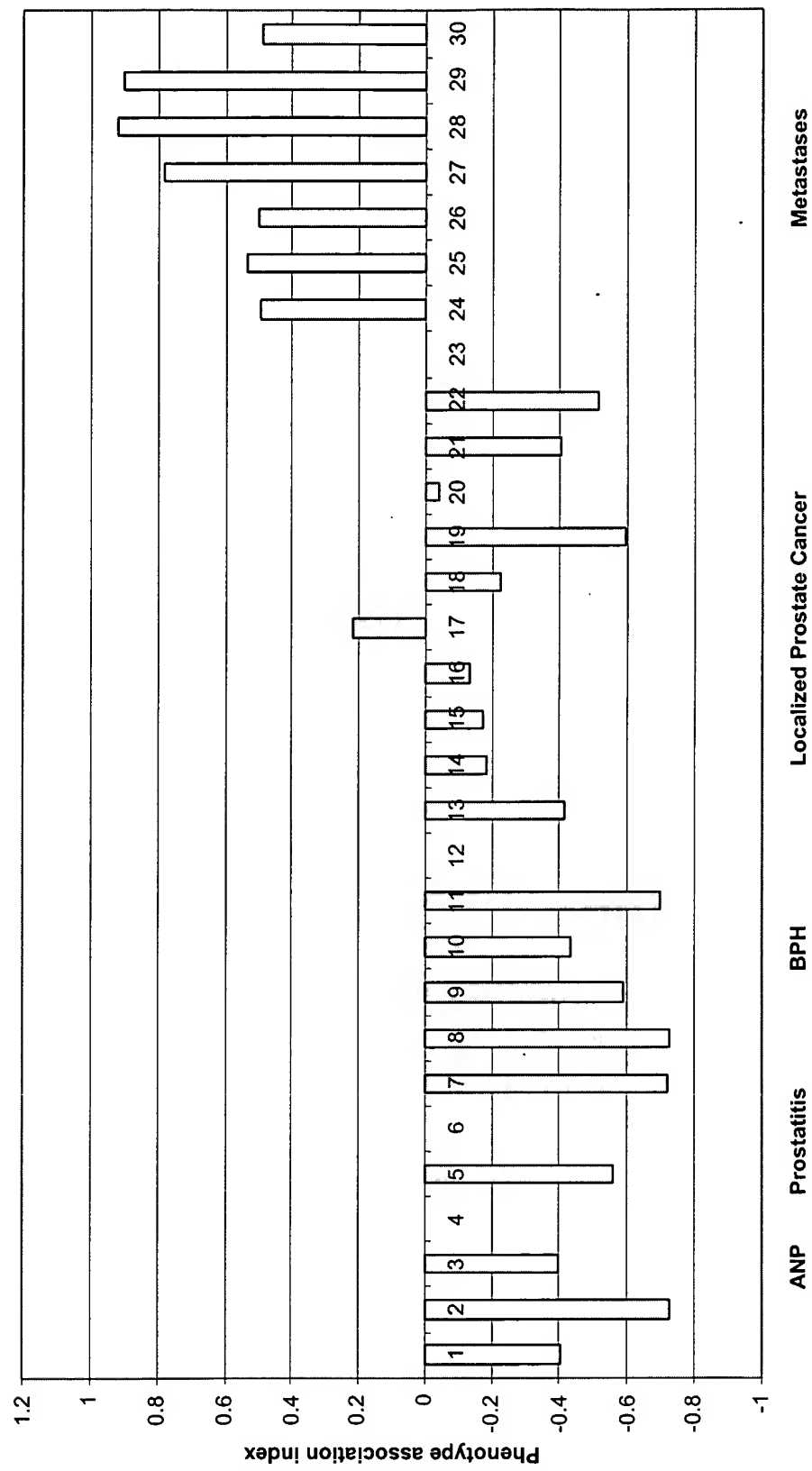


Figure 32. Phenotype association indices for 17 genes of metastasis segregation class in 14 BPH samples, 4 ANP samples, prostatitis, 14 samples of localized prostate cancer (LPC), and 20 samples of metastatic prostate cancer (MPC).

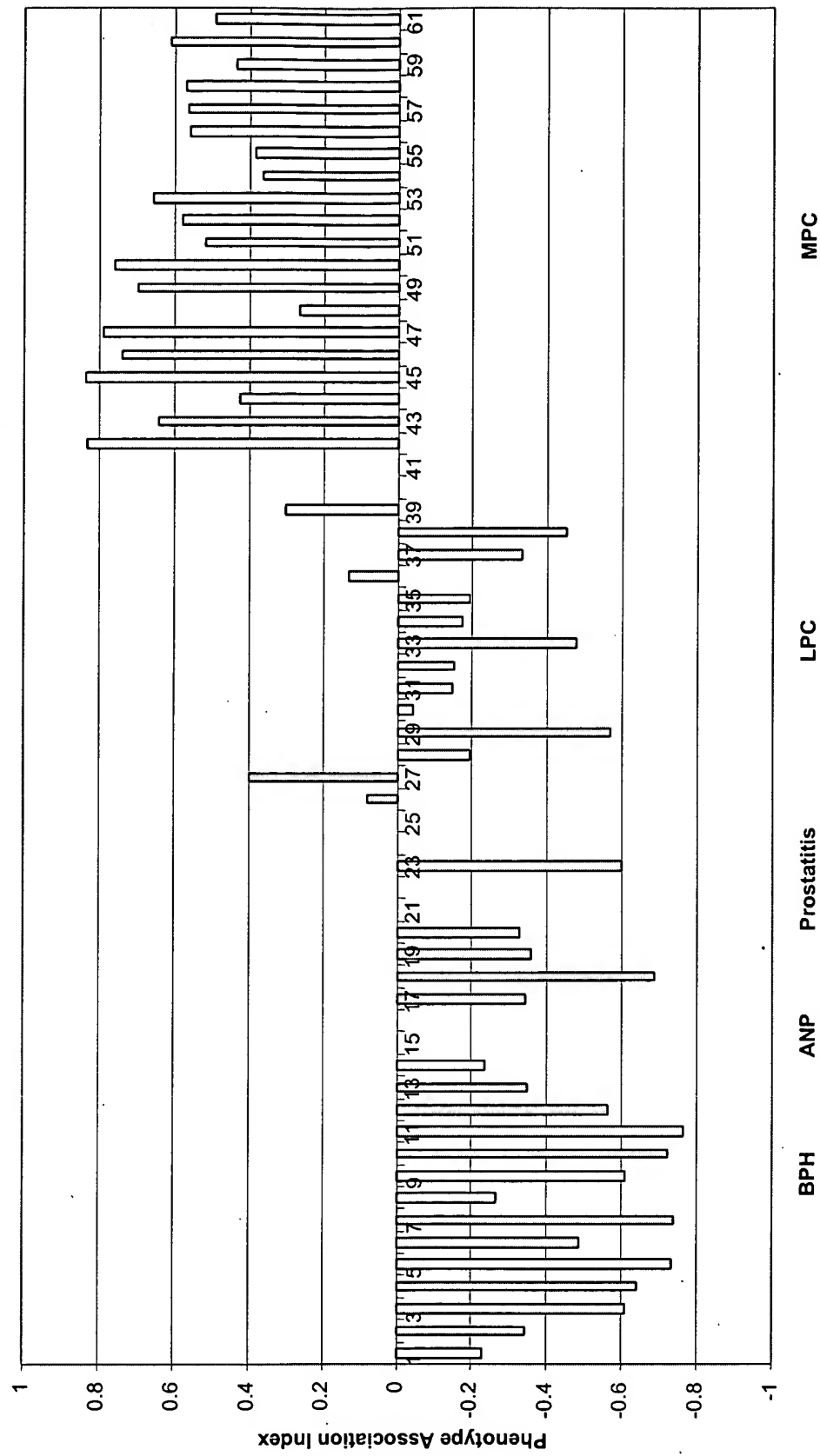


Figure 33. Phenotype association indices for 19 genes of metastasis segregation class 2 in 14 BPH samples, 4 ANP samples, prostatitis, 14 samples of localized prostate cancer (LPC), and 20 samples of metastatic prostate cancer (MPC).

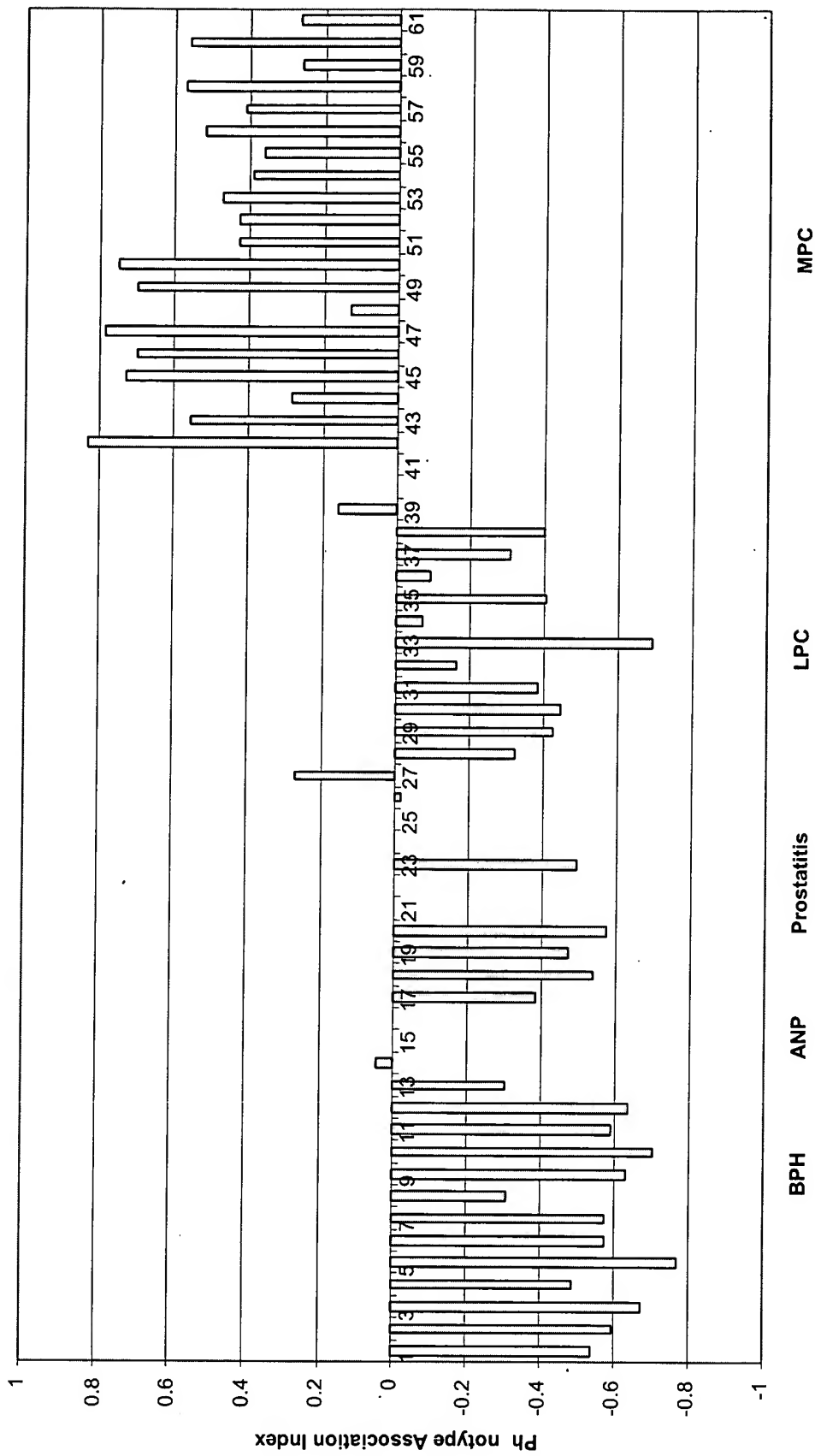


Figure 34. Phenotype association indices for 6 genes of the Q-PCR-based poor prognosis predictor class in 34 breast cancer patients who developed distant metastases within 5 years of diagnosis and 44 patients who continued to be disease-free

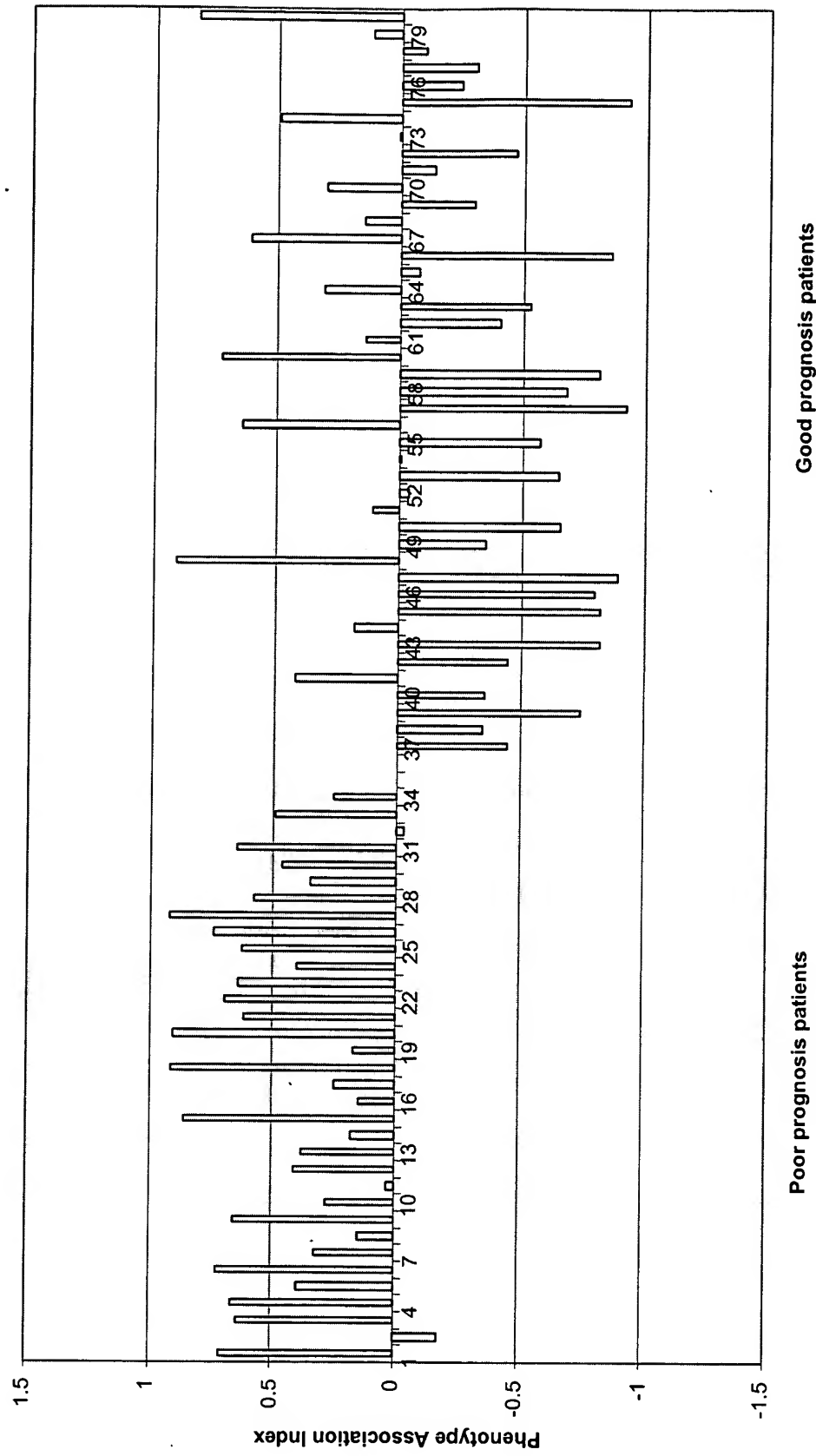


Figure 35. Phenotype association indexes for 14 genes of the Q-PCR-based good prognosis predictor class in 34 breast cancer patients who developed distant metastases within 5 years of diagnosis and 44 patients who continued to be disease-free

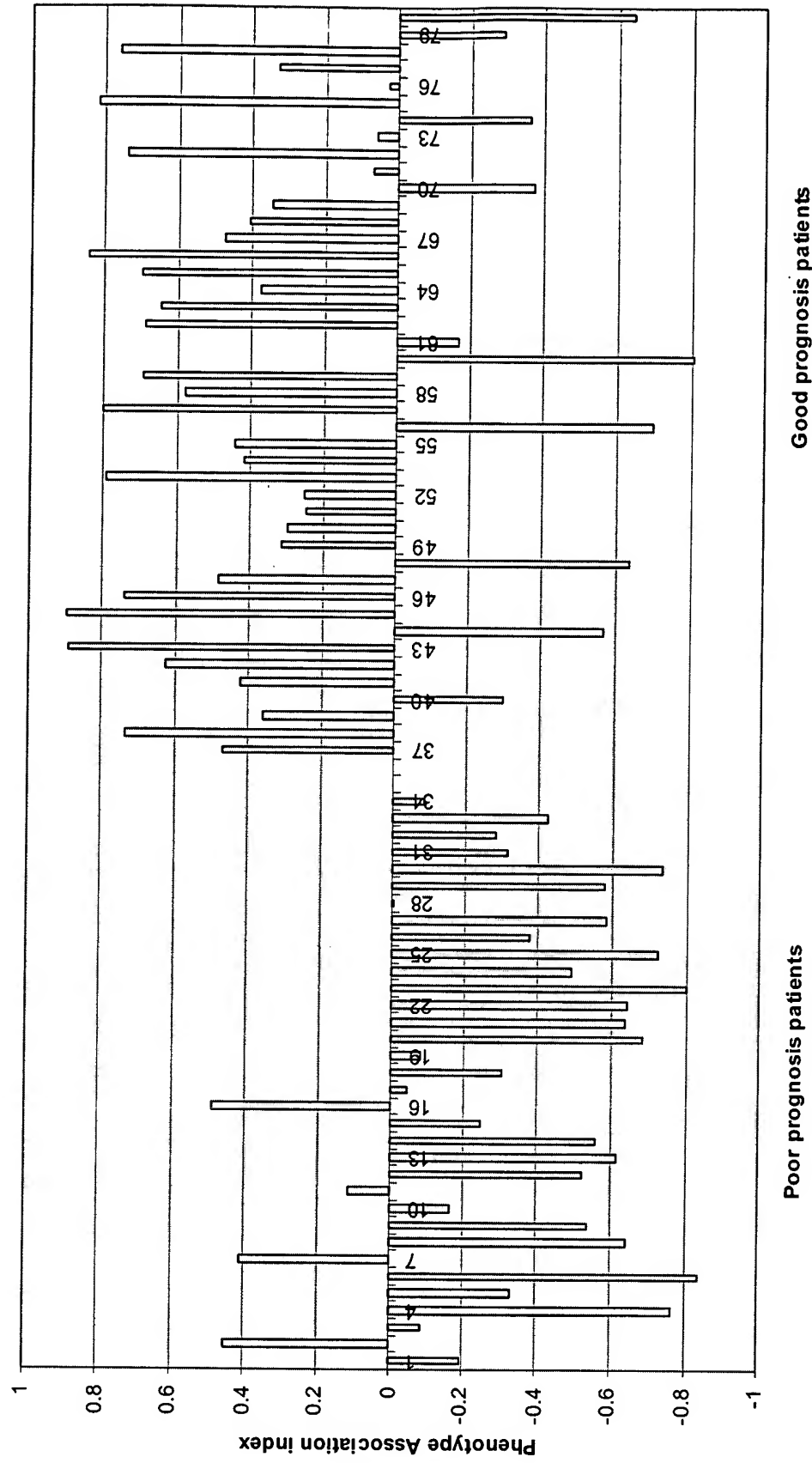


Figure 36. Phenotype association indices for 13 genes of the Q-PCR-based good prognosis predictor class in 34 breast cancer patients who developed distant metastases within 5 years of diagnosis and 44 patients who continued to be disease-free

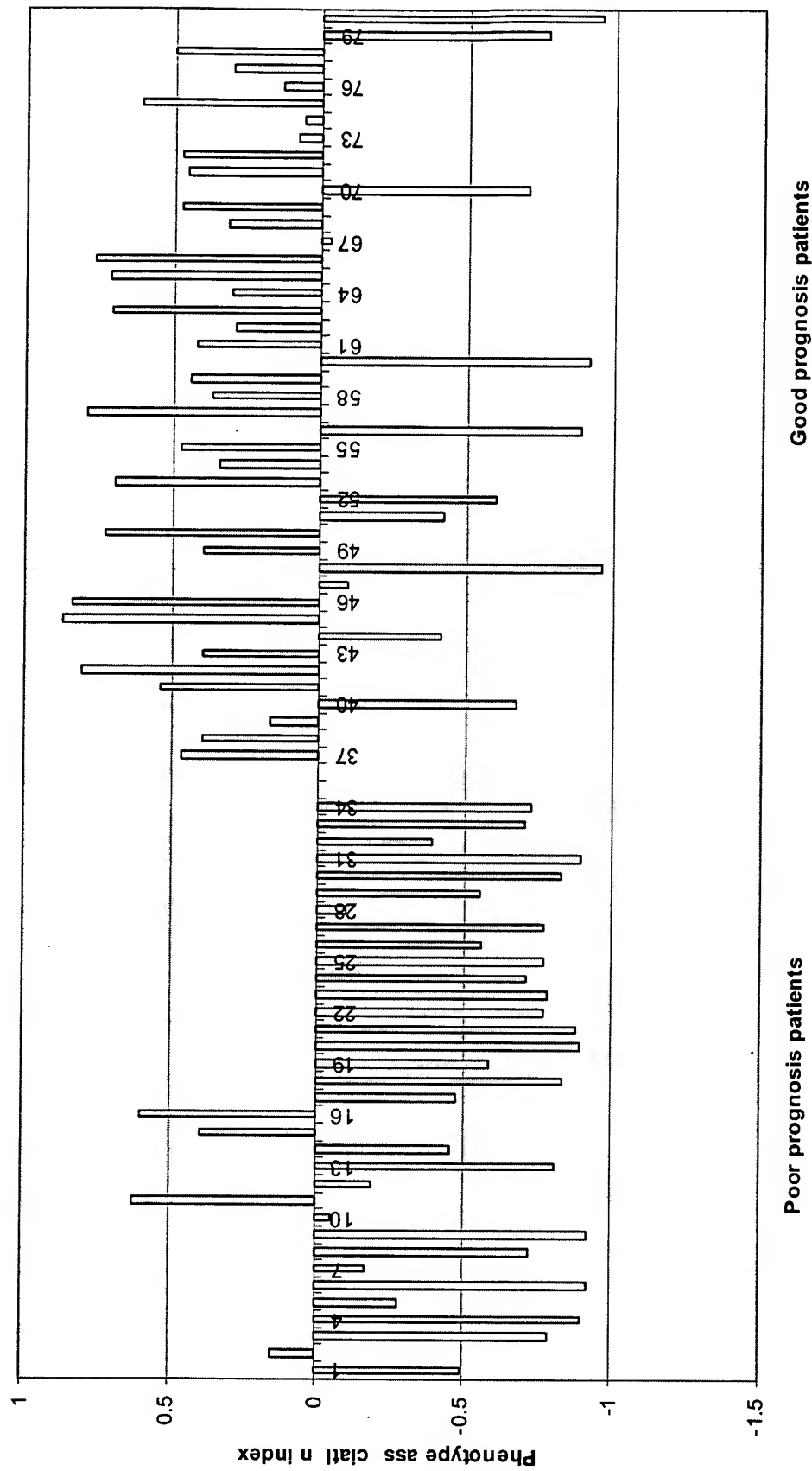


Figure 37. Phenotype association indices for 13 genes of the Q-PCR-based good prognosis predictor class in 11 breast cancer patients who developed distant metastases within 5 years of diagnosis and 8 patients who continued to be disease-free

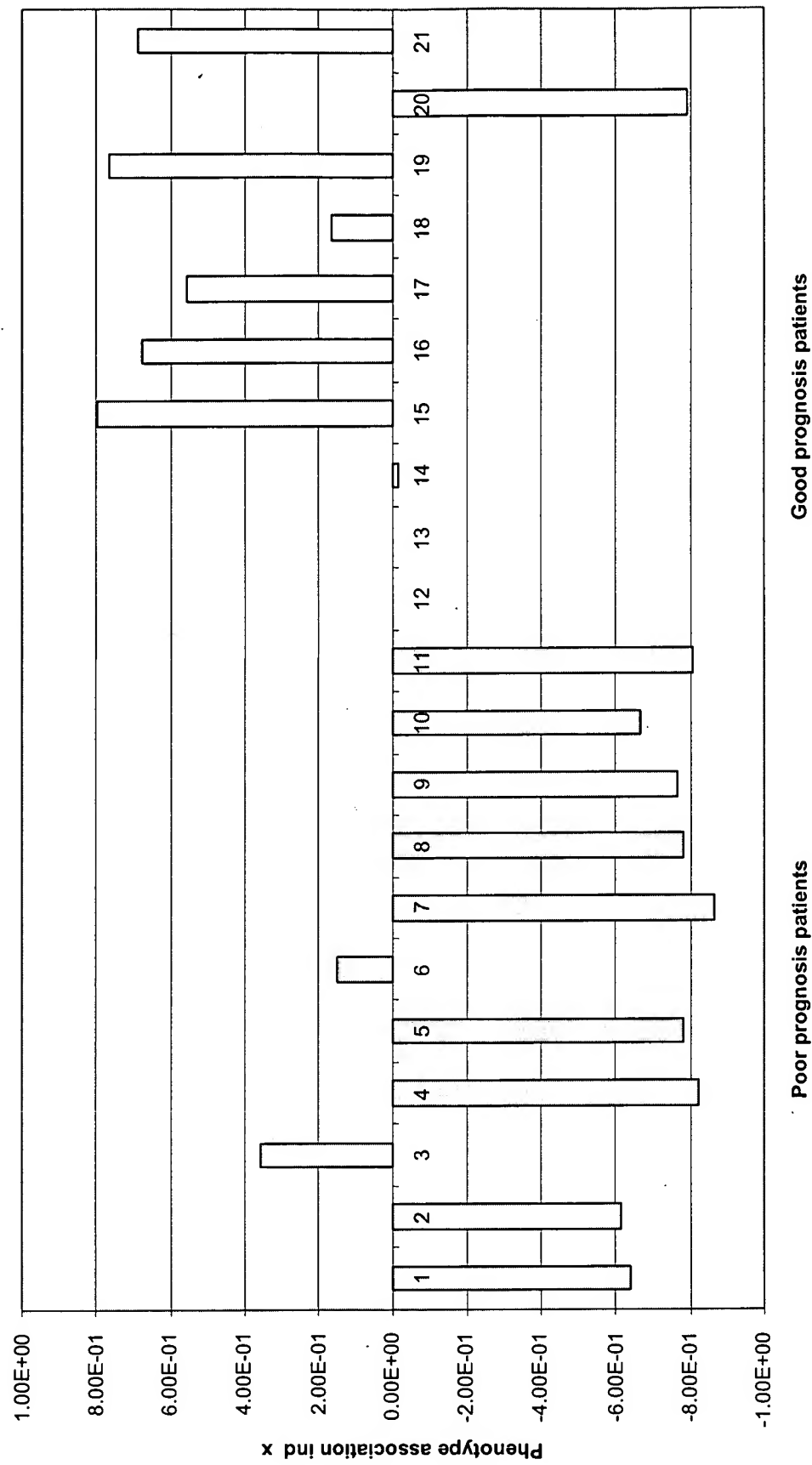


Figure 38. Phenotype association indices for 11 genes of the ovarian cancer poor prognosis predictor class in 11 tumors of well and moderate differentiation and 3 tumors of poor differentiation

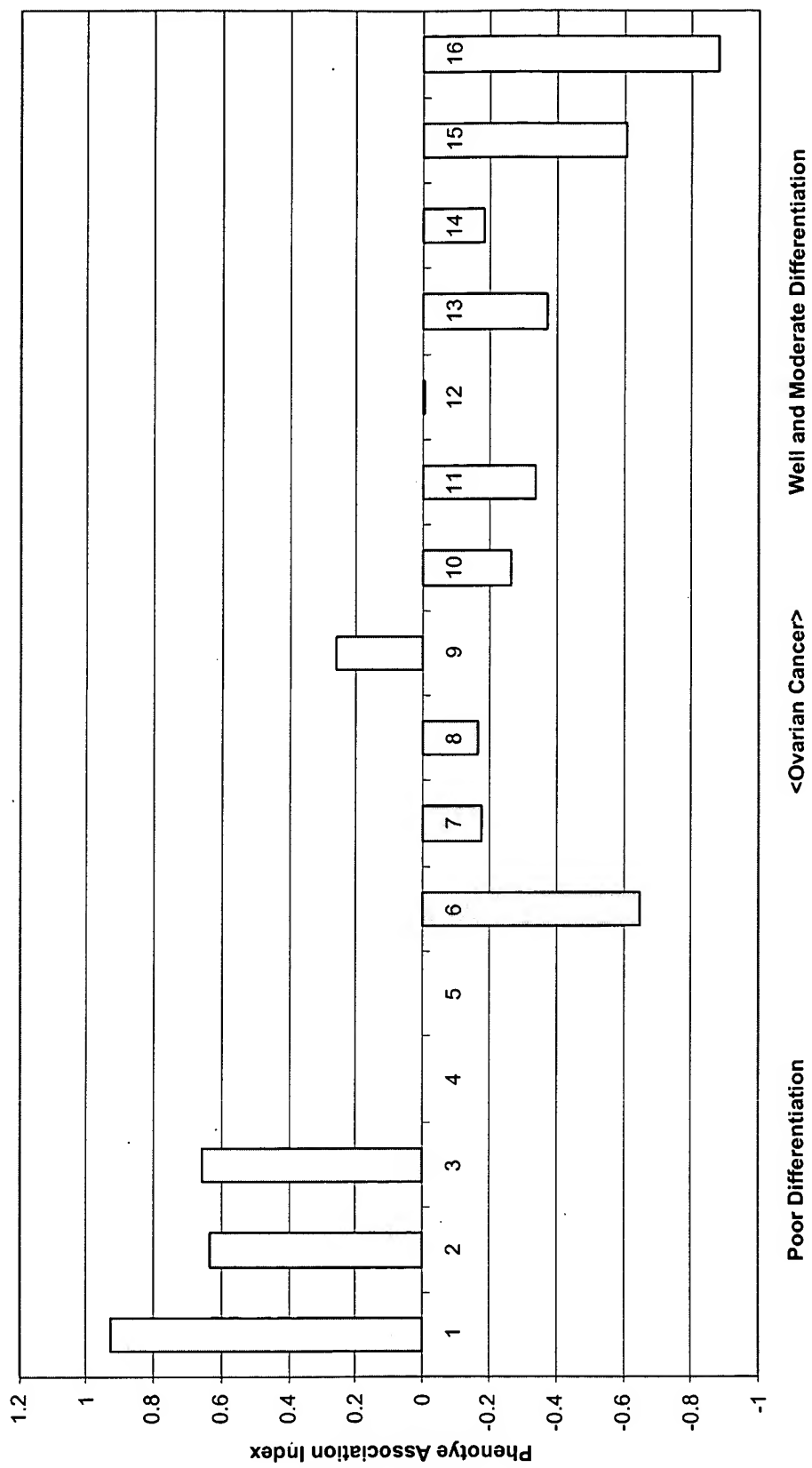


Figure 39. Phenotype association indices for 10 genes of the ovarian cancer good prognosis predictor class in 11 tumors of well and moderate differentiation and 3 tumors of poor differentiation

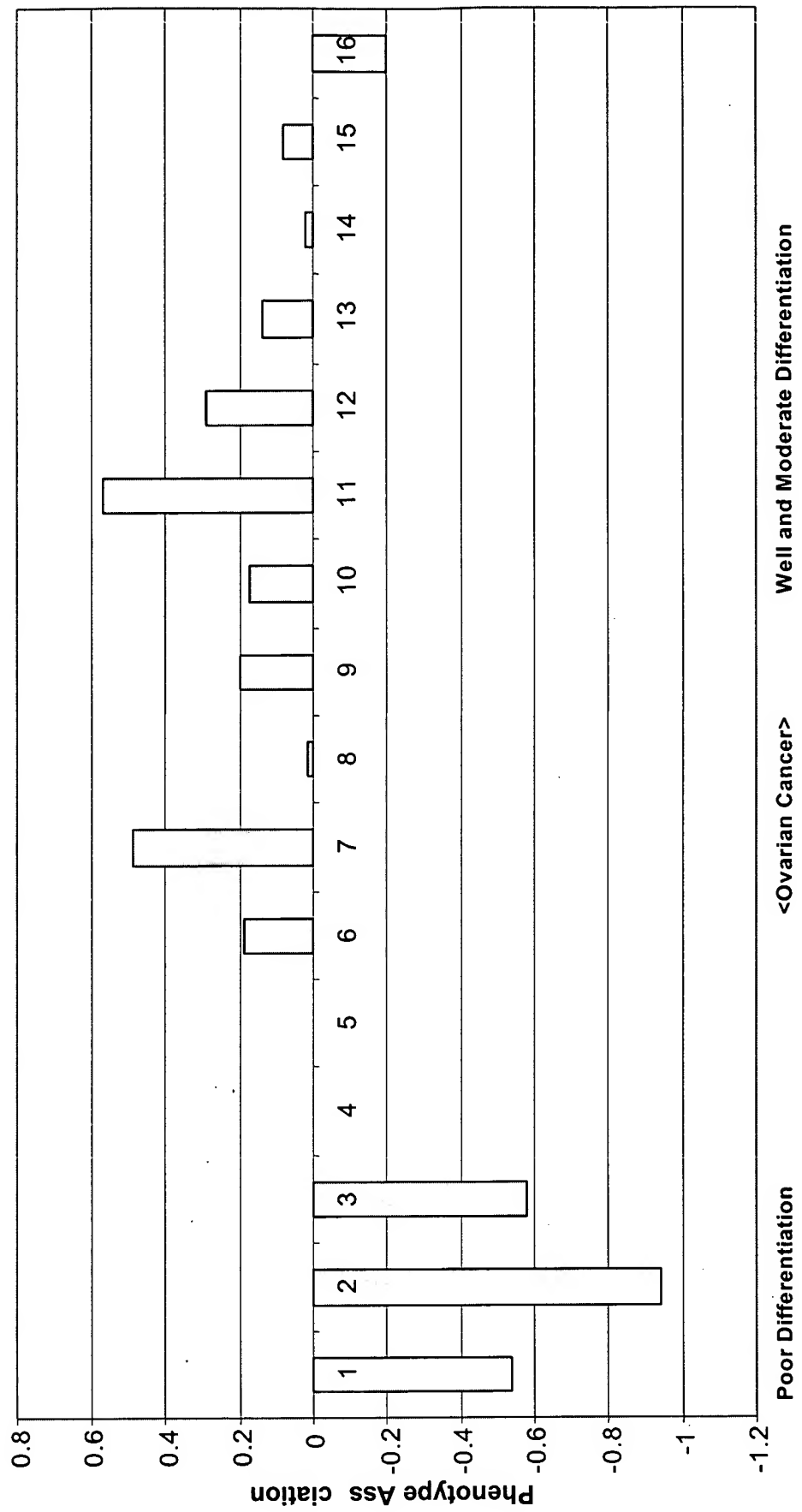


Figure 40. Correlation of the expression profiles in NSCLC cell lines versus normal bronchial epithelial cells and 139 adenocarcinoma samples versus 17 normal lung specimens for 13 genes of the human lung adenocarcinoma minimum segregation cluster 1

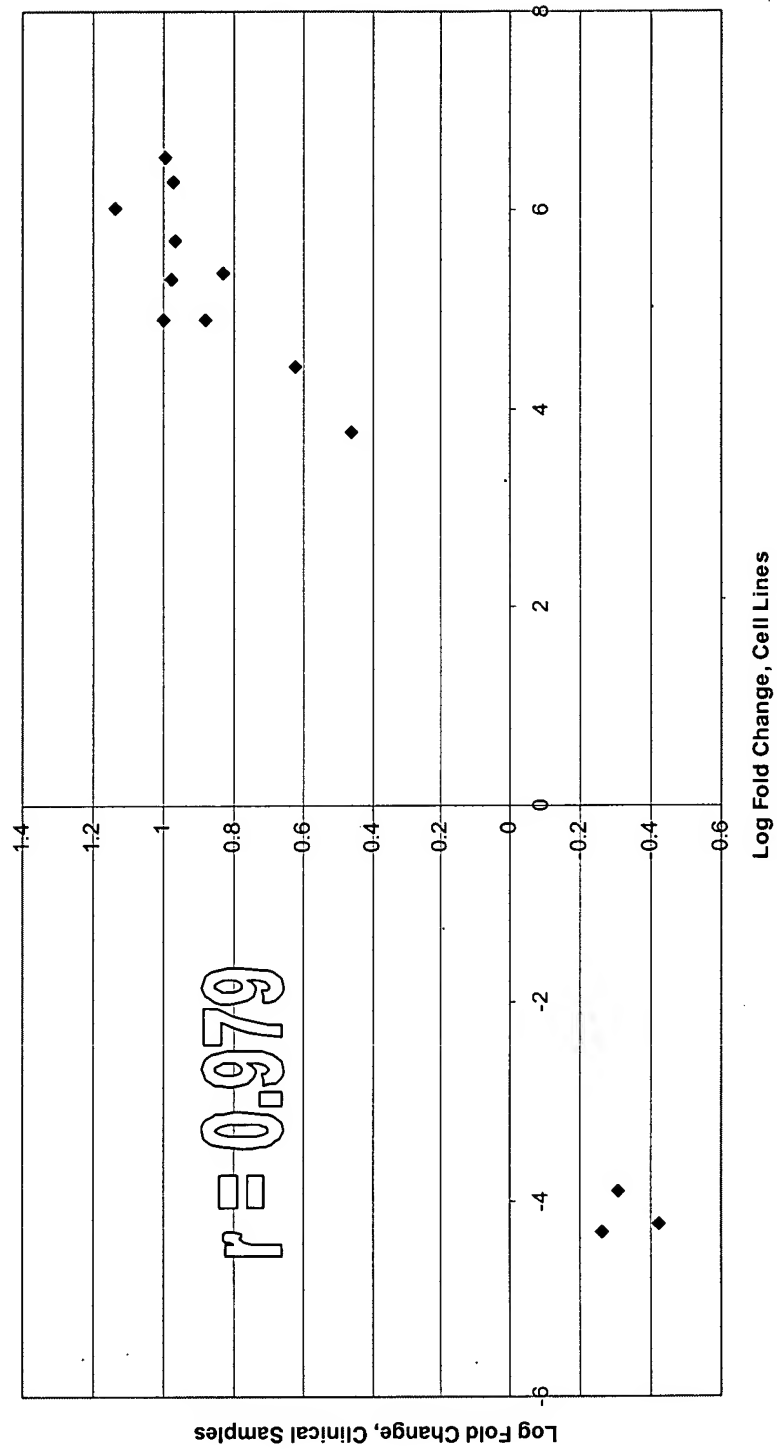


Figure 41. Correlation of the expression profiles in NSCLC cell lines versus normal bronchial epithelial cells and 139 adenocarcinoma samples versus 17 normal lung specimens for 26 genes of the human lung adenocarcinoma minimum segregation cluster 2

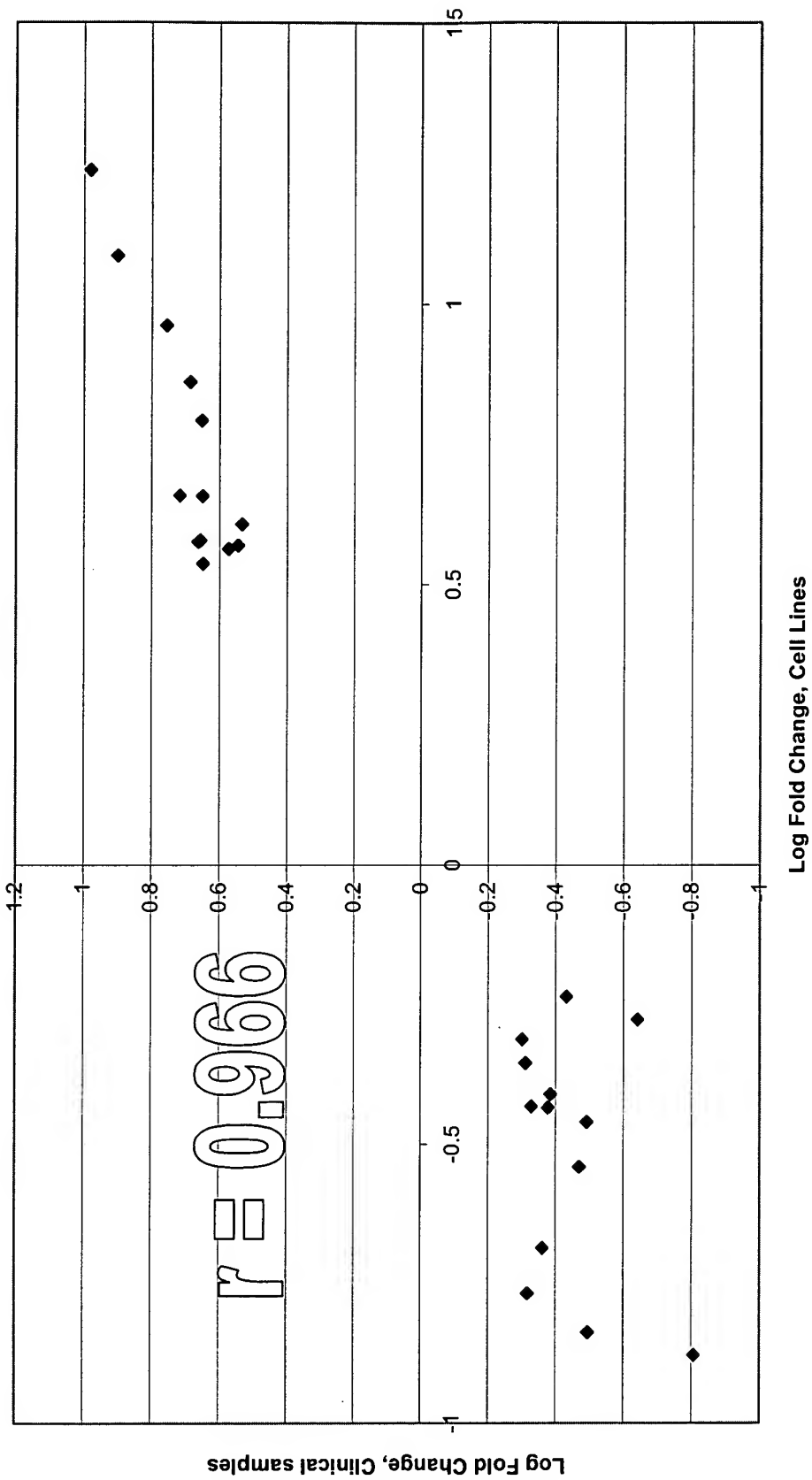


Figure 42. Phenotype association indices for 13 genes of the lung adenocarcinoma cluster 1 in 17 normal lung specimens and 139 lung adenocarcinoma samples

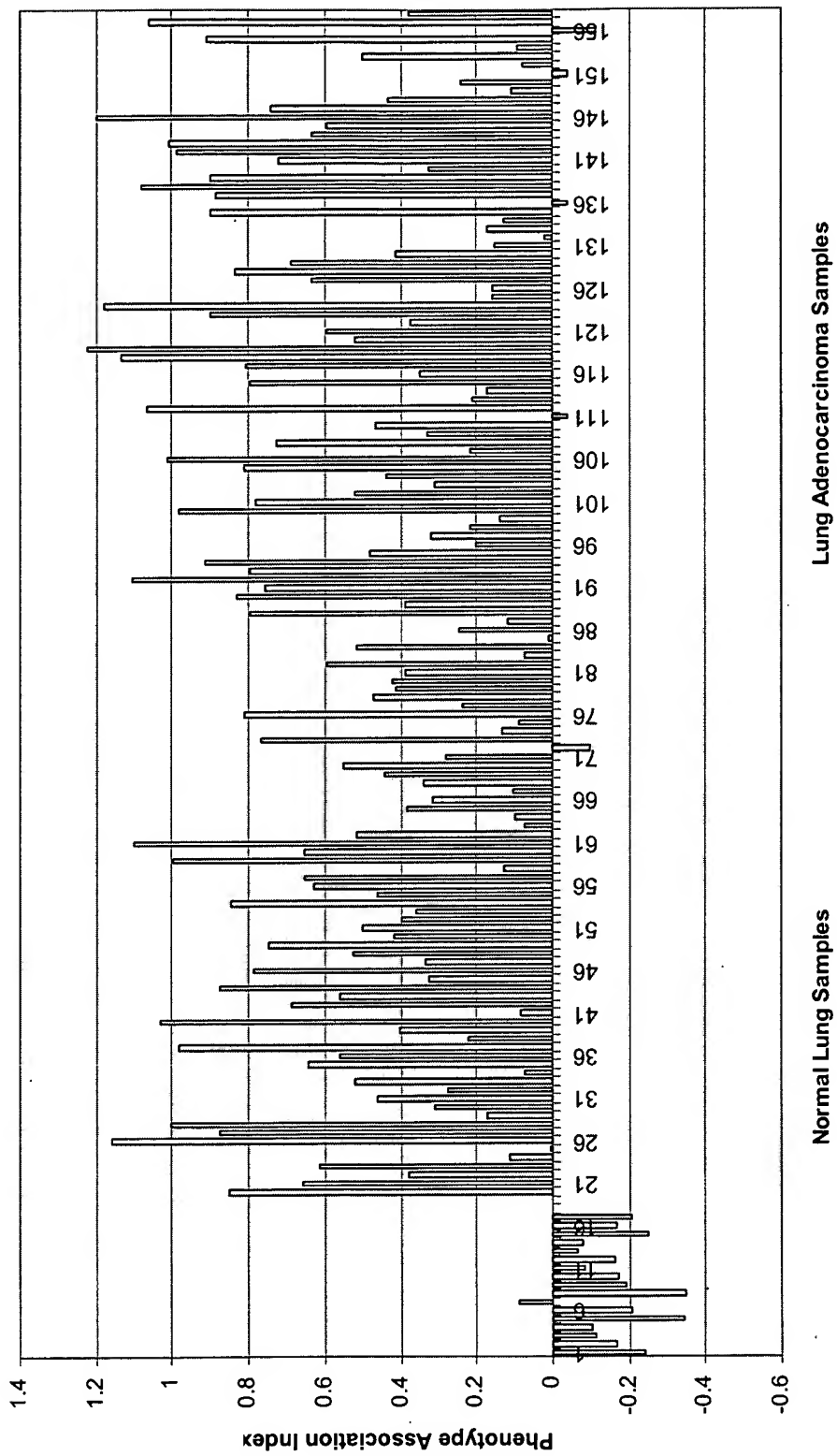


Figure 43. Phenotype association indices for 26 genes of the lung adenocarcinoma cluster 2 in 17 normal lung specimens and 139 lung adenocarcinoma samples

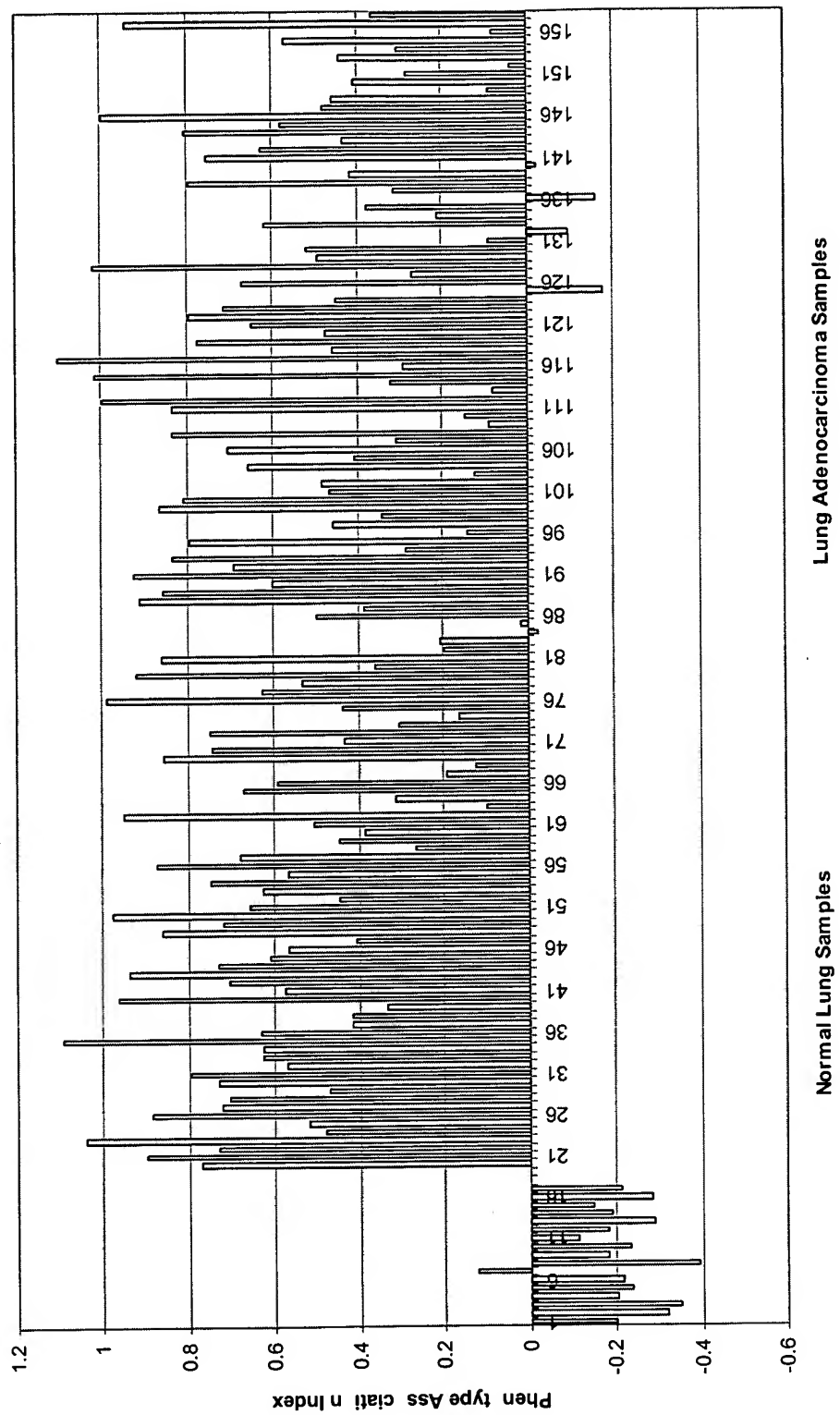


Figure 44. Correlation of the expression profiles in NSCLC cell lines versus normal bronchial epithelial cells and 34 NSCLC patients with poor prognosis versus 16 patients with good prognosis for 38 genes of lung adenocarcinoma poor prognosis cluster 1

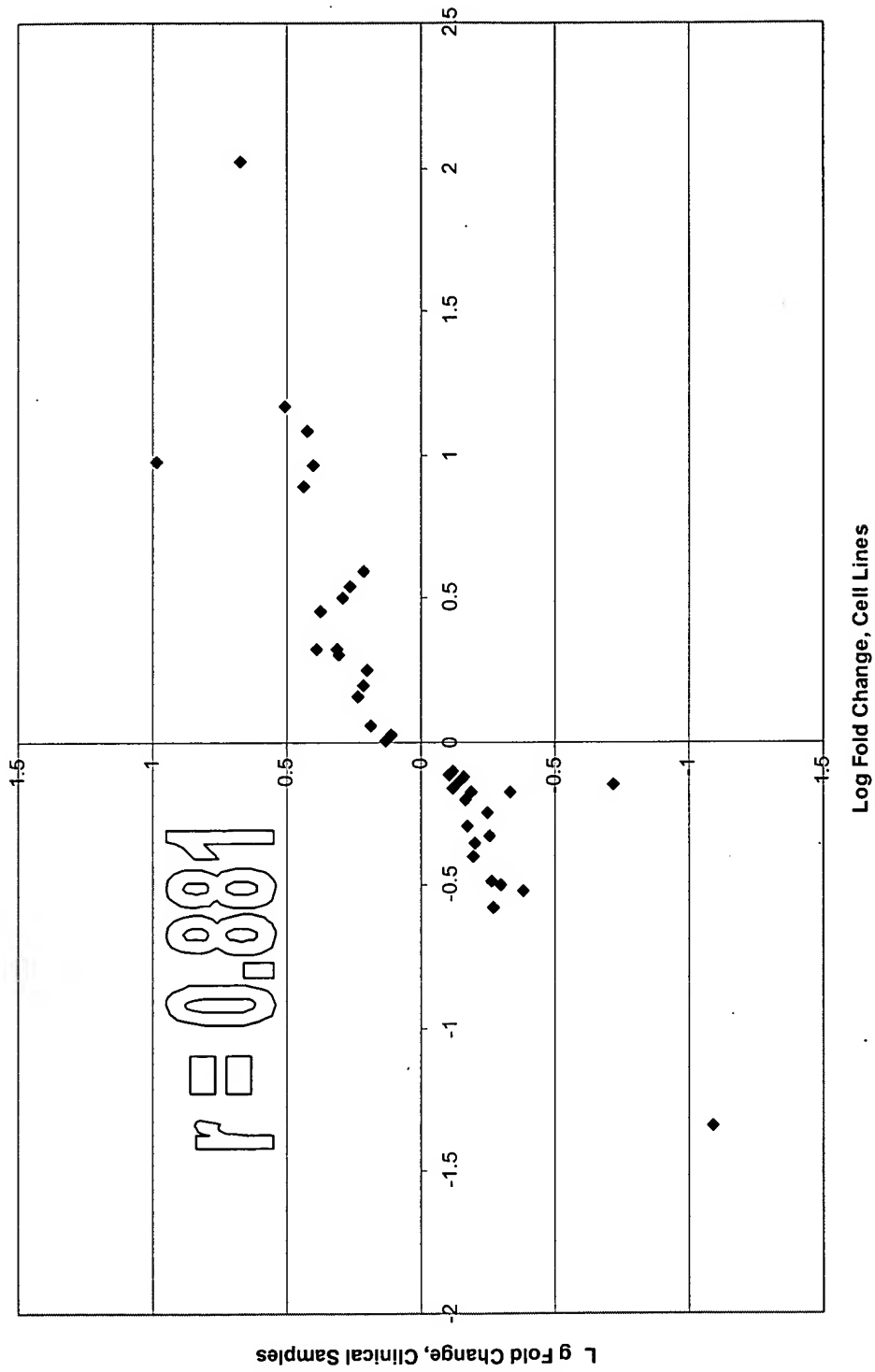
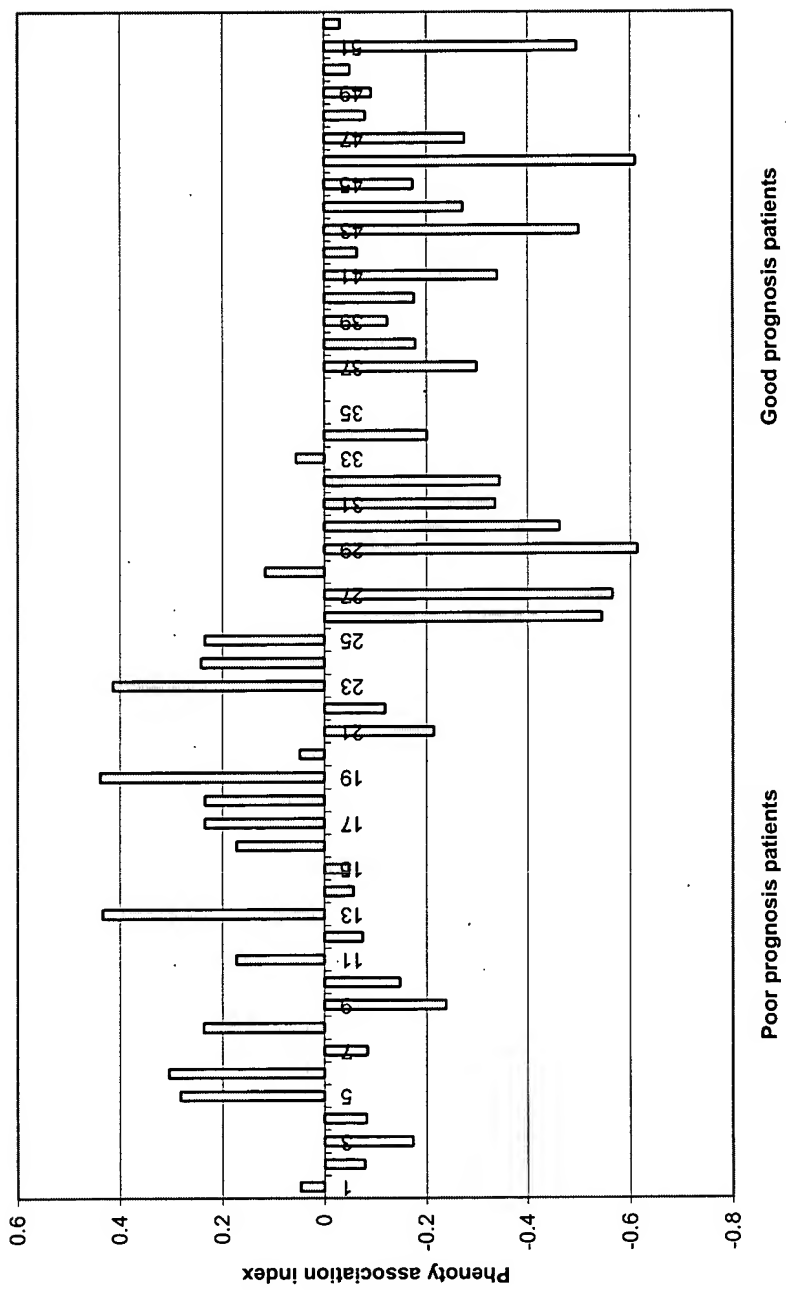
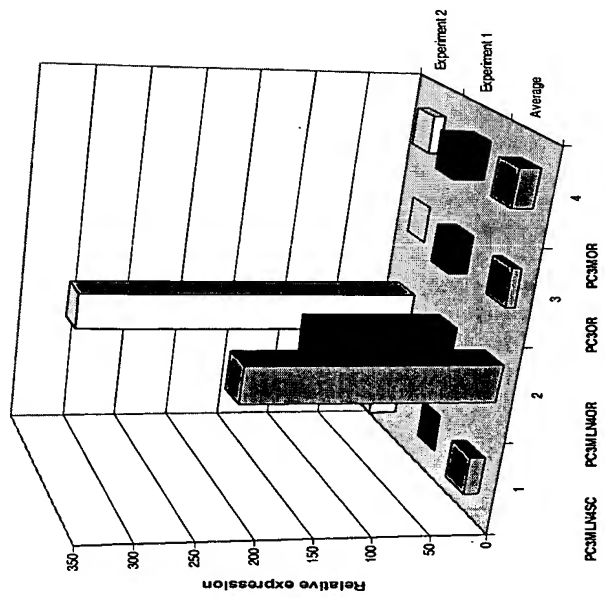


Figure 45. Phenotype association indices for 38 genes of the lung adenocarcinoma poor prognosis predictor cluster 1 in 34 NSCLC patients with poor prognosis and 16 patients with good prognosis

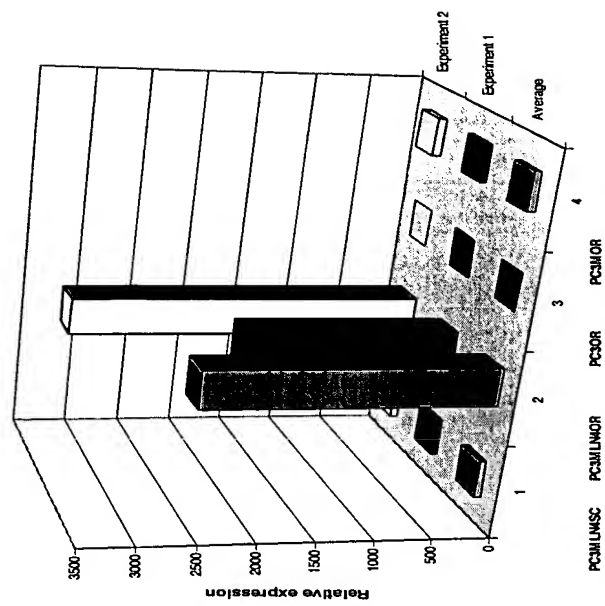


MMP9 expression in human prostate carcinoma xenografts



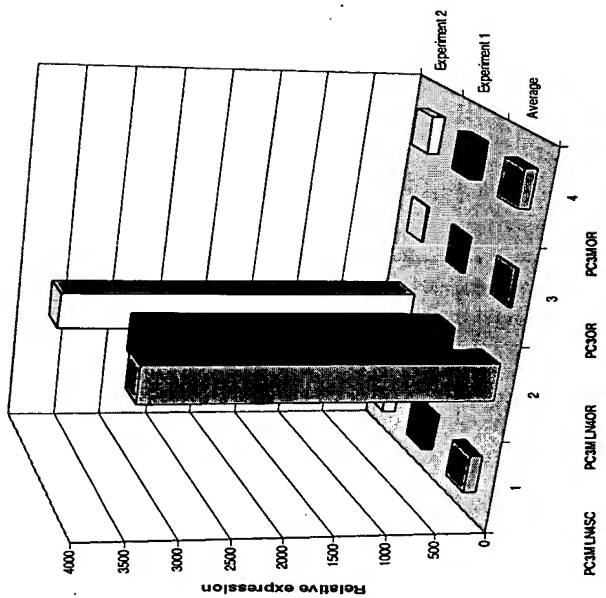
A1

MMP10 expression in human prostate carcinoma xenografts



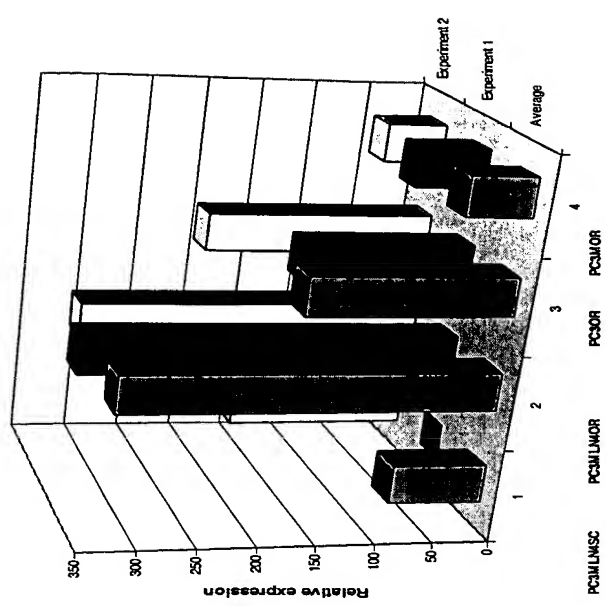
A2.

MMP1 expression in human prostate carcinoma xenografts



A3

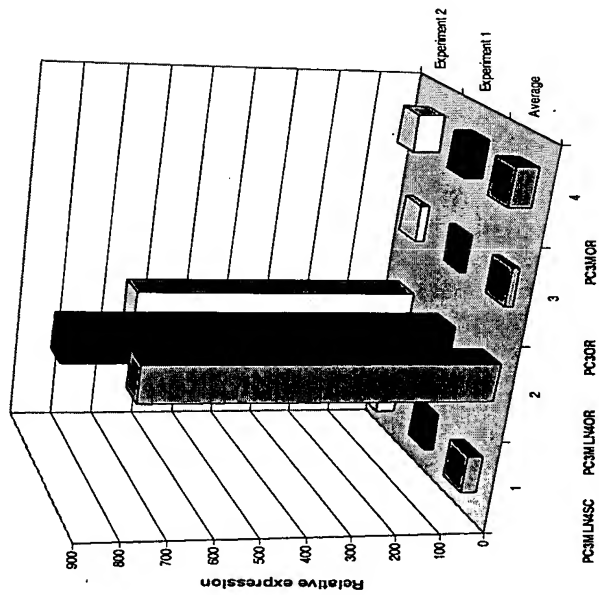
MMP14 expression in human prostate carcinoma xenografts



A4.

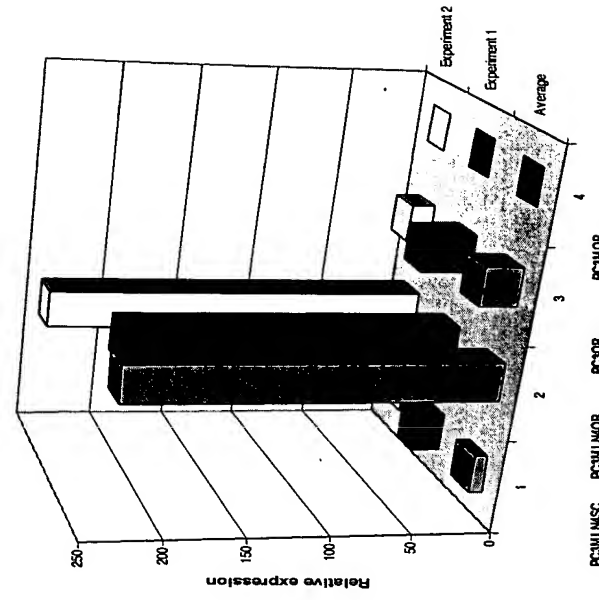
46

tPA expression in human prostate carcinoma xenografts



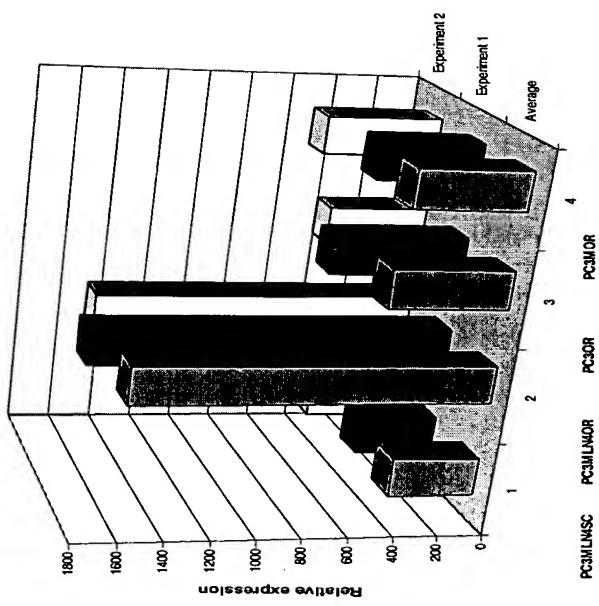
B1

uPA receptor expression in human prostate carcinoma xenografts



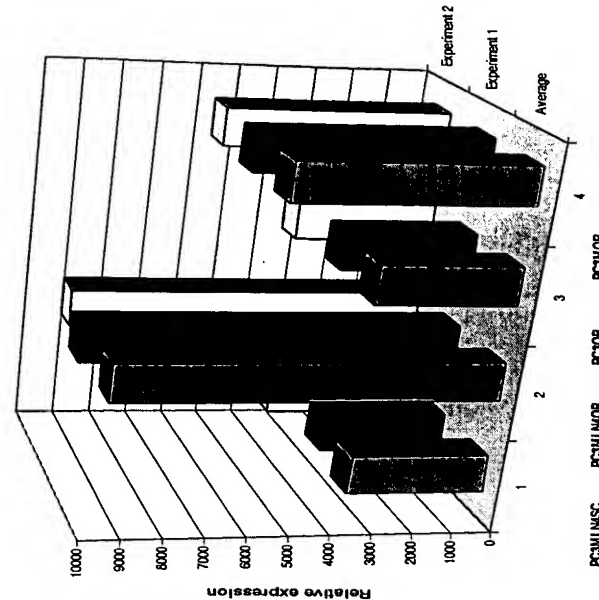
B2.

Plasminogen receptor expression in human prostate carcinoma xenografts



B3

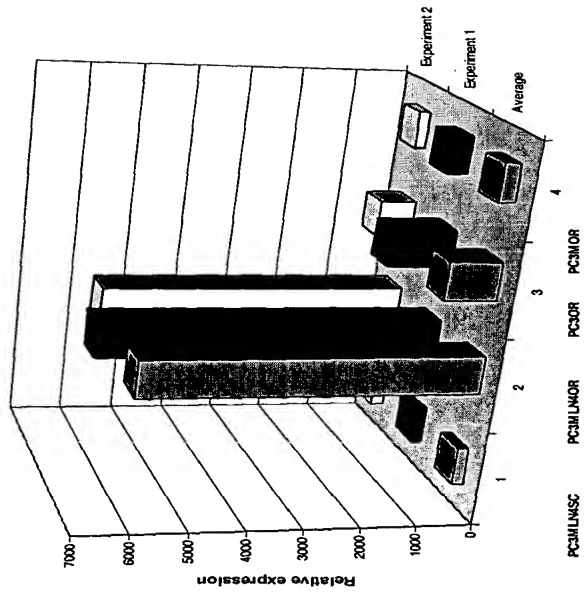
uPA expression in human prostate carcinoma xenografts



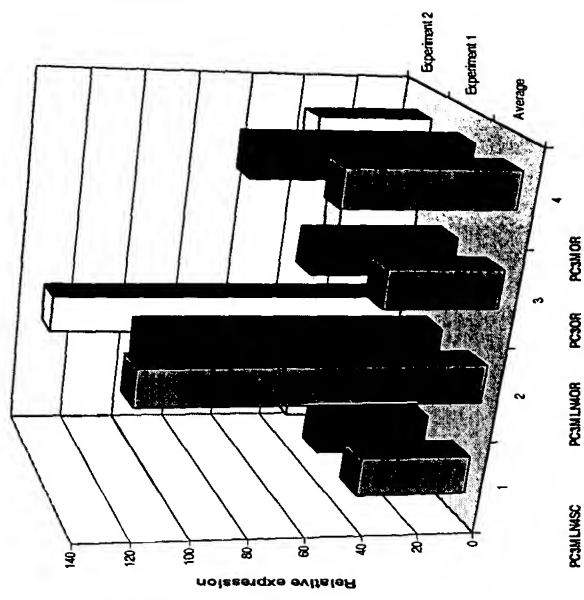
B4.

46

Interleukin 8 expression in human prostate carcinoma xenografts

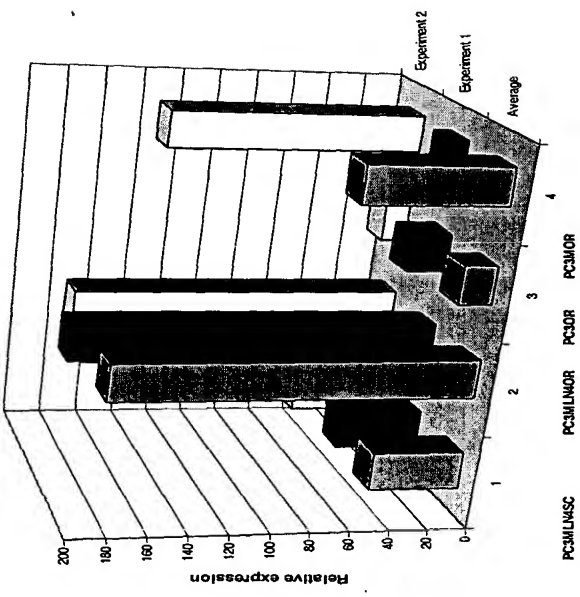


Angiopoietin-2 expression in human prostate carcinoma xenografts

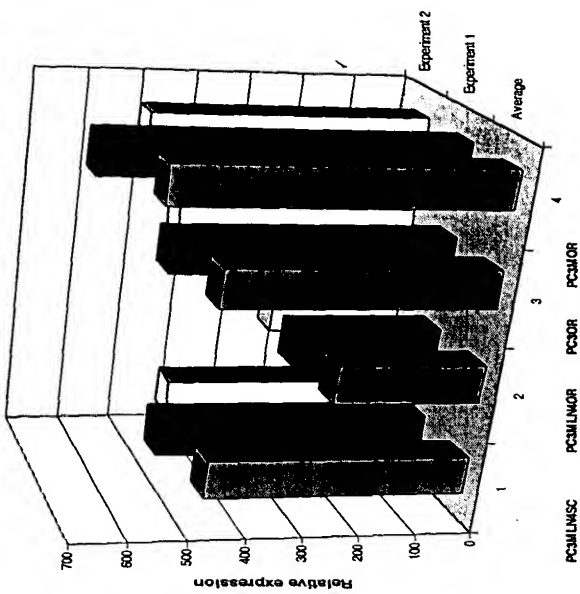


46

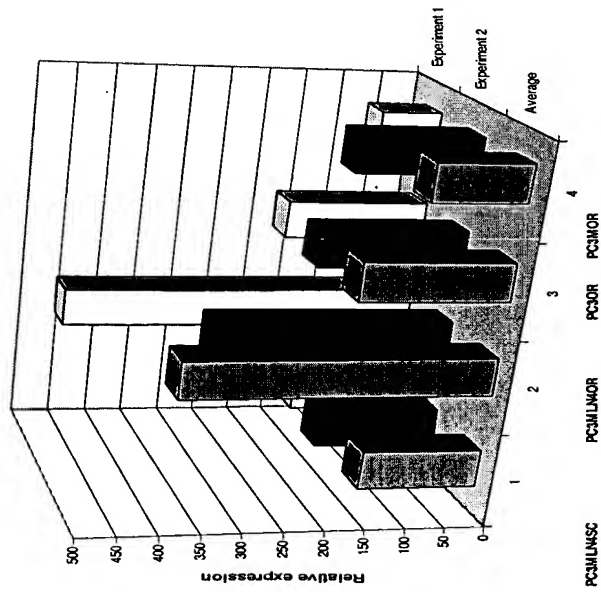
Osteopontin expression in human prostate carcinoma xenografts



Maspin expression in human prostate carcinoma xenografts

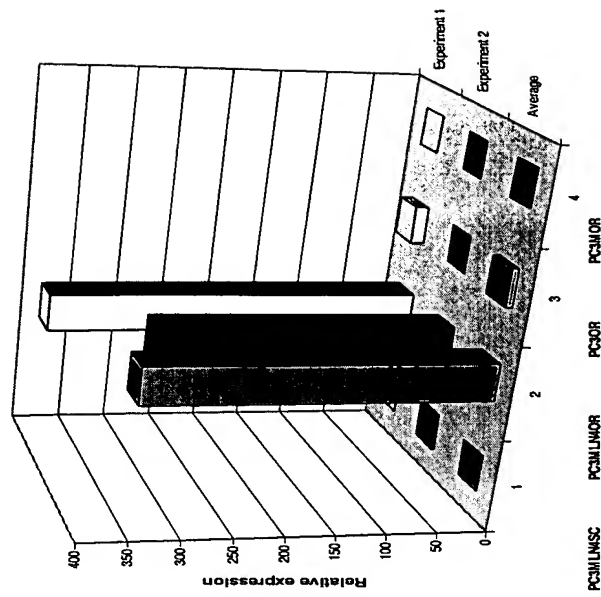


OB-cadherin-2 expression in human prostate carcinoma xenografts



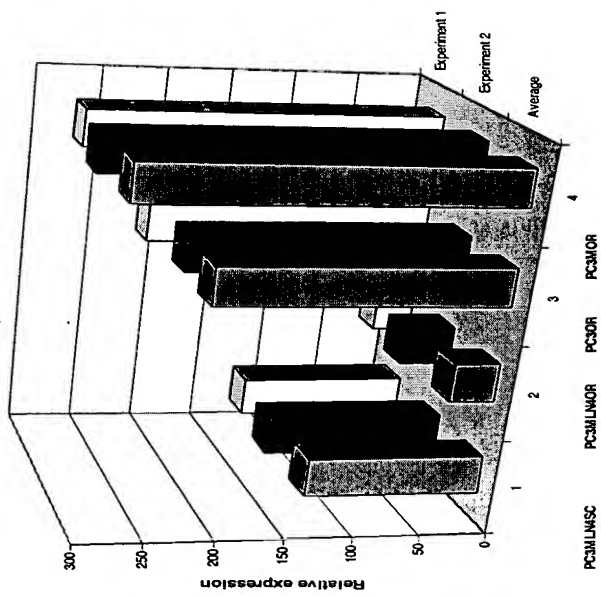
D1

VE-cadherin expression in human prostate carcinoma xenografts



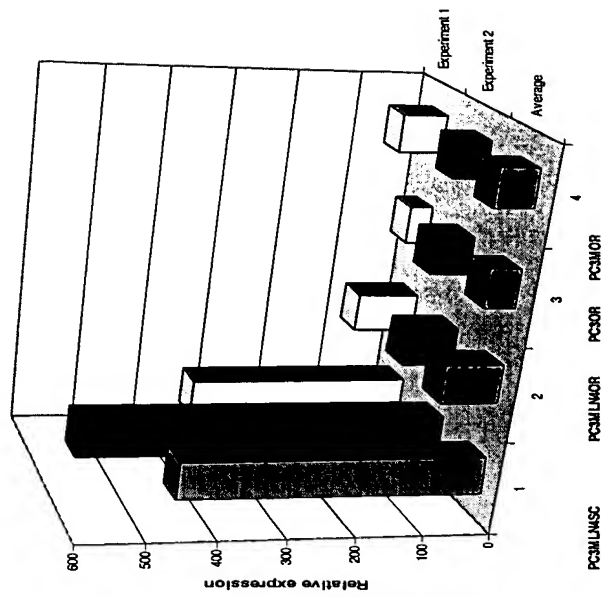
D2.

E-cadherin expression in human prostate carcinoma xenografts



D3.

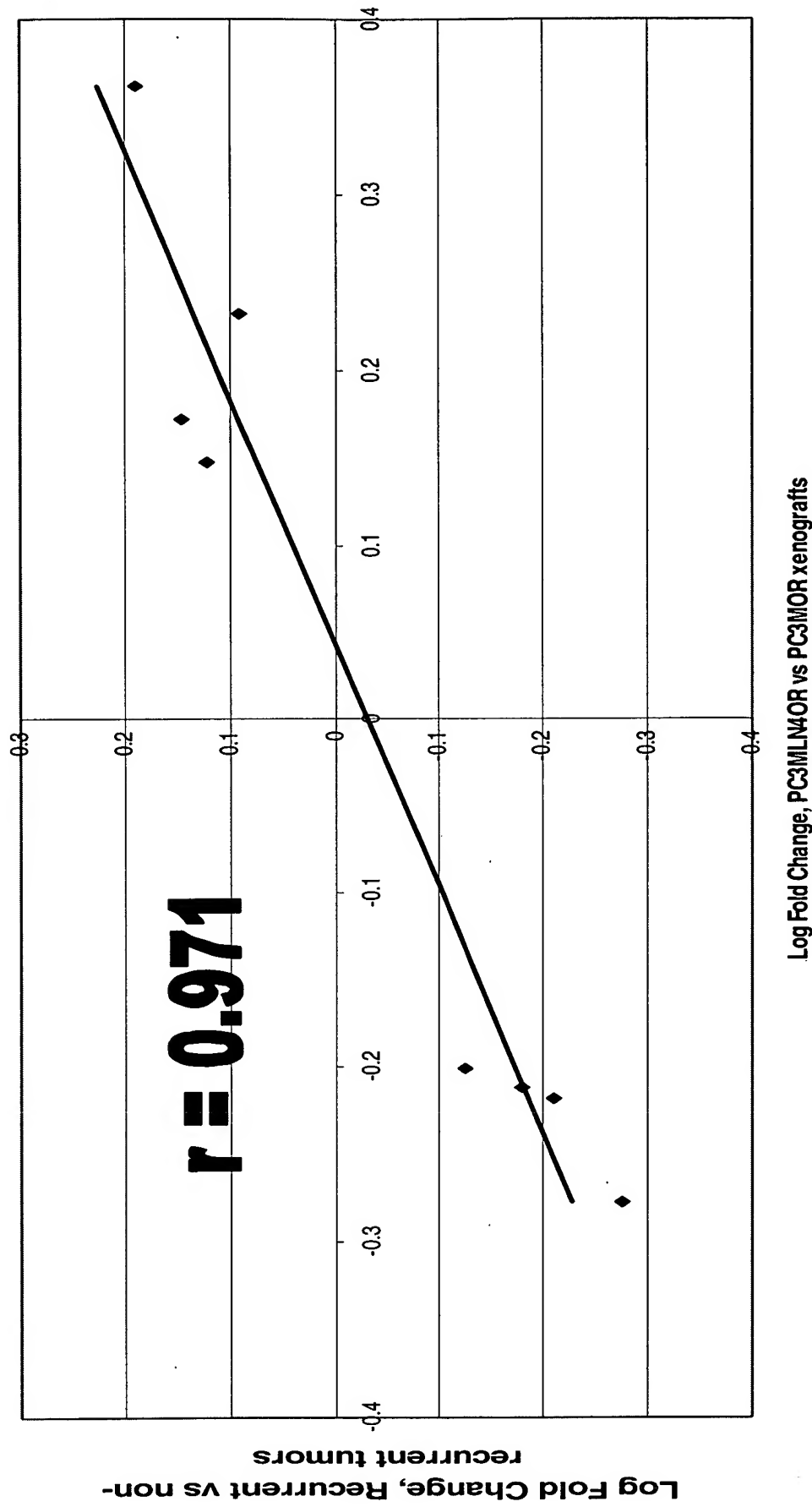
N-cadherin expression in human prostate carcinoma xenografts



D4.

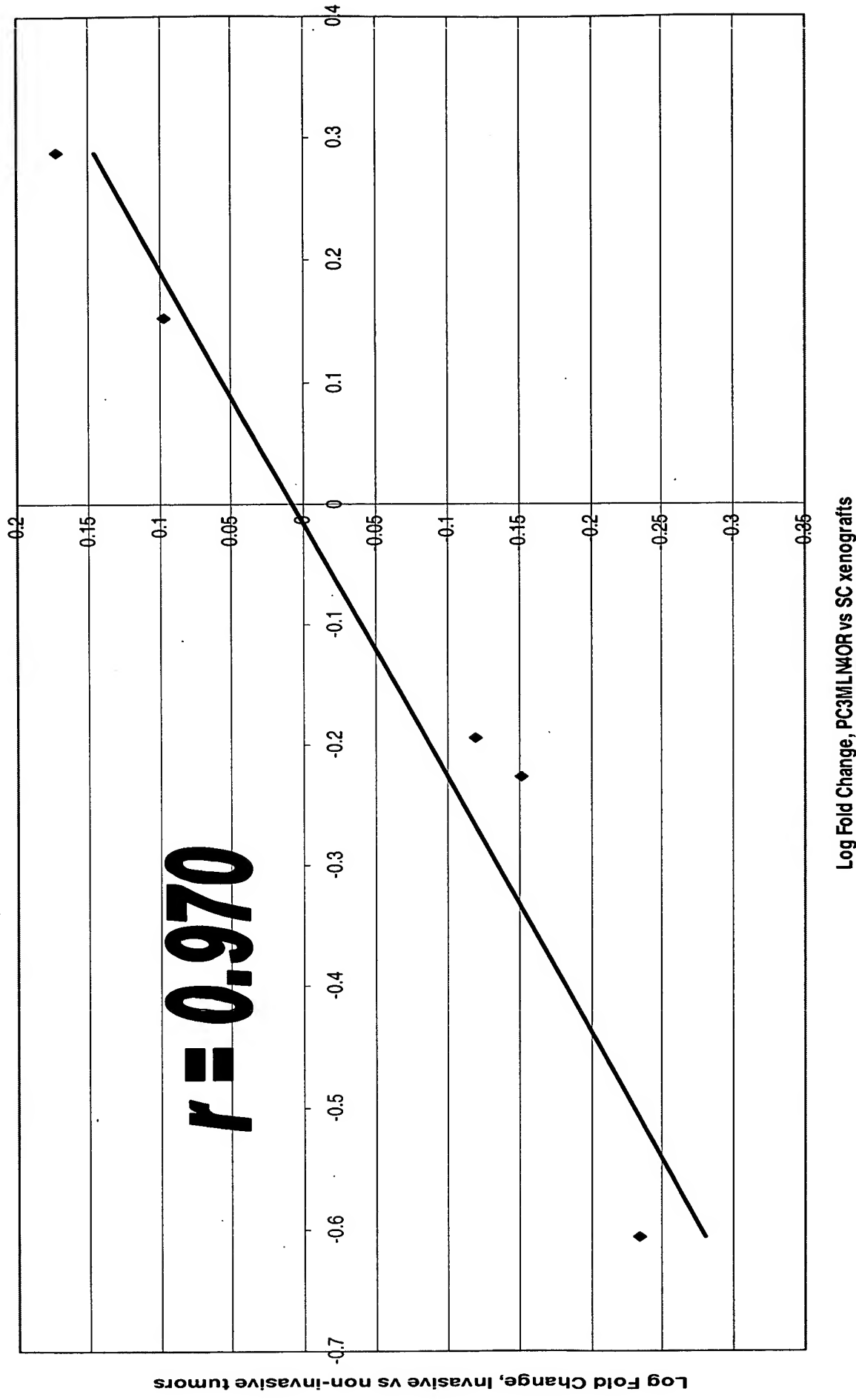
46

47A. Correlation of the expression profiles for 8 genes of the prostate cancer recurrence predictor class in orthotopic xenografts and 8 recurrent versus 13 non-recurrent human prostate tumors

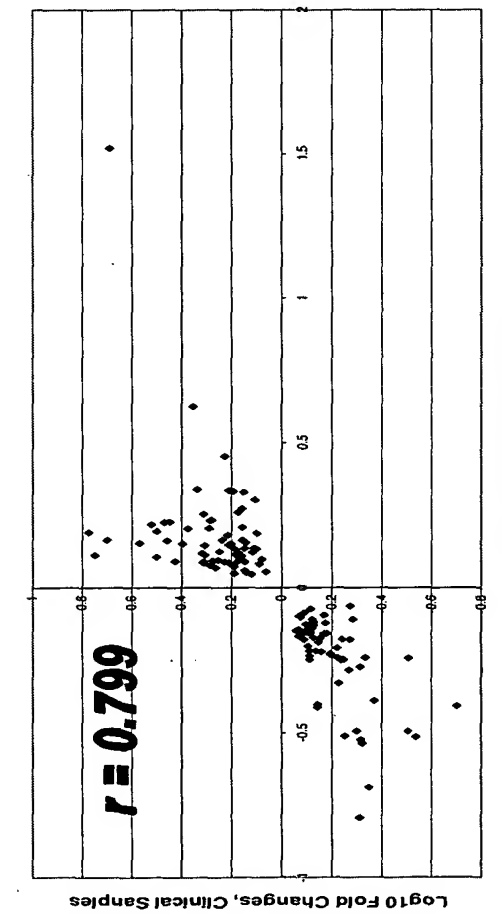


47B.

Correlation of the expression profiles for 5 genes of the prostate cancer invasion predictor cluster in orthotopic xenografts and 26 invasive versus 26 non-invasive human prostate tumors



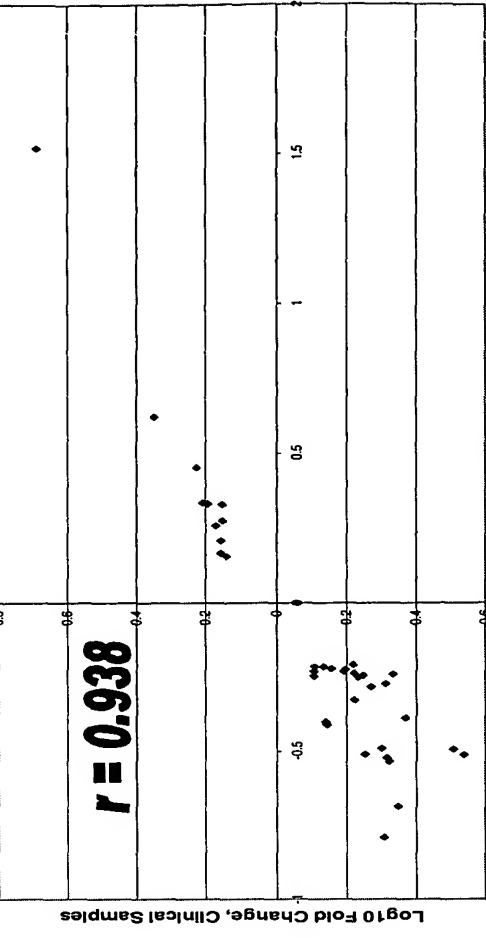
48A. Correlation of the expression profiles for 131 transcripts of the prostate cancer metastasis segregation cluster in PC-3MLN4 orthotopic versus s.c. xenografts and metastatic versus primary human prostate tumors



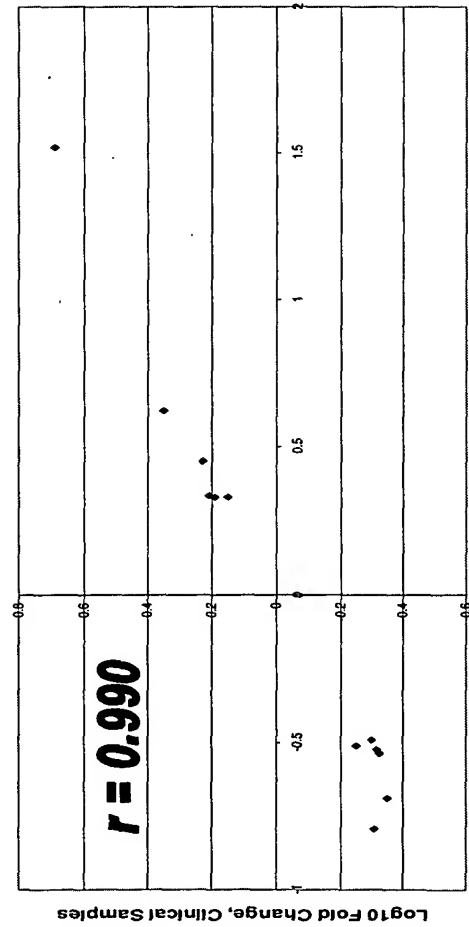
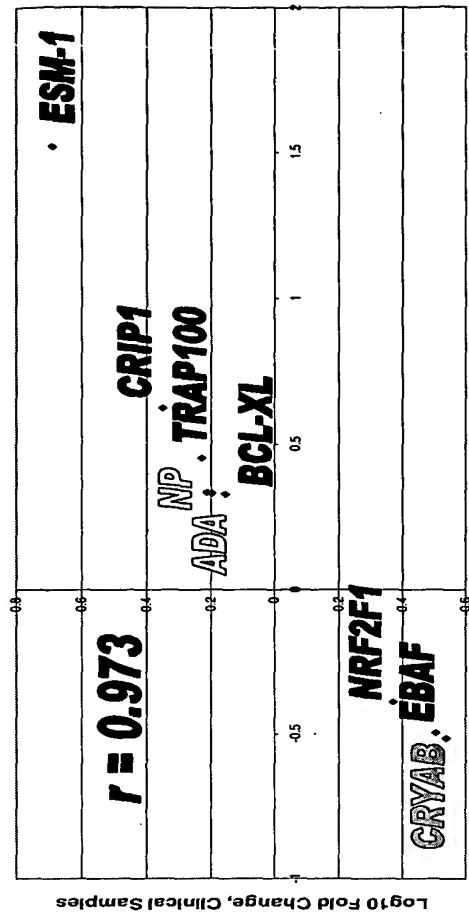
48C. Correlation of the expression profiles for 12 transcripts of the prostate cancer metastasis segregation cluster in PC-3MLN4 orthotopic versus s.c. xenografts and metastatic versus primary human prostate tumors

Log10 Fold Changes, Xenografts

48B. Correlation of the expression profiles for 37 transcripts of the prostate cancer metastasis segregation cluster in PC-3MLN4 orthotopic versus s.c. xenografts and metastatic versus primary human prostate tumors

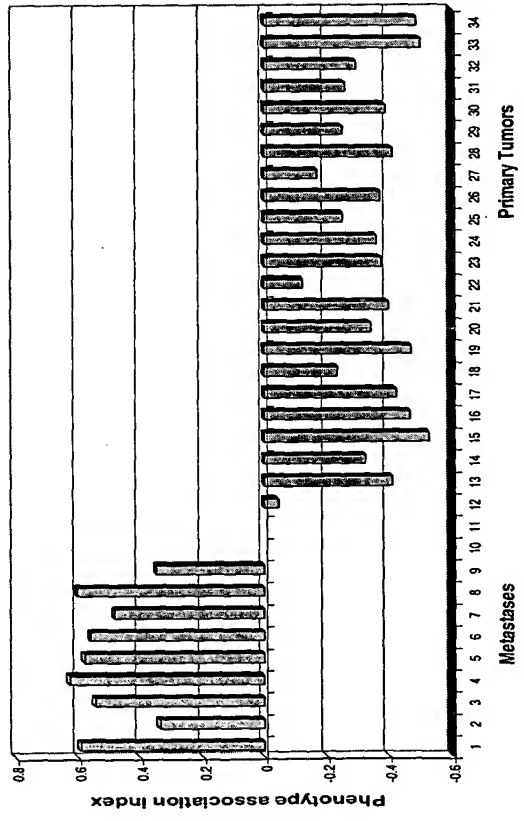


48D. Correlation of the expression profiles for 9 transcripts of the prostate cancer metastasis segregation cluster in PC-3MLN4 orthotopic versus s.c. xenografts and metastatic versus primary human prostate tumors

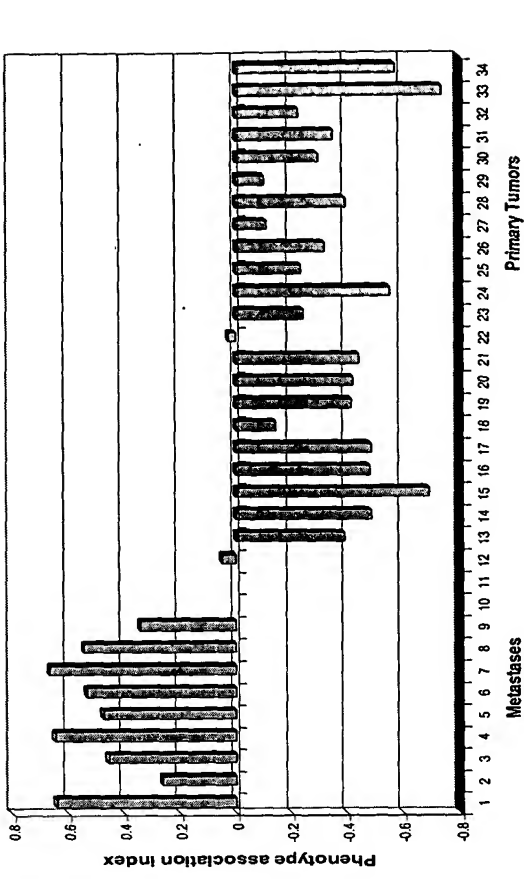


Log10 Fold Changes, Xenografts

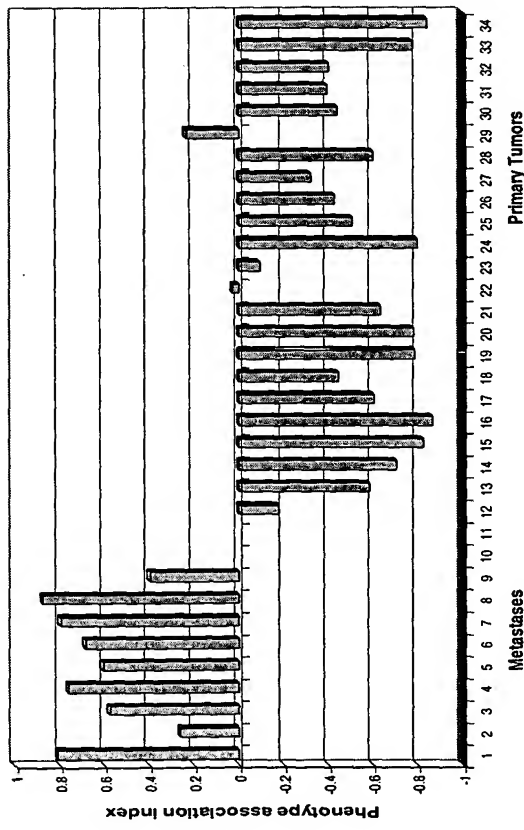
49A. Phenotype association indices of the 131 gene signature of the human prostate cancer metastasis in 9 metastatic and 23 primary human prostate tumors



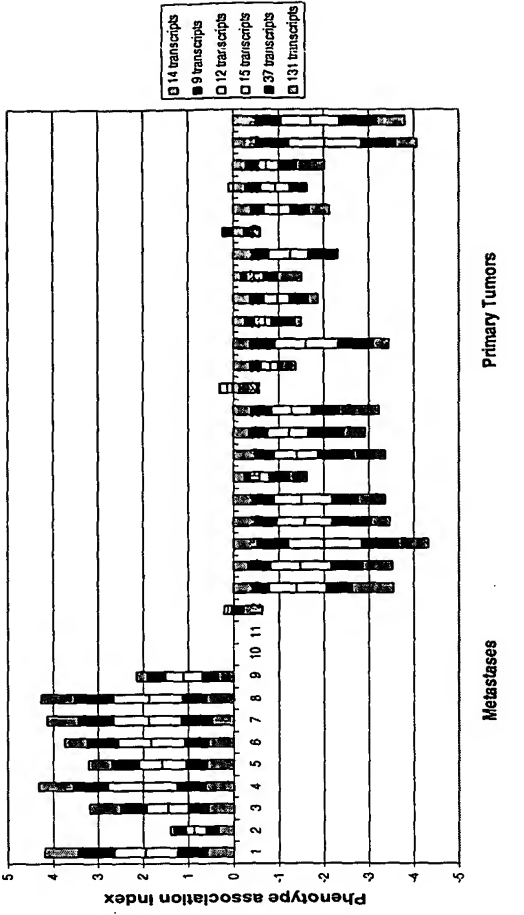
49B. Phenotype association indices of the 37 gene signature of the human prostate cancer metastasis in 9 metastatic and 23 primary human prostate tumors



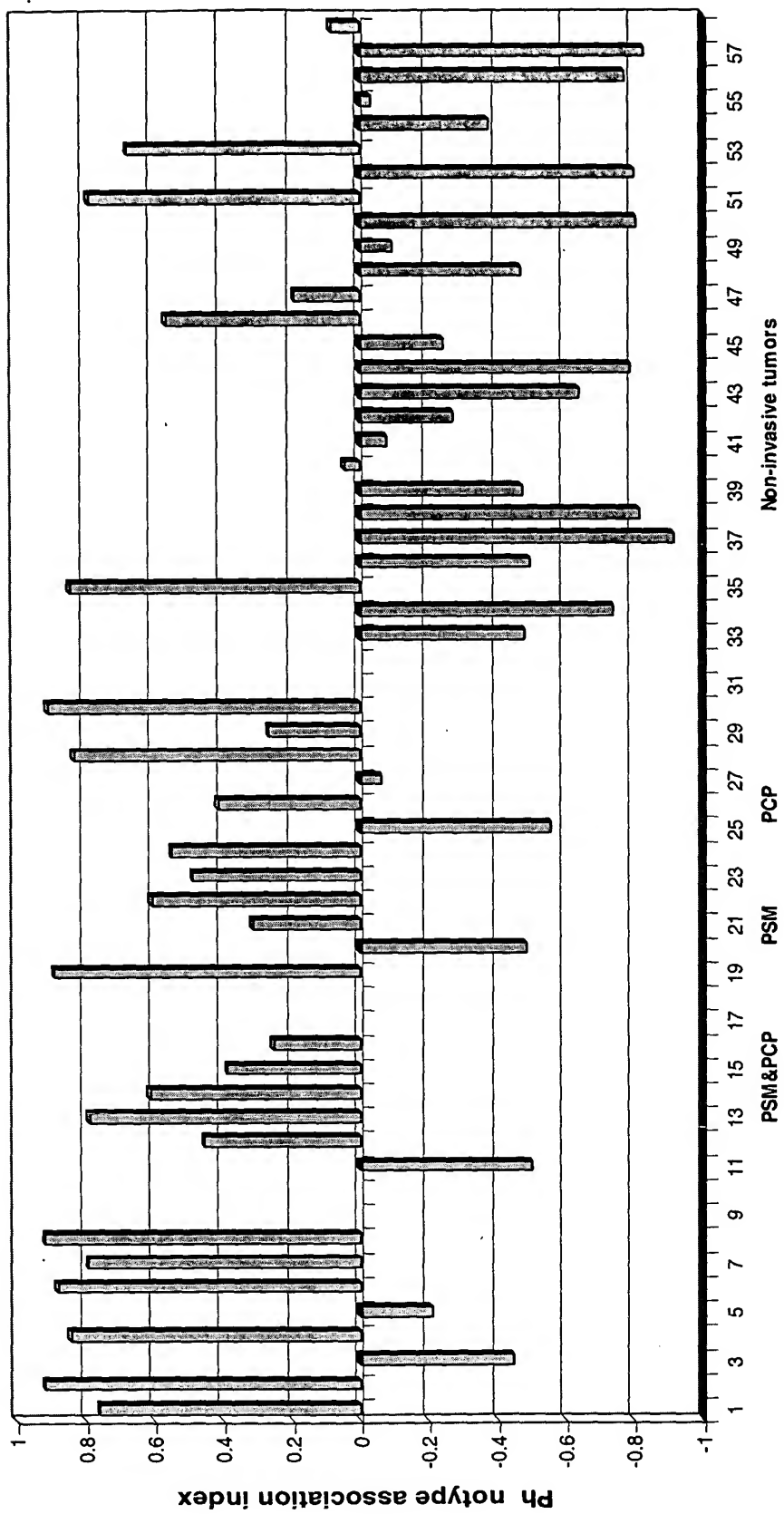
49C. Phenotype association indices of the 9 gene signature of the human prostate cancer metastasis in 9 metastatic and 23 primary human prostate tumors



49D. Phenotype association indices for transcripts of 6 prostate cancer metastasis signature gene clusters in 9 metastatic and 23 primary human prostate tumors



50A. Phenotype association indices for transcripts of the 5 genes prostate cancer invasion predictor cluster in 26 invasive and 26 non-invasive human prostate tumors



50B. Phenotype association indices for transcripts of the 8 genes prostate cancer recurrence predictor cluster in 8 recurrent and 13 non-recurrent human prostate tumors

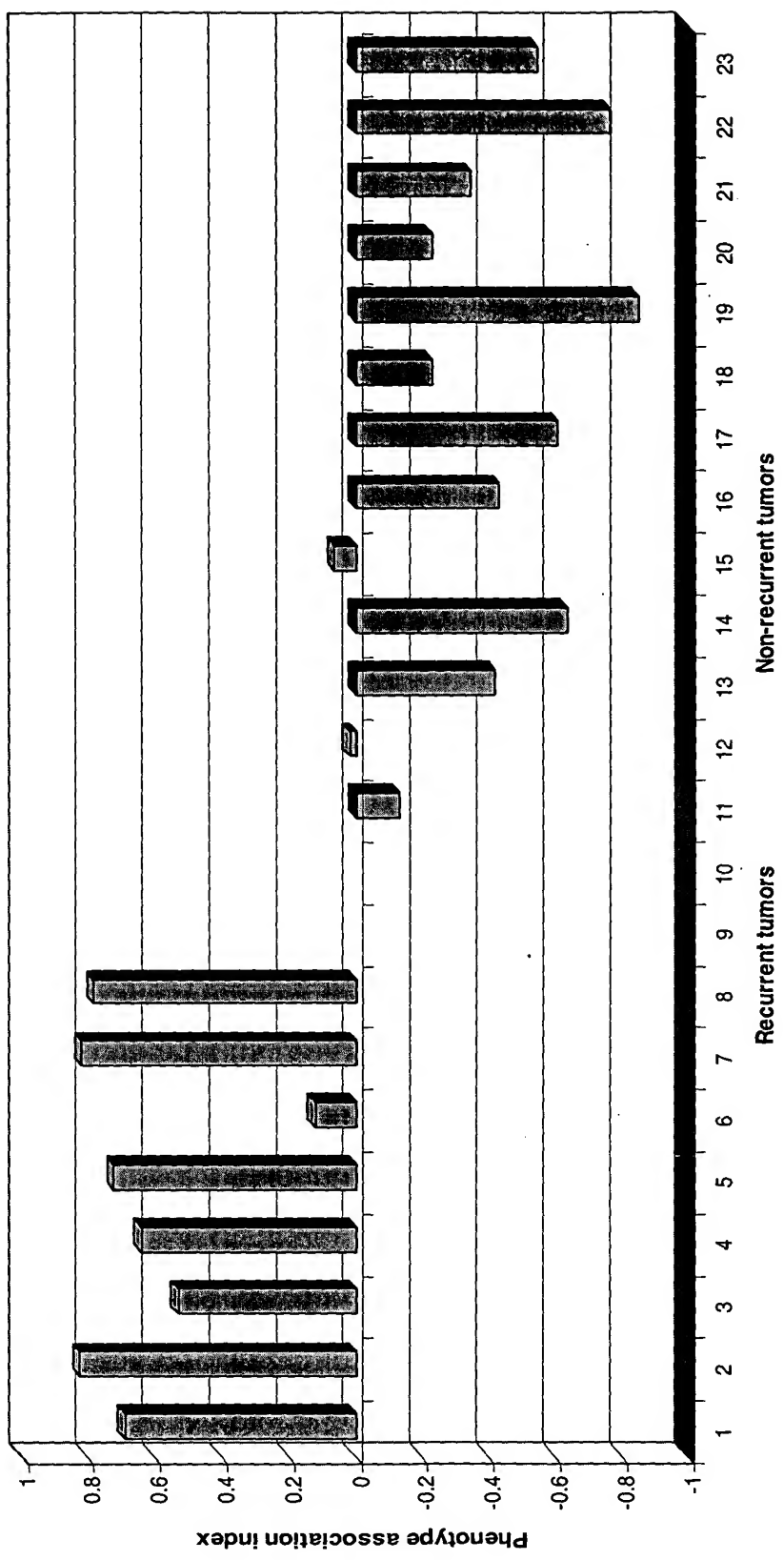


Figure 51A. Expression profiles of the 8 gene recurrence predictor signature in PC3MLN4 orthotopic xenografts and recurrent human prostate tumors

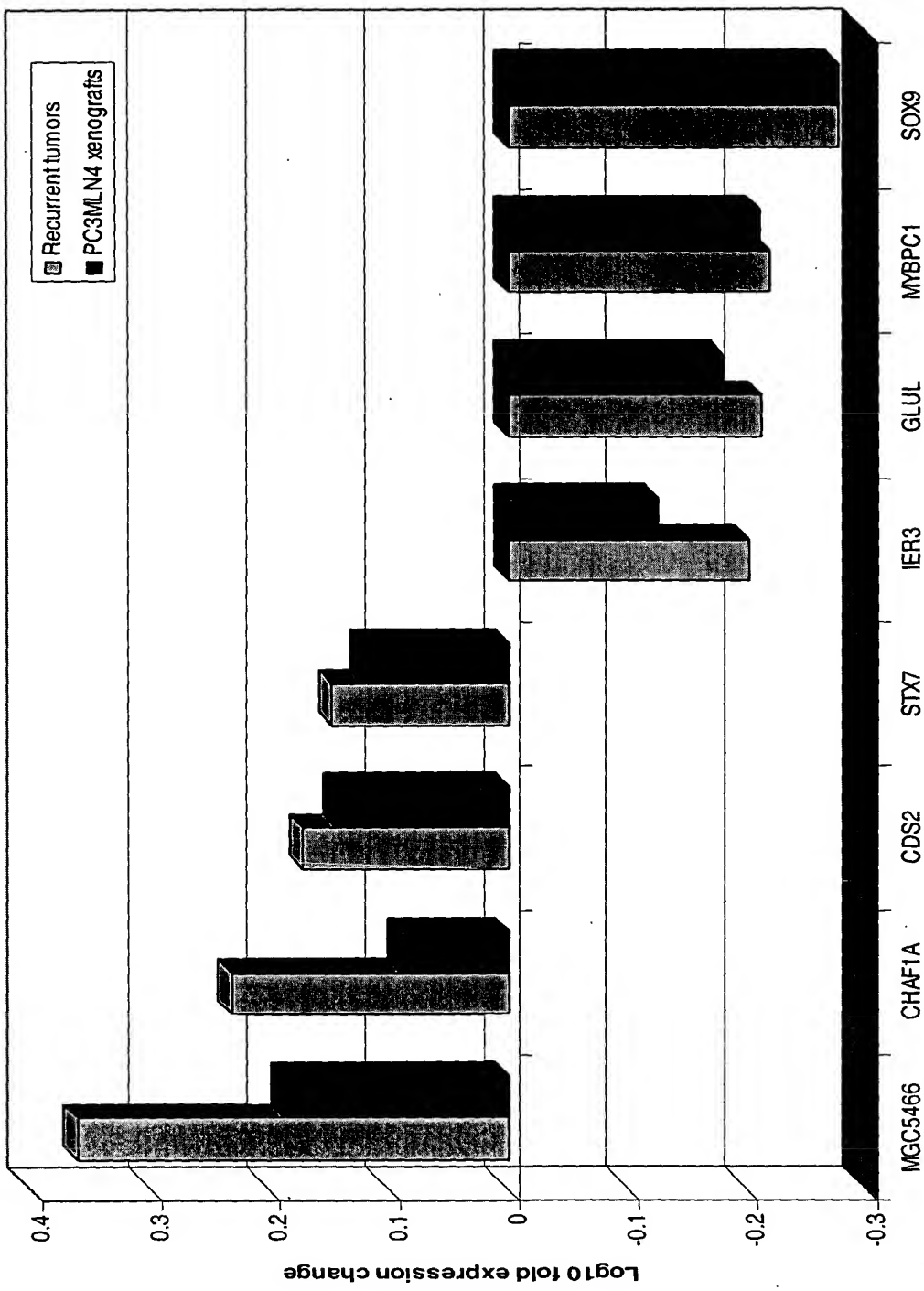


Figure 51B. Expression profiles of the 5 gene invasion signature in PC3MLN4 orthotopic xenografts and invasive human prostate tumors

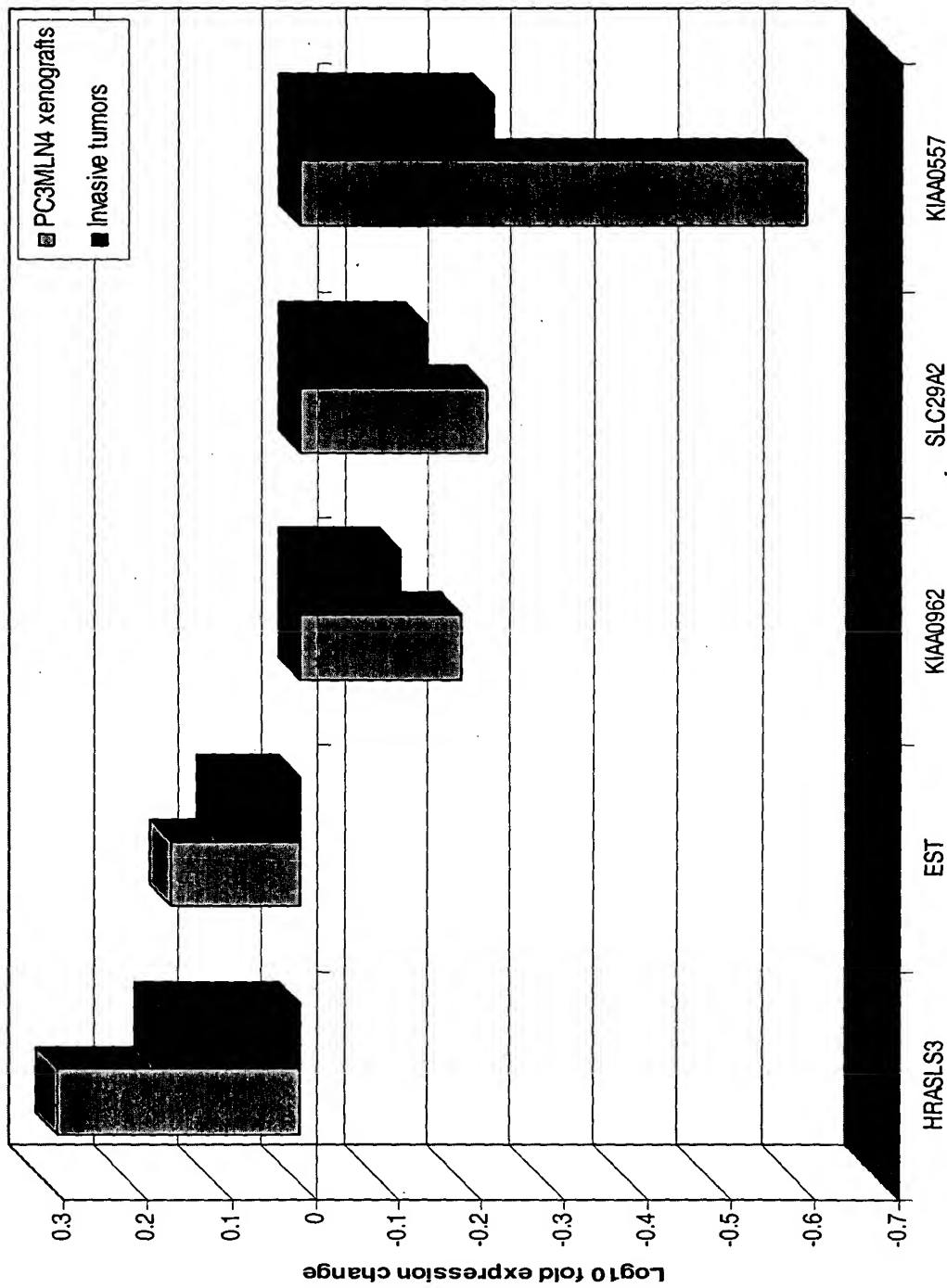


Figure 51C. Expression profiles of the 9 gene metastasis signature in PC3MLN4 orthotopic xenografts and metastatic human prostate tumors

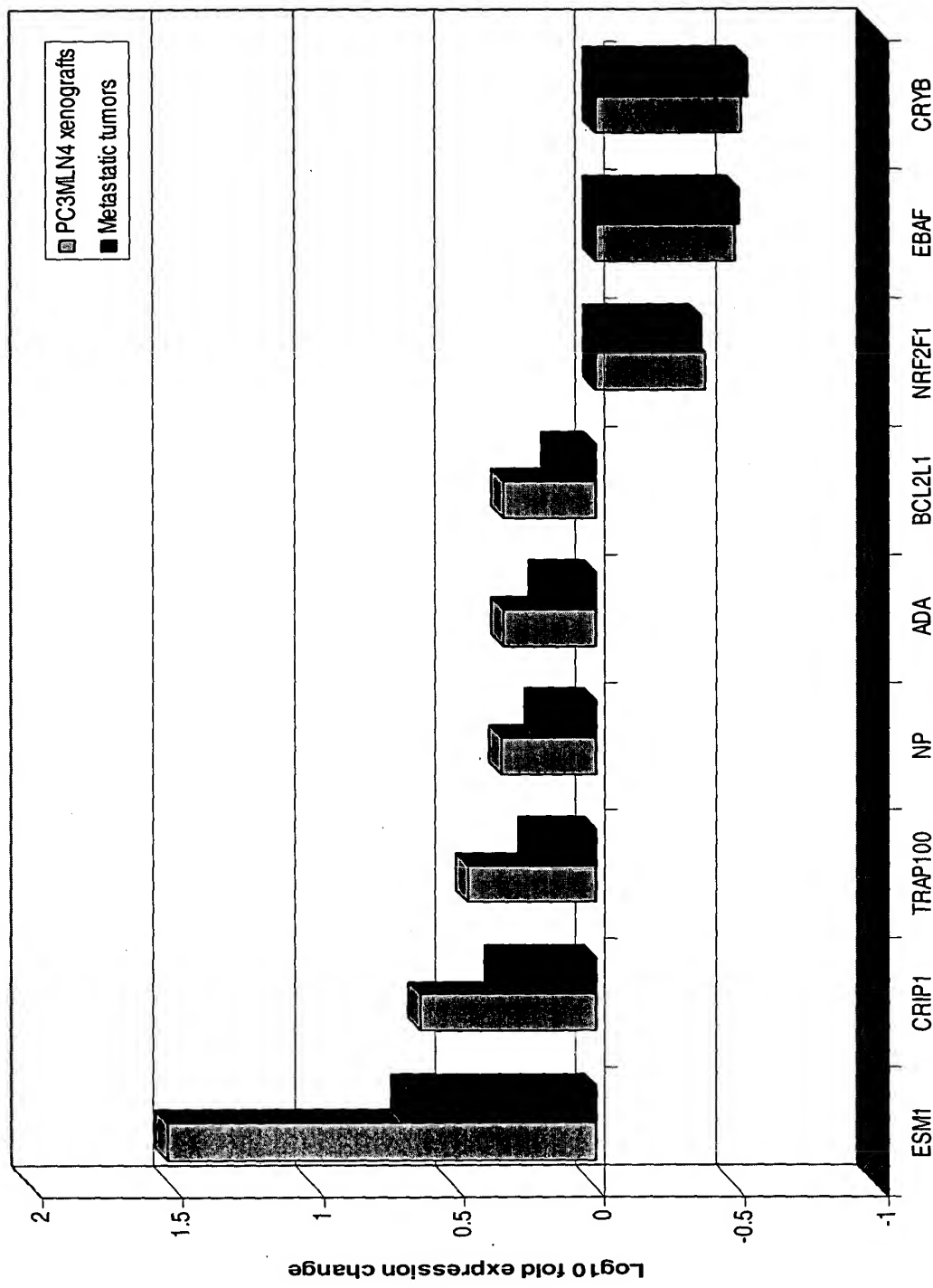


Figure 52A. Expression profiles of the 25 gene recurrence predictor signature in PC3MLN4 orthotopic xenografts and recurrent human prostate tumors

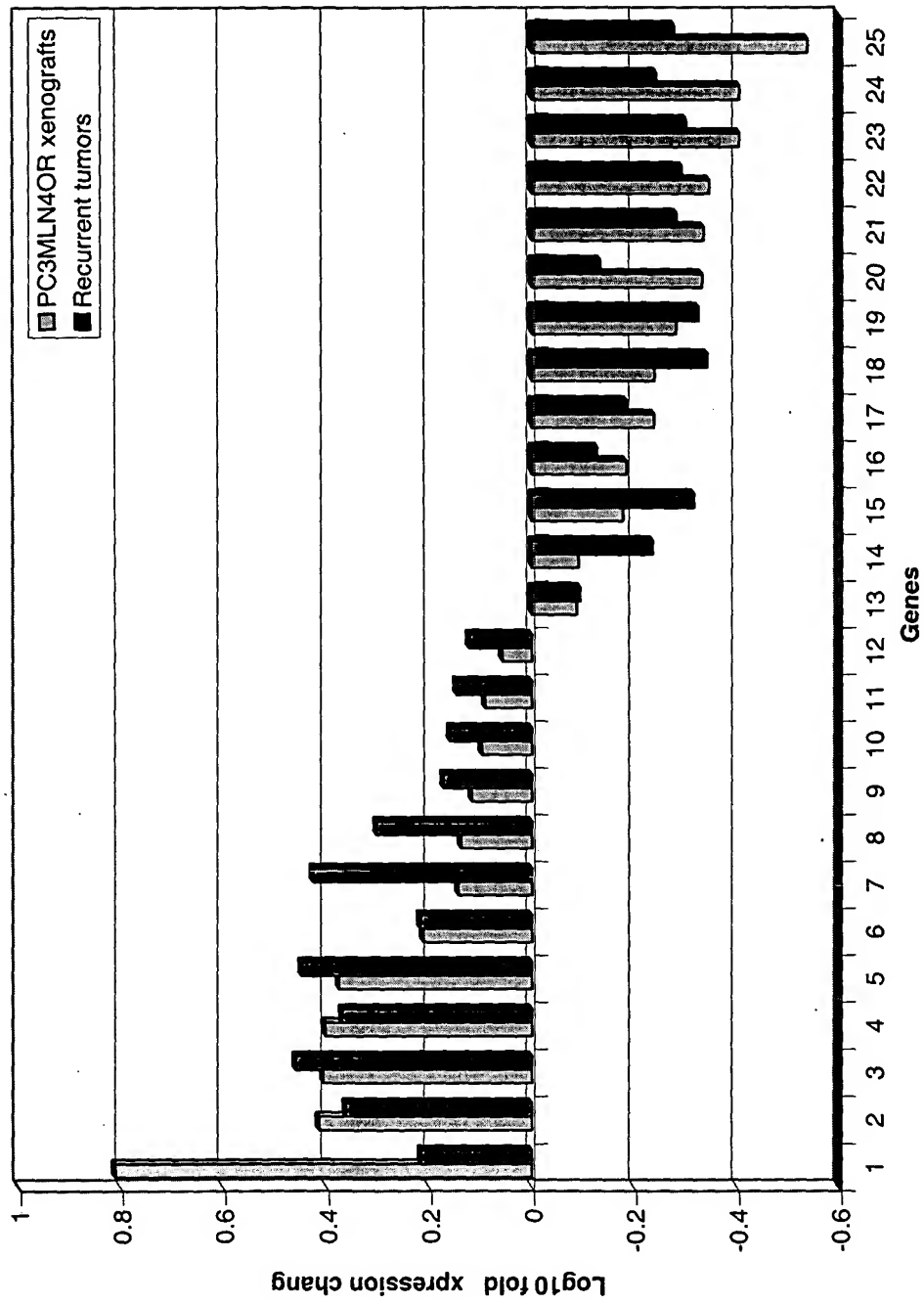


Figure 52B. Correlation of the expression profiles of the 25 genes recurrence predictor cluster in PC3MLN4 orthotopic xenografts and recurrent human prostate tumors

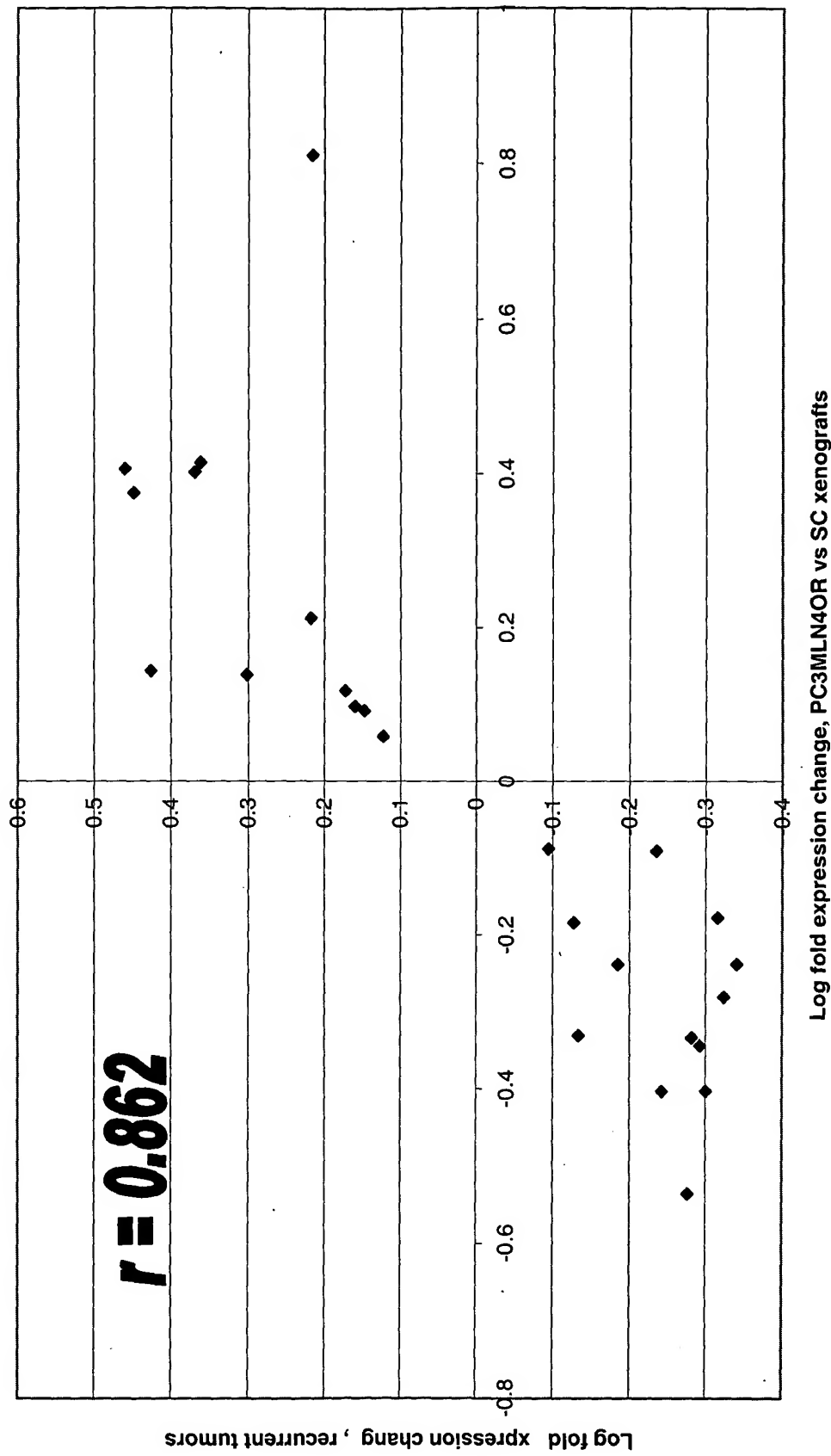


Figure 53. Phenotype association idices for transcripts of the 25 genes prostate cancer recurrence predictor cluster in 8 recurrent and 13 non-recurrent human prostate tumors

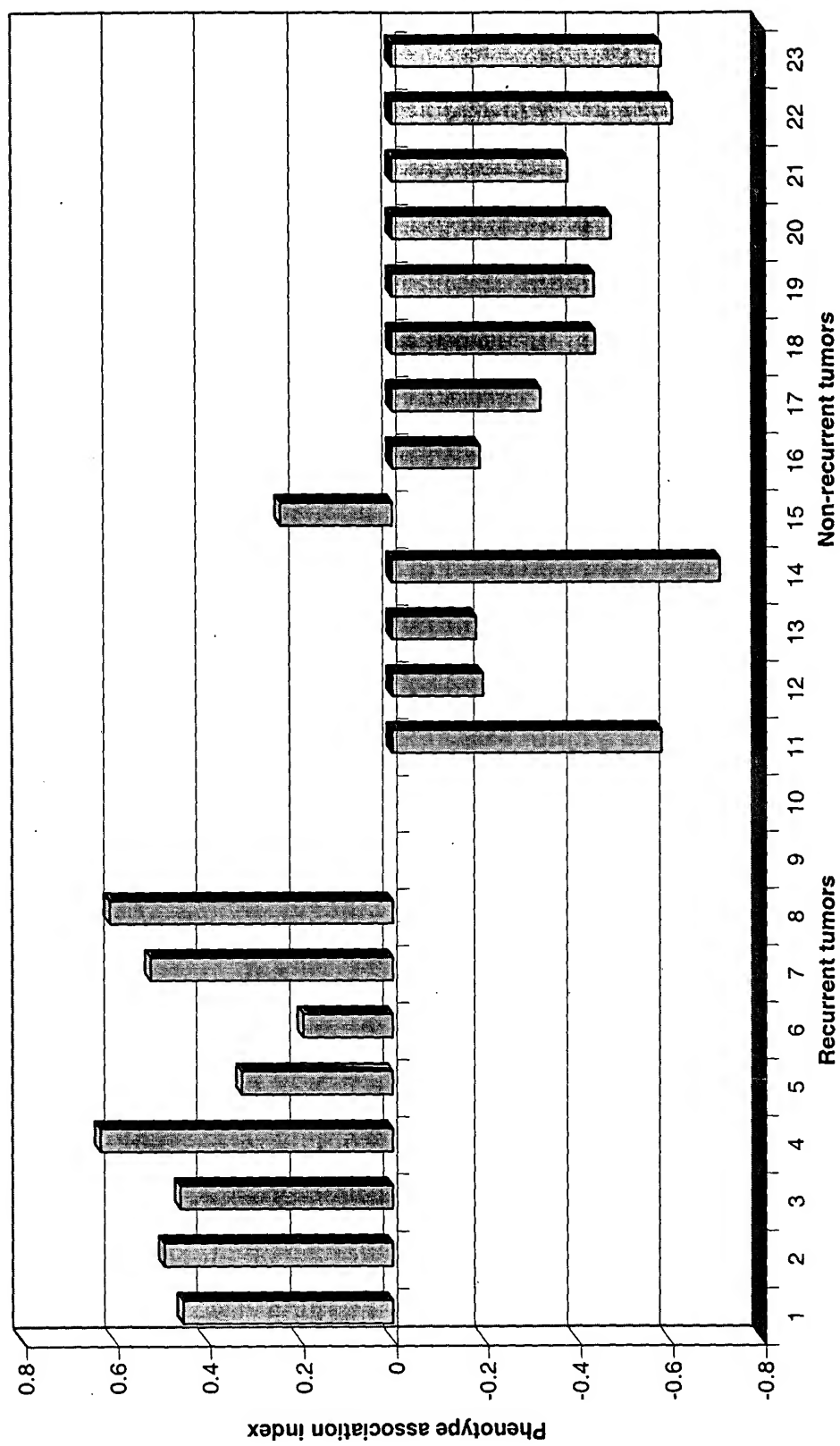


Figure 54. Expression profiles of the 12 gene recurrence predictor signature in PC3MLN4 orthotopic xenografts and recurrent human prostate tumors

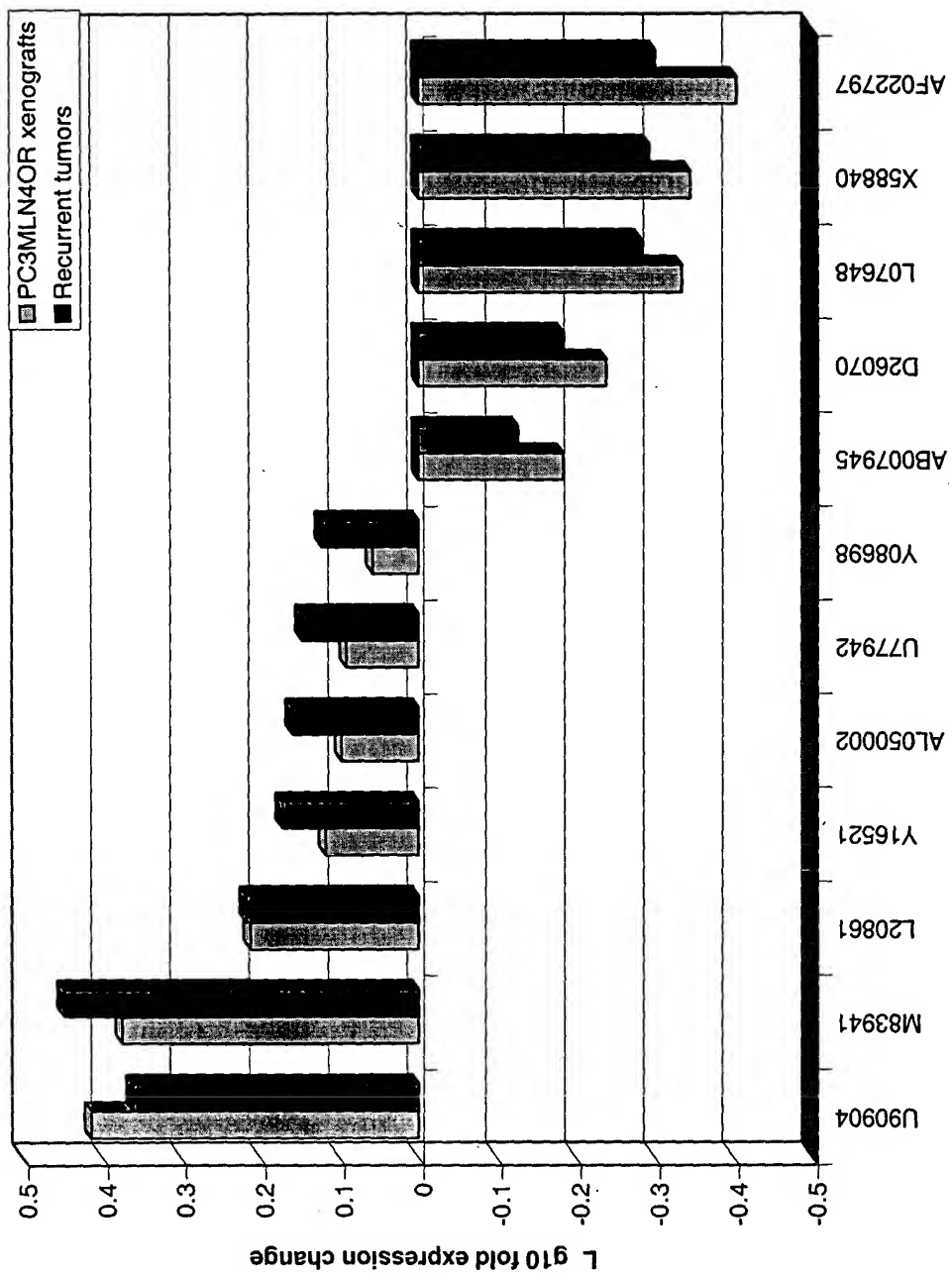


Figure 55. Correlation of the expression profiles of the 12 genes recurrence predictor cluster in PC3MLN4 orthotopic xenografts and recurrent human prostate tumors

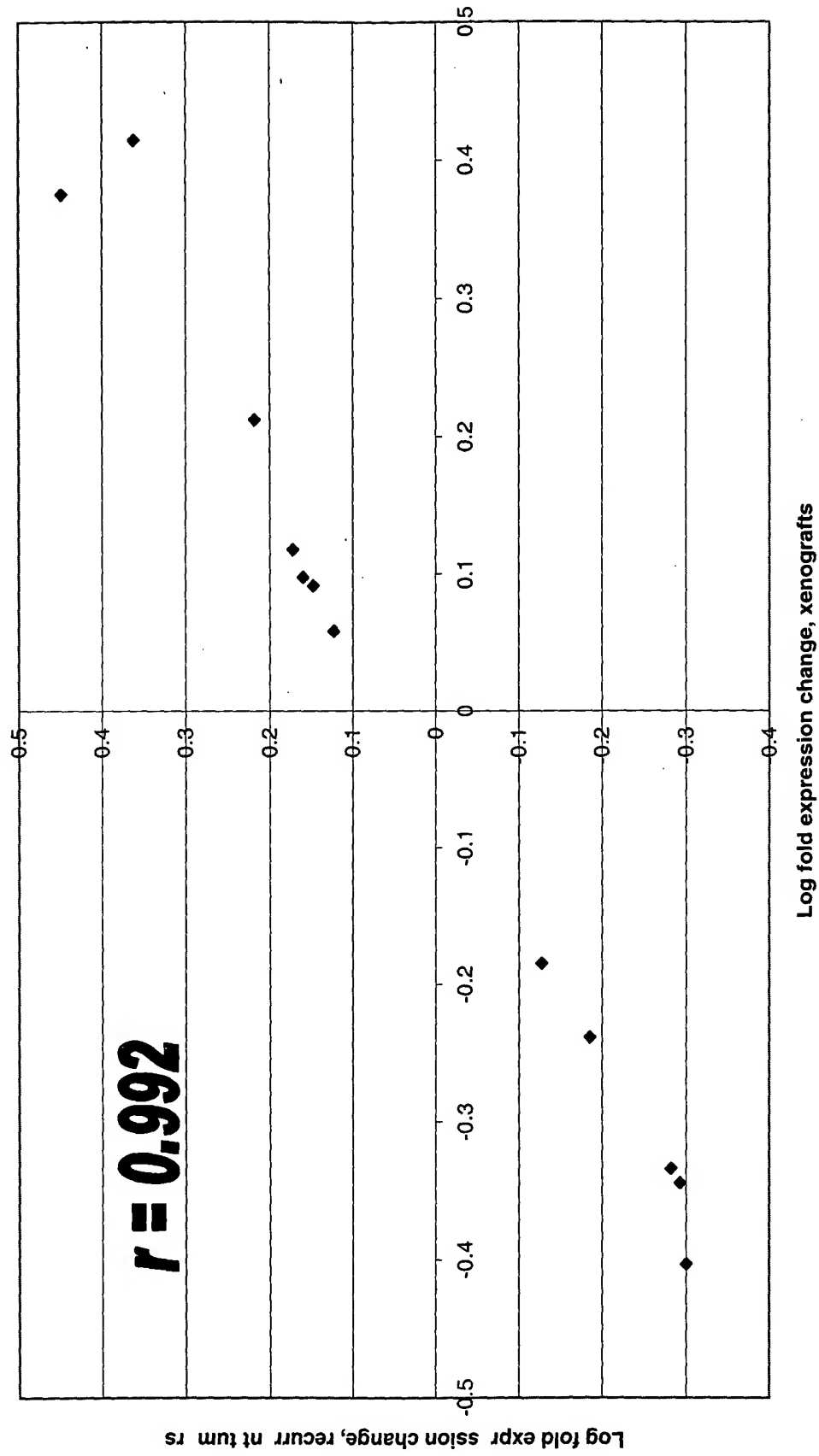


Figure 56. Phenotype association indices for transcripts of the 12 genes prostate cancer recurrence predictor cluster in 8 recurrent and 13 non-recurrent human prostate tumors

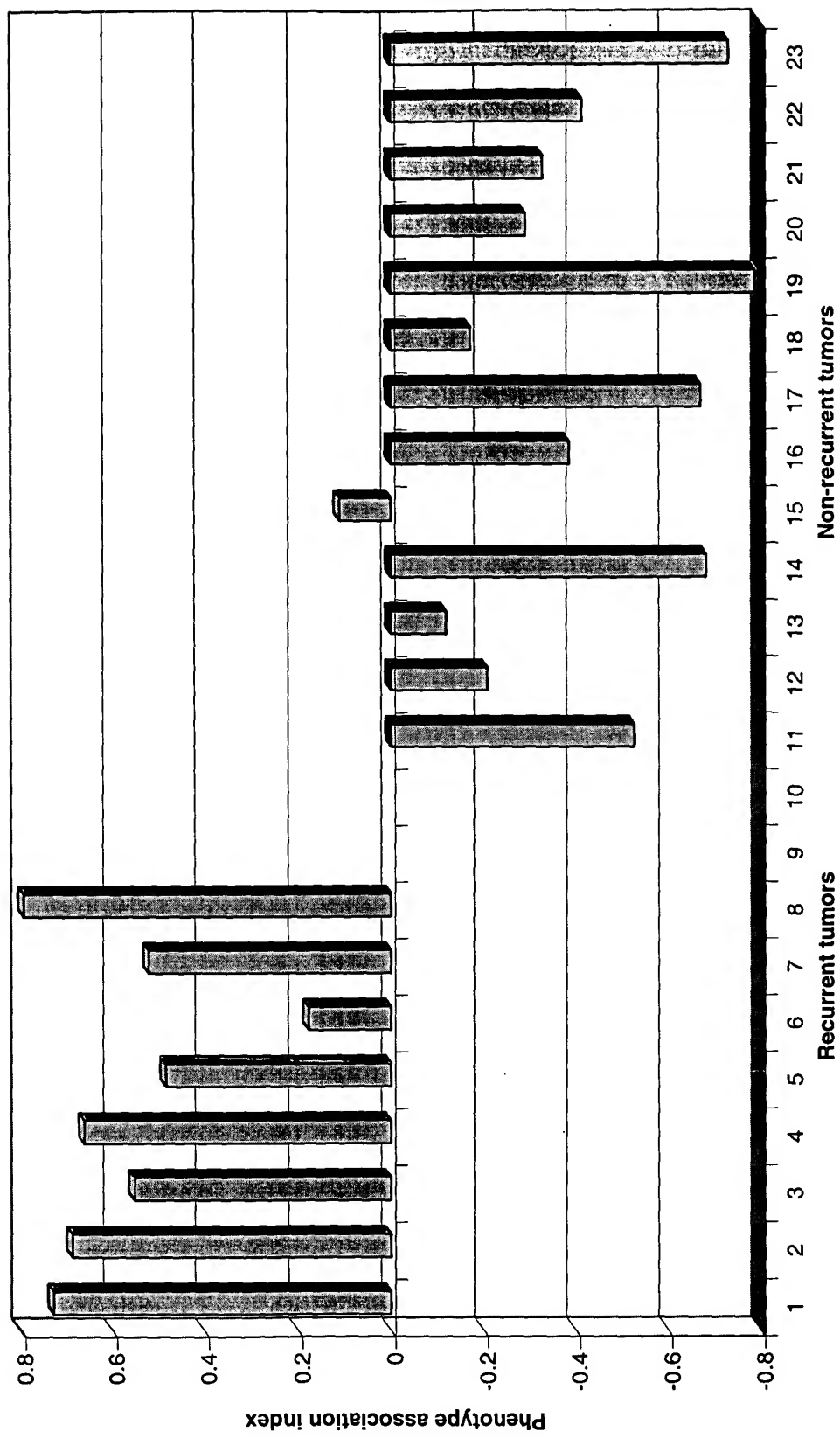
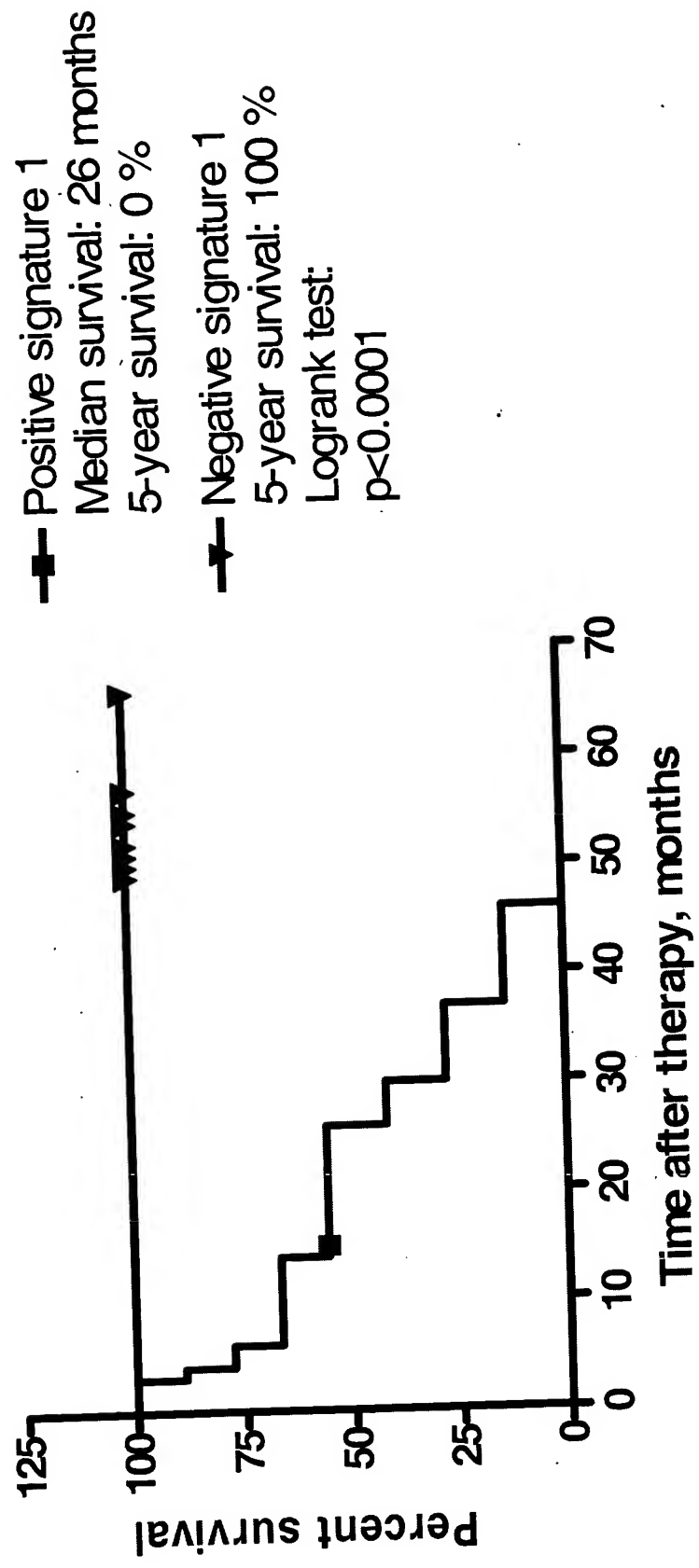


Figure 57. Phenotype association indices defined by expression profiles of transcripts of the recurrence predictor signature 1 in 8 recurrent and 13 non-recurrent human prostate tumors



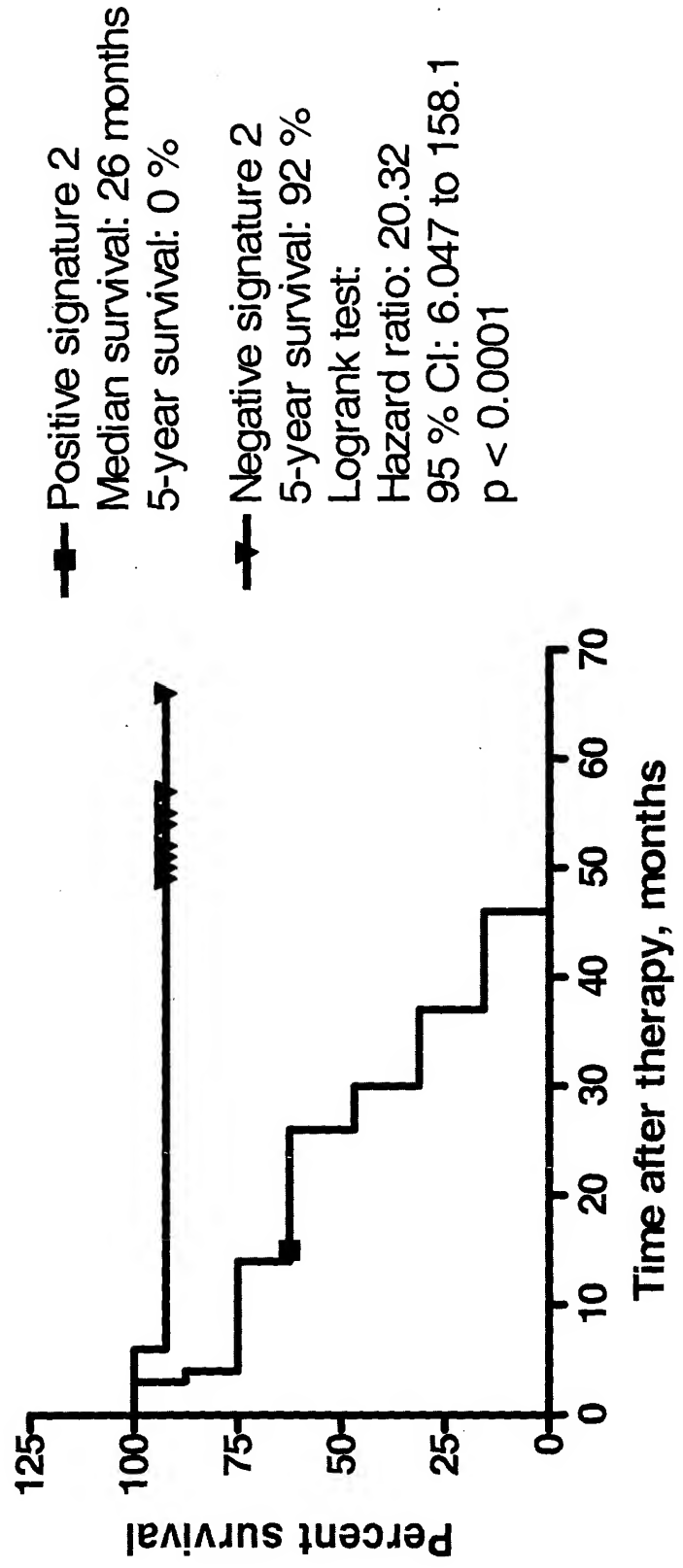
58A.

Relapse-free survival of prostate cancer patients



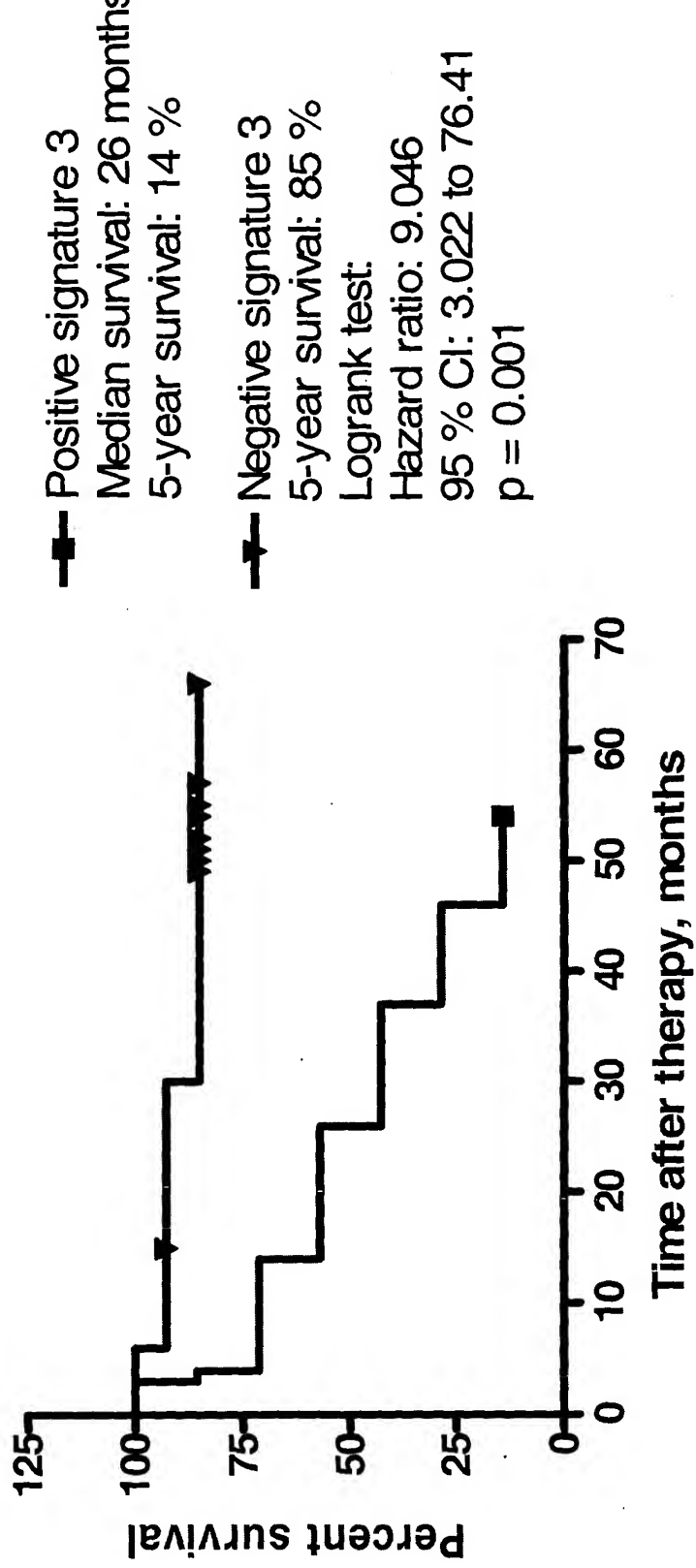
58B.

Relapse-free survival of prostate cancer patients



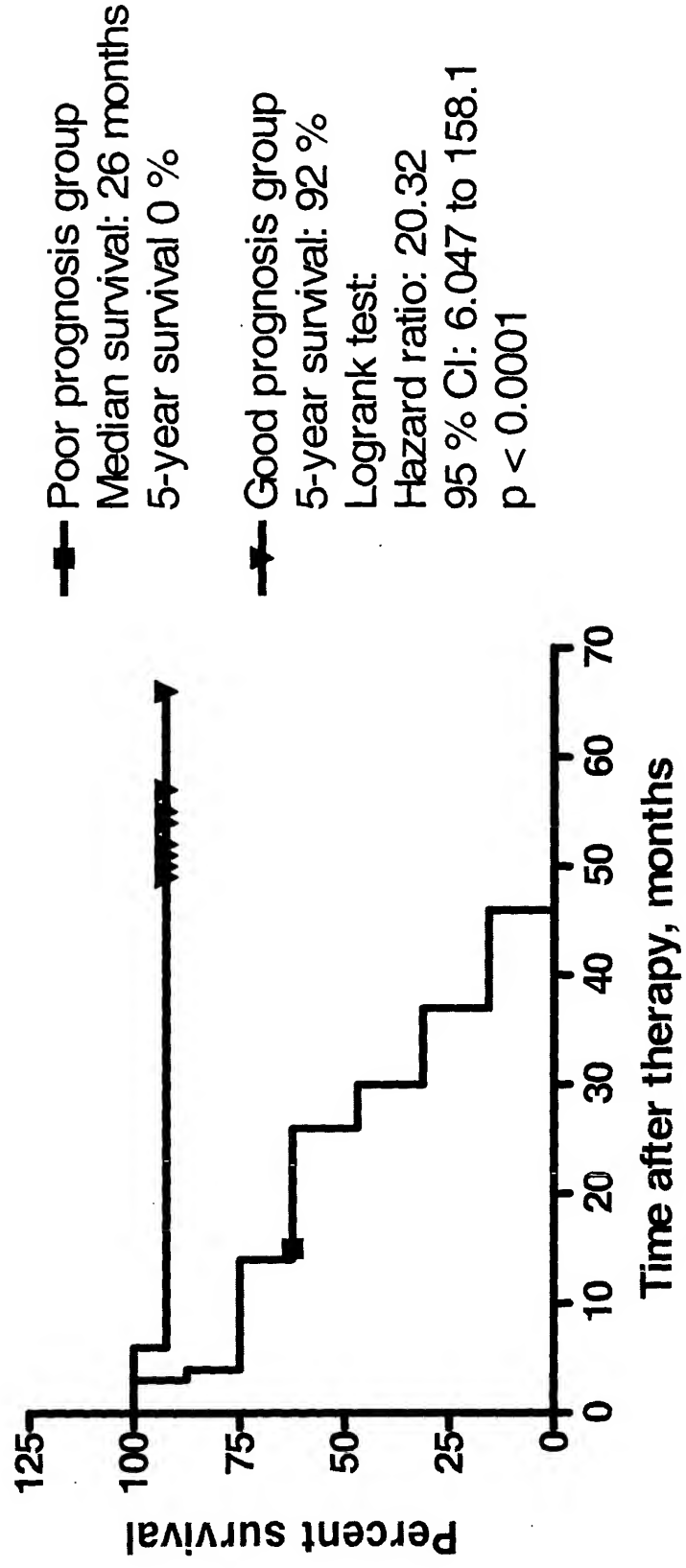
58C.

Relapse-free survival of prostate cancer patients



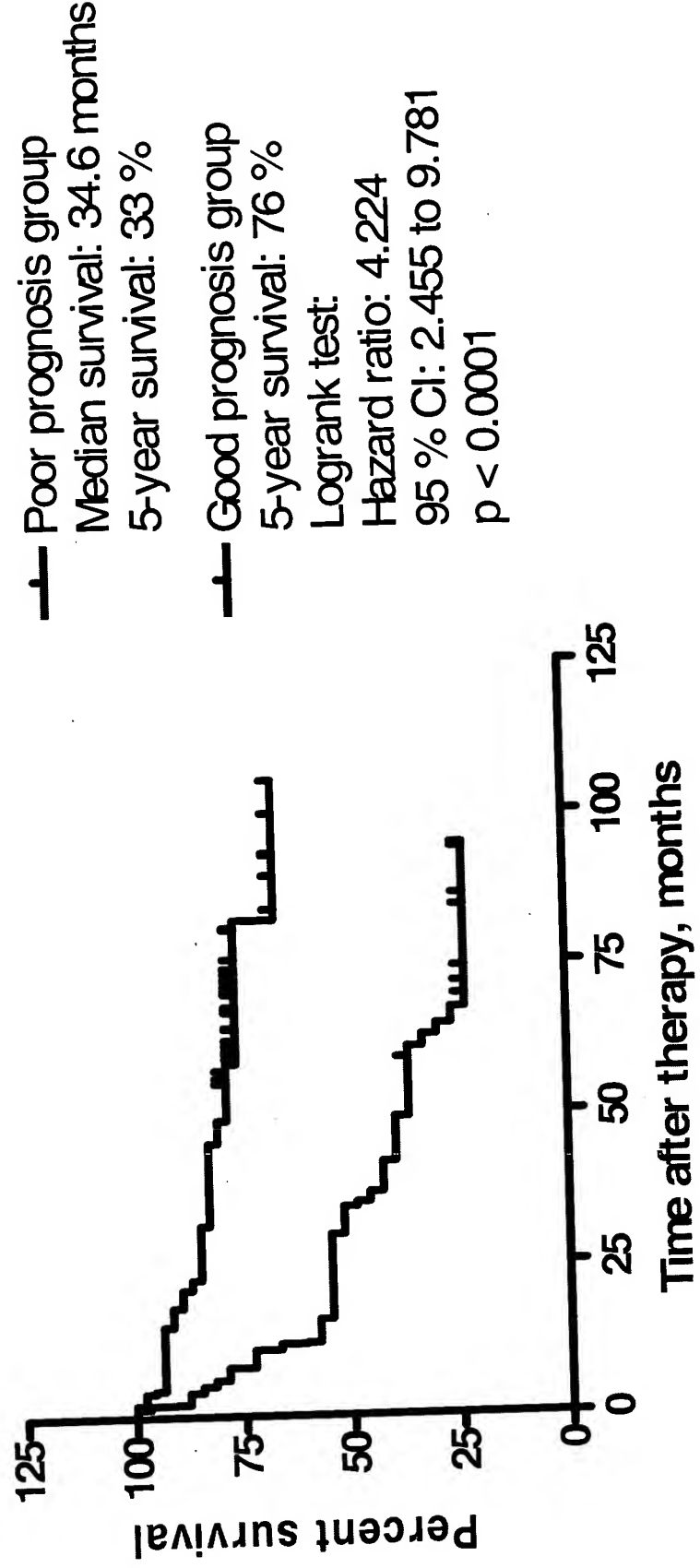
58D.

Relapse-free survival of prostate cancer patients



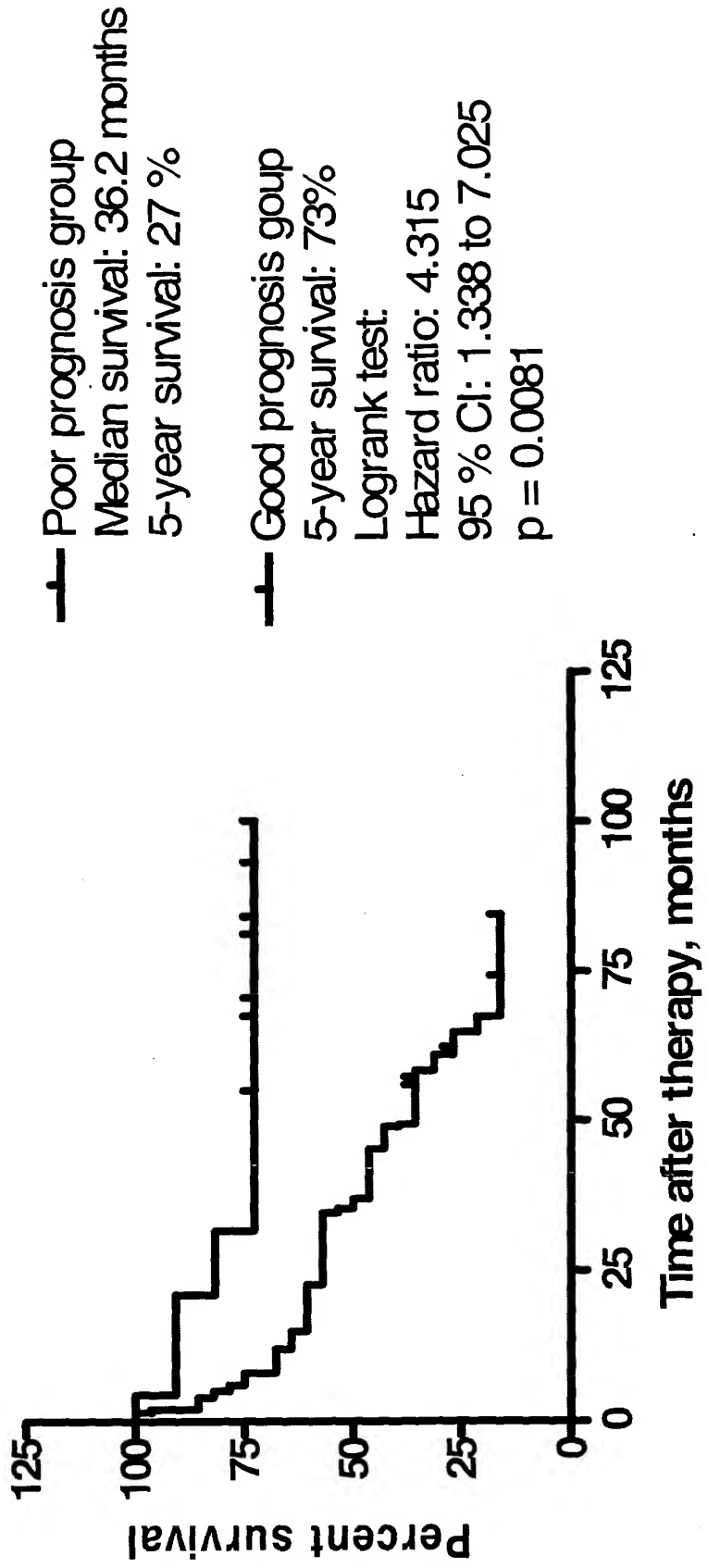
59A.

Relapse-free survival of prostate cancer patients



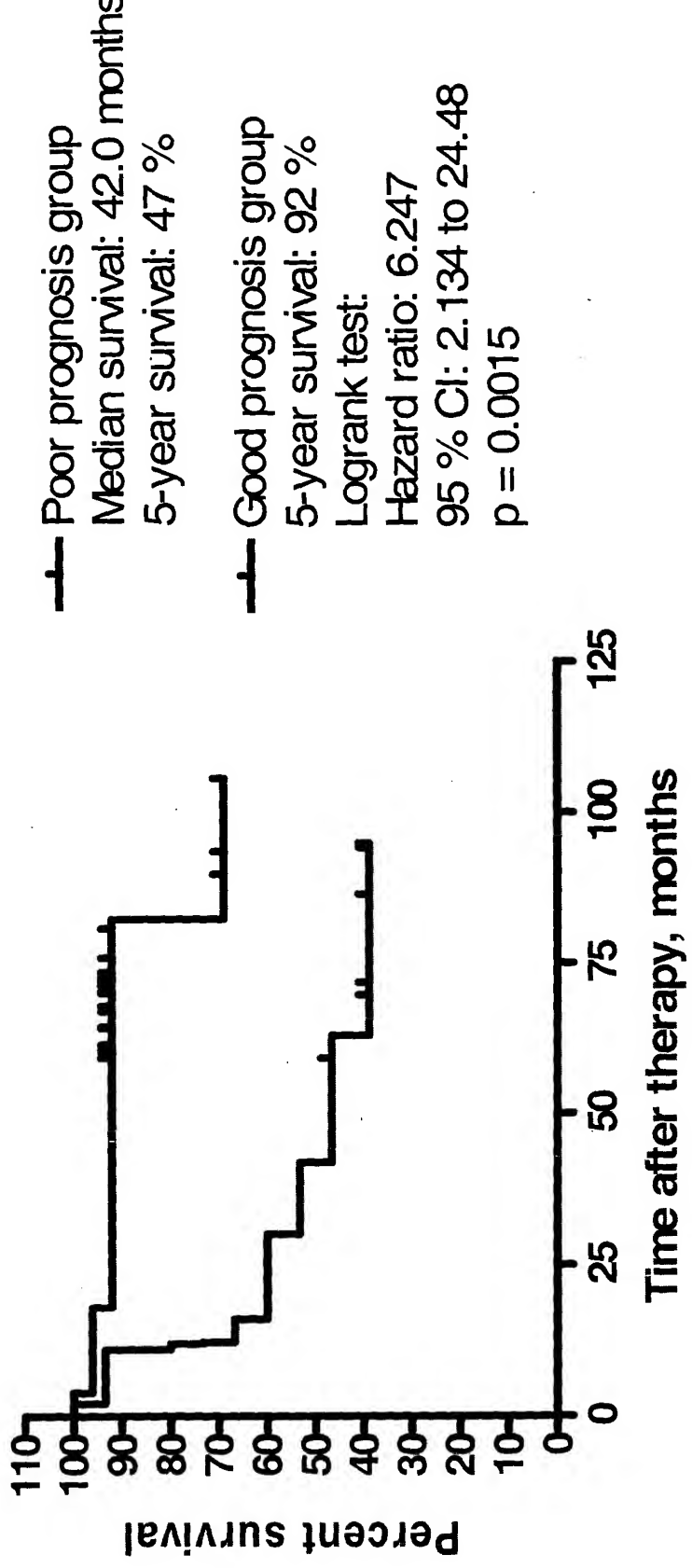
59B

Relapse-free survival of prostate cancer patients with high preoperative PSA level



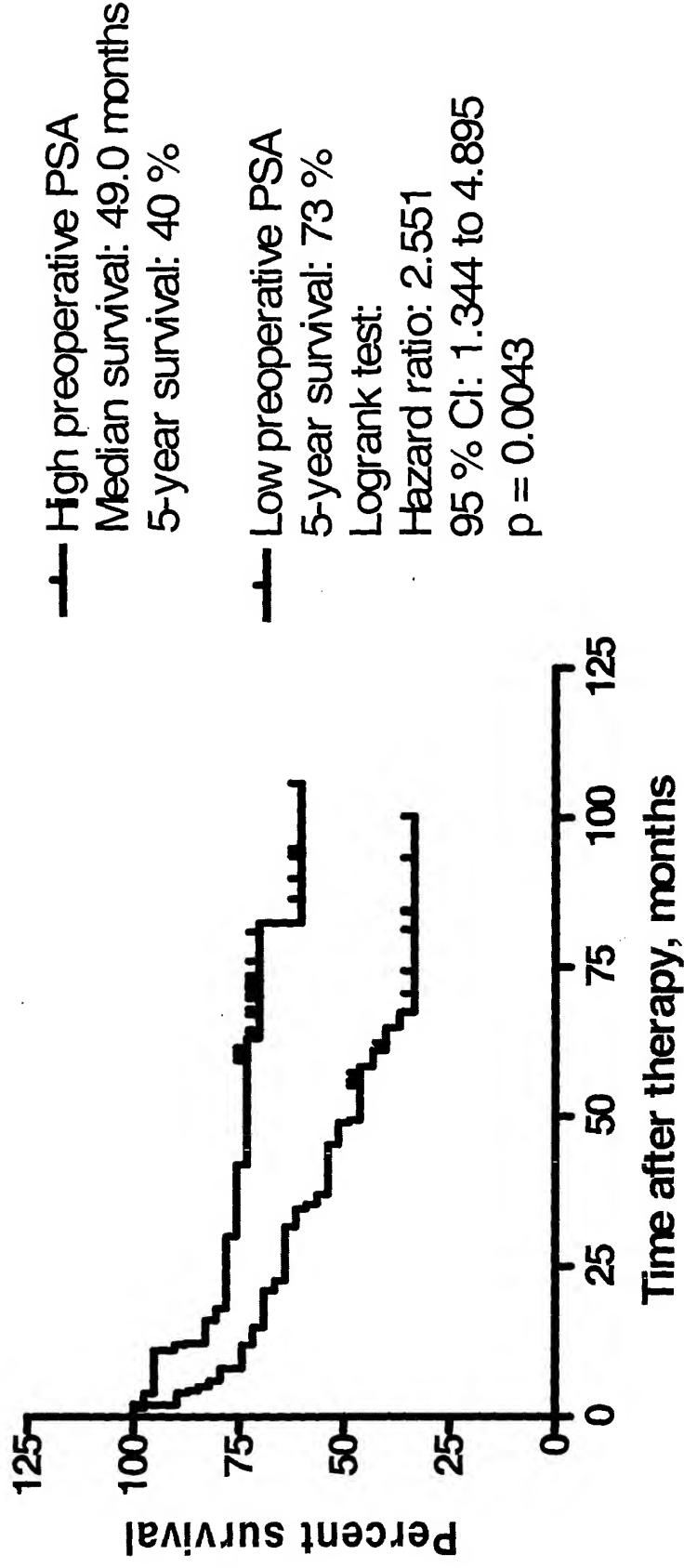
59C.

Relapse-free survival of prostate cancer patients with low preoperative PSA level



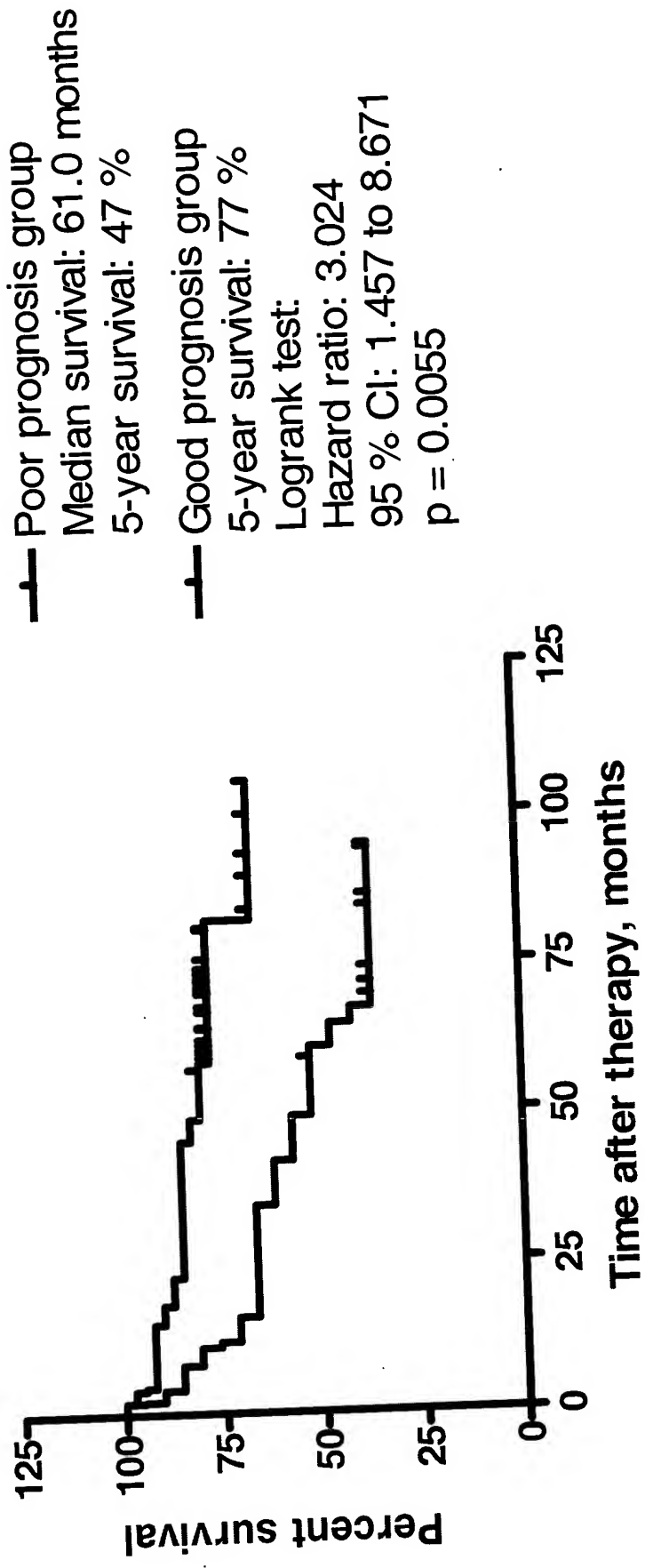
59D.

Relapse-free survival of prostate cancer patients

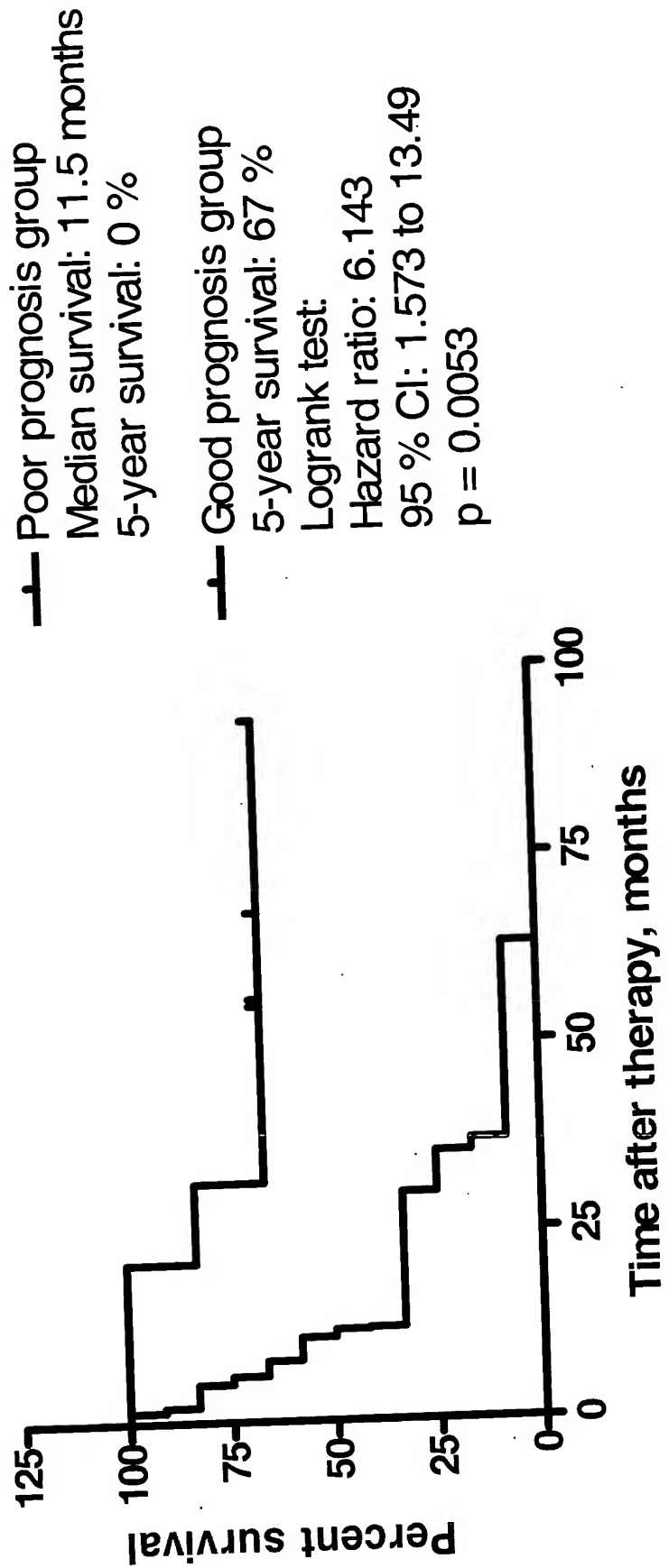


60A.

Relapse-free survival of prostate cancer patients with RP Gleason sum 6 & 7

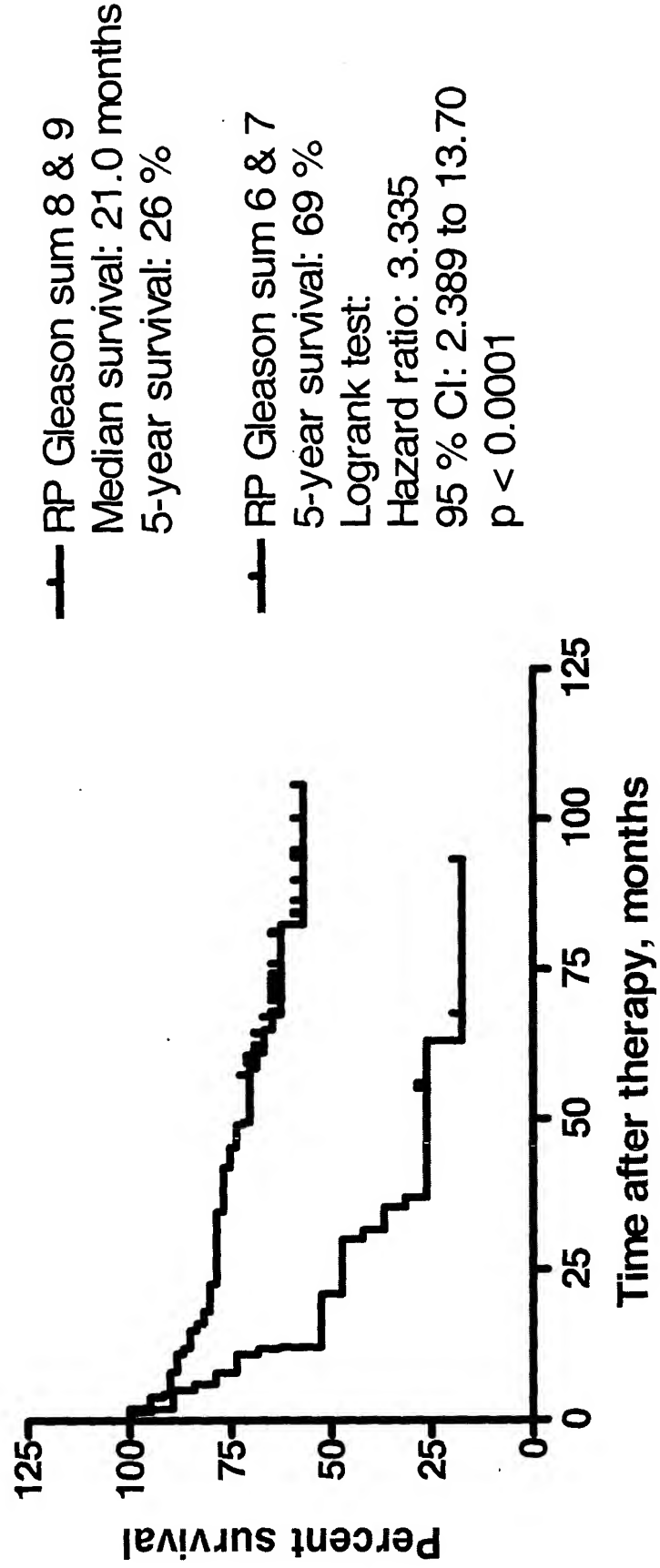


Relapse-free survival of prostate cancer patients with RP Gleason sum 8 & 9



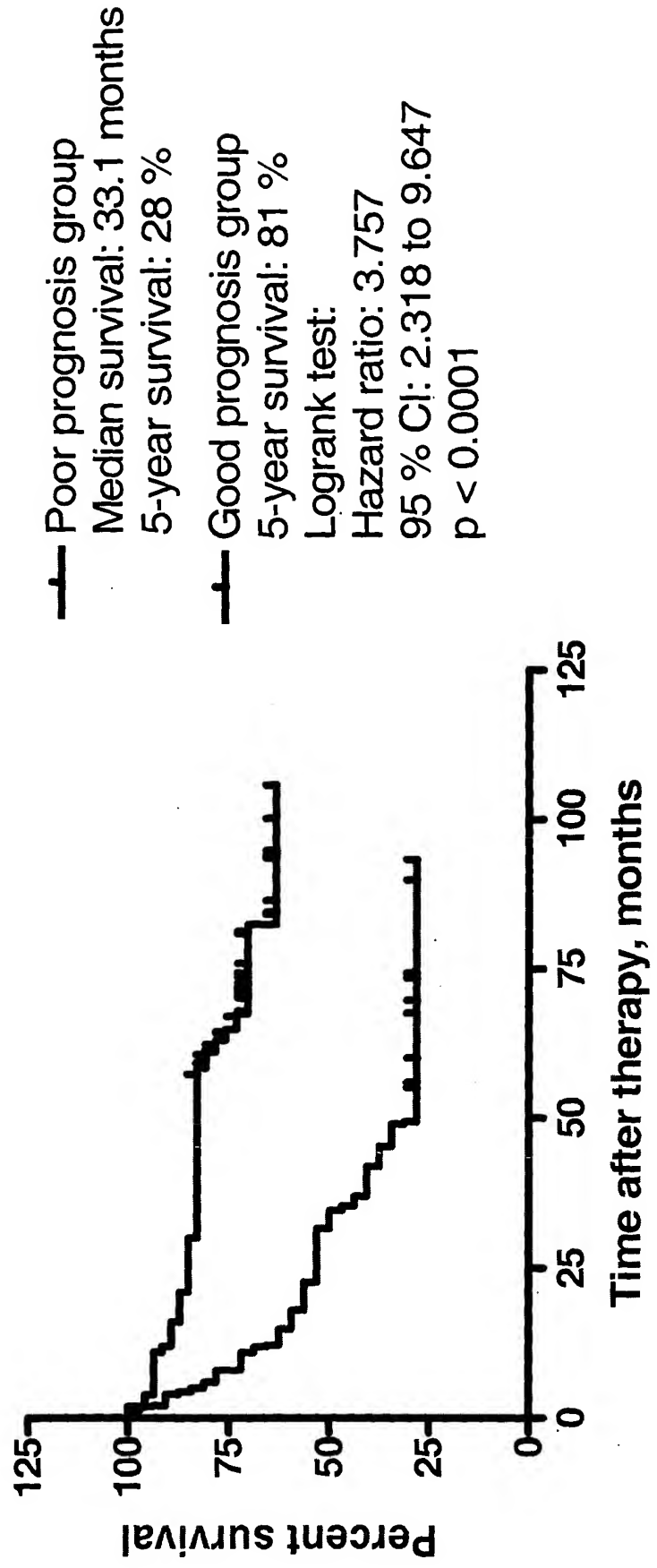
60C

Relapse-free survival of prostate cancer patients with different RP Gleason sum



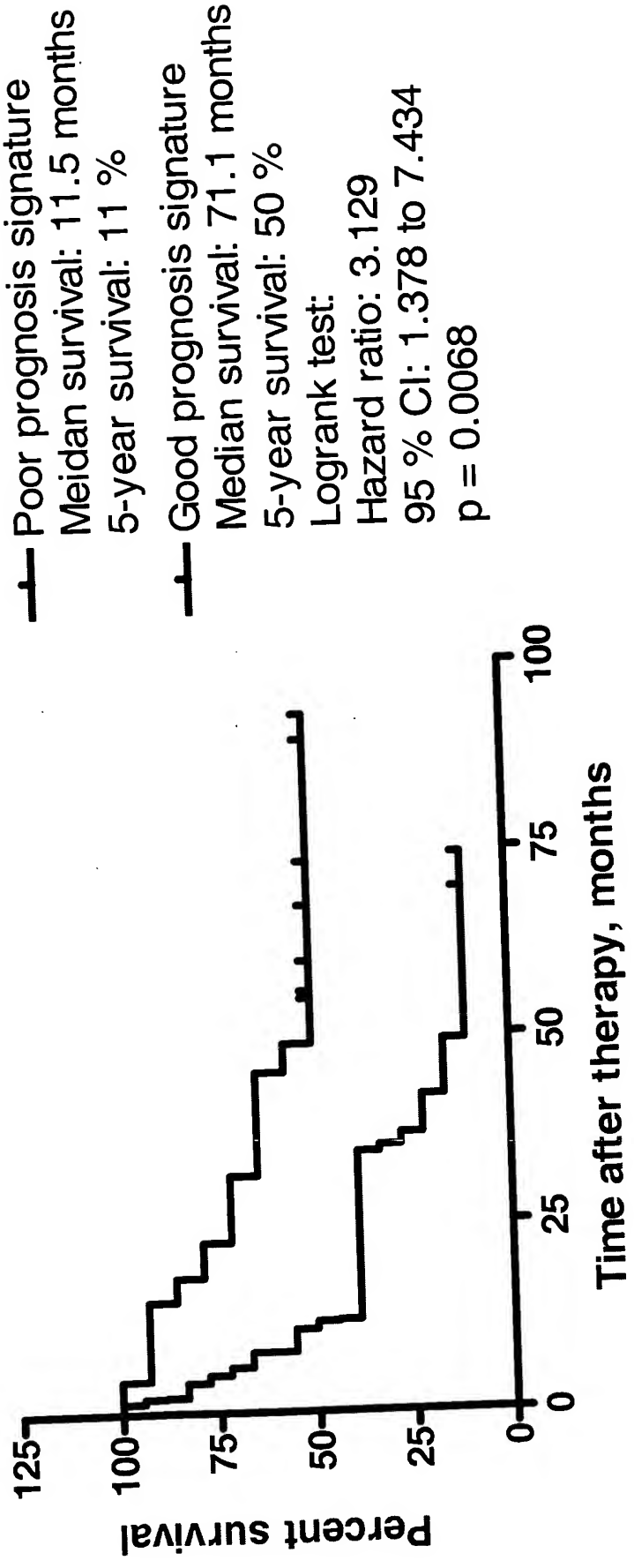
61A

Relapse-free survival of prostate cancer patients in distinct nomogram-defined subgroups



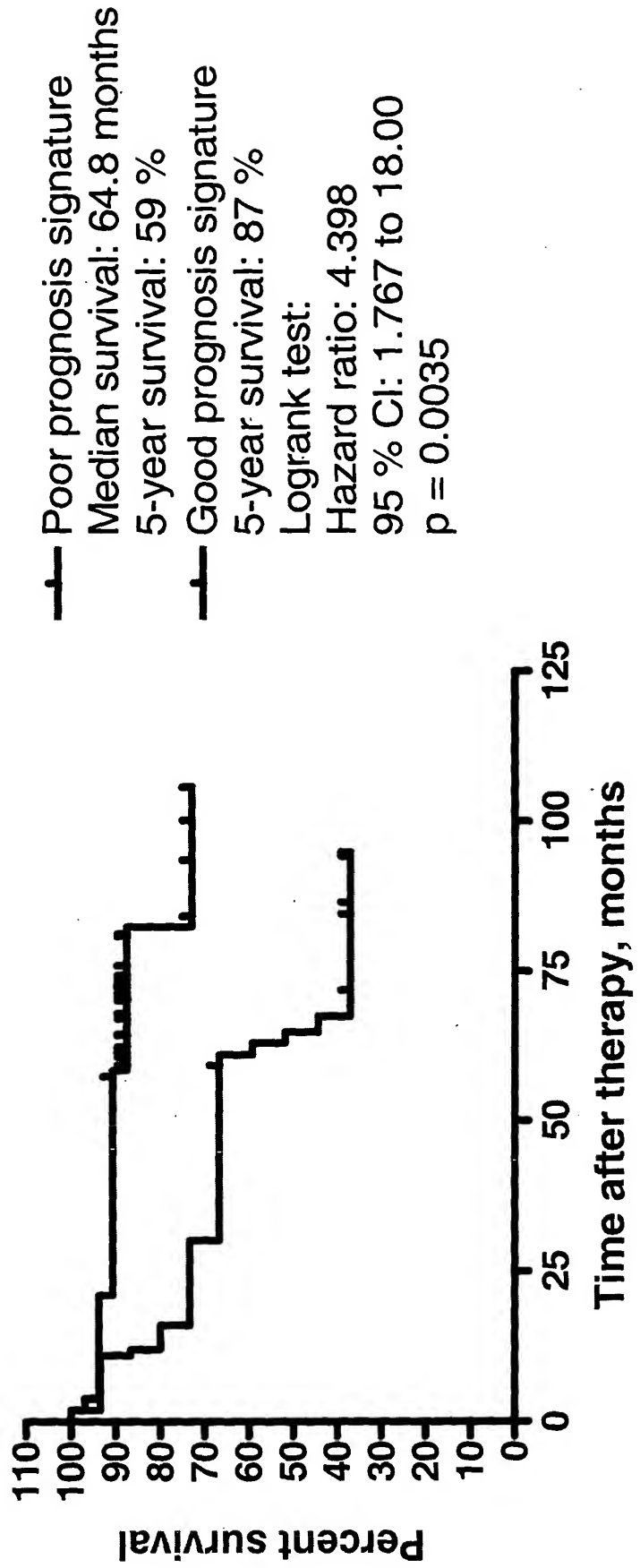
61B

Relapse-free survival of prostate cancer patients (nomogram-defined poor prognosis group)



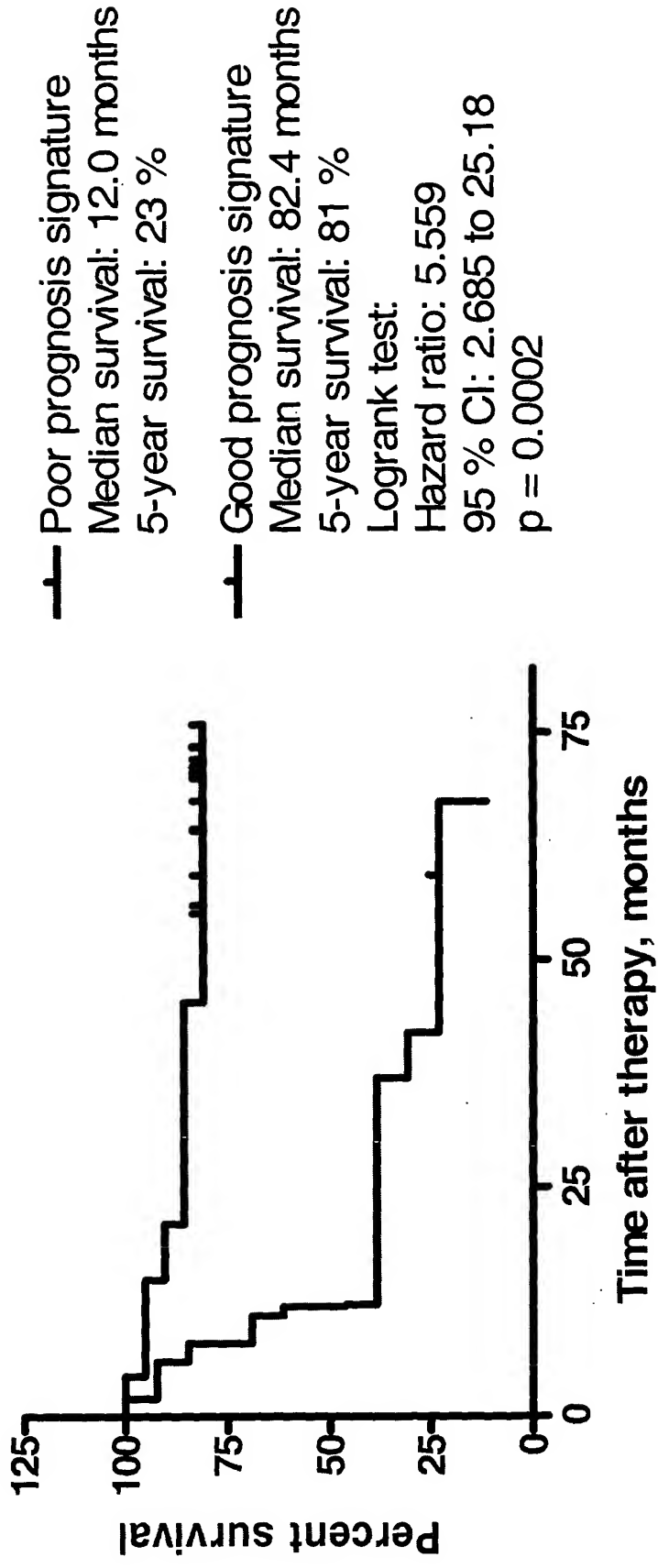
61C.

Relapse-free survival of prostate cancer patients (nomogram-defined good prognosis group)



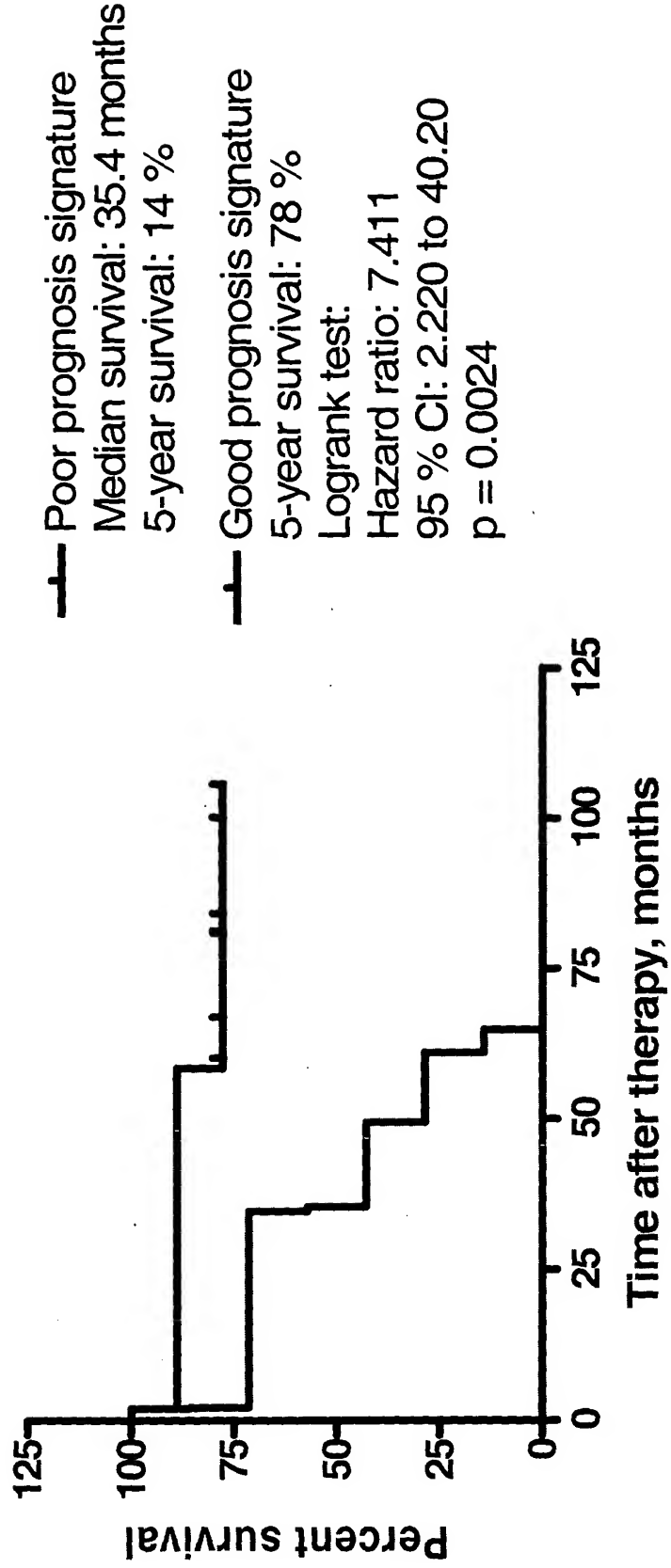
62A.

Relapse-free survival of prostate cancer patients with stage 1C tumors



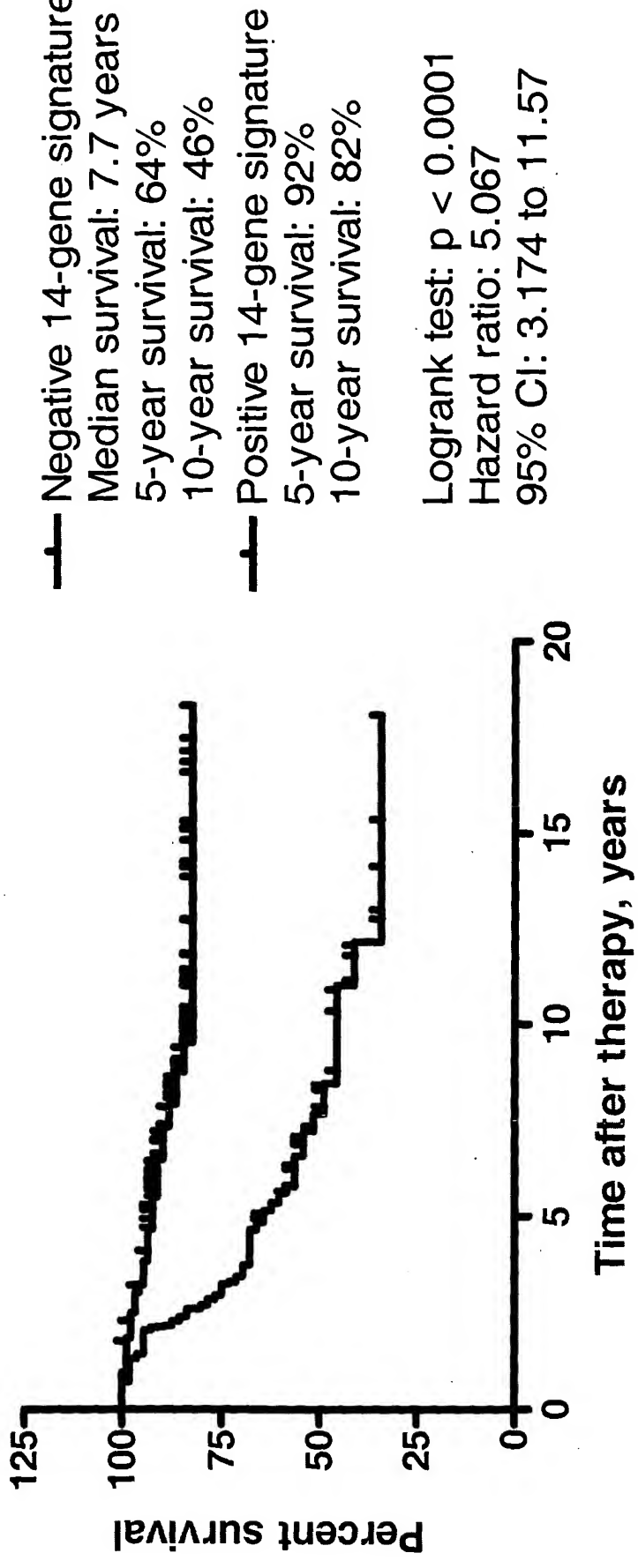
62B.

Relapse-free survival of prostate cancer patients with stage 2A tumors



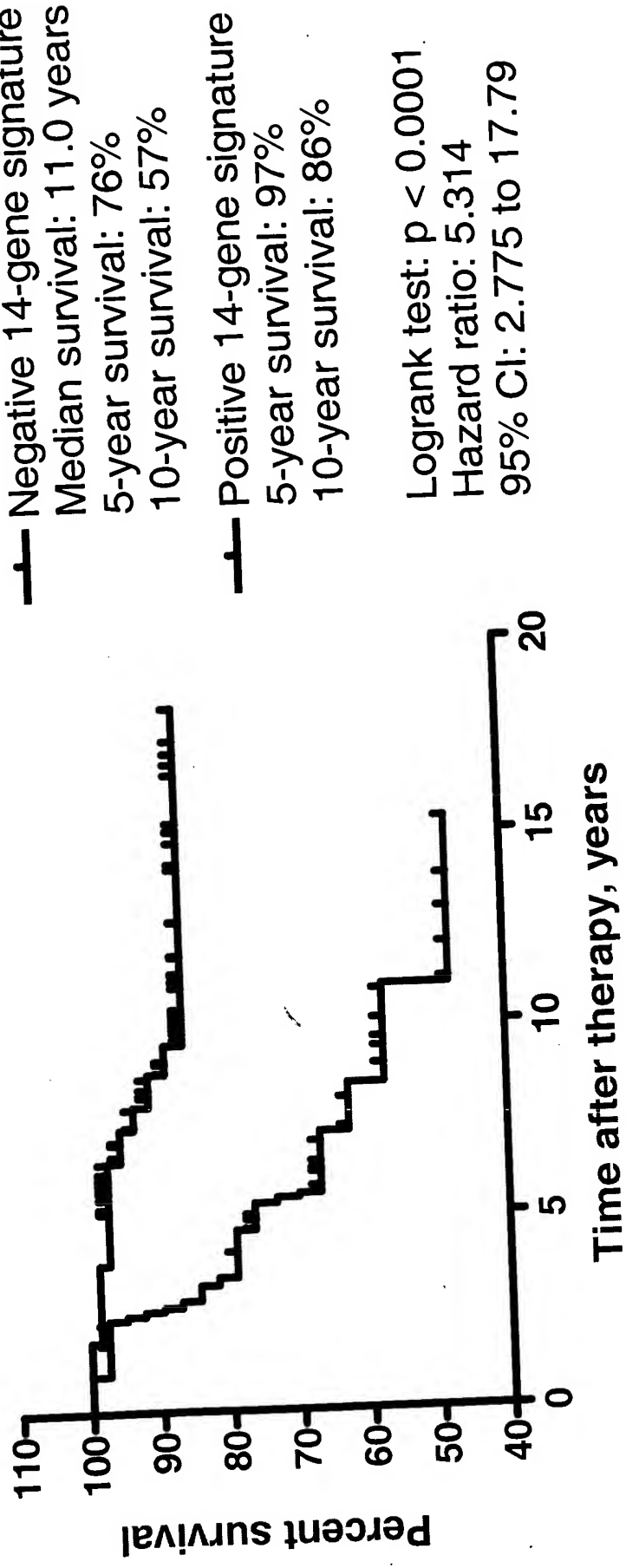
63A

Survival of 151 breast cancer patients with LN- disease



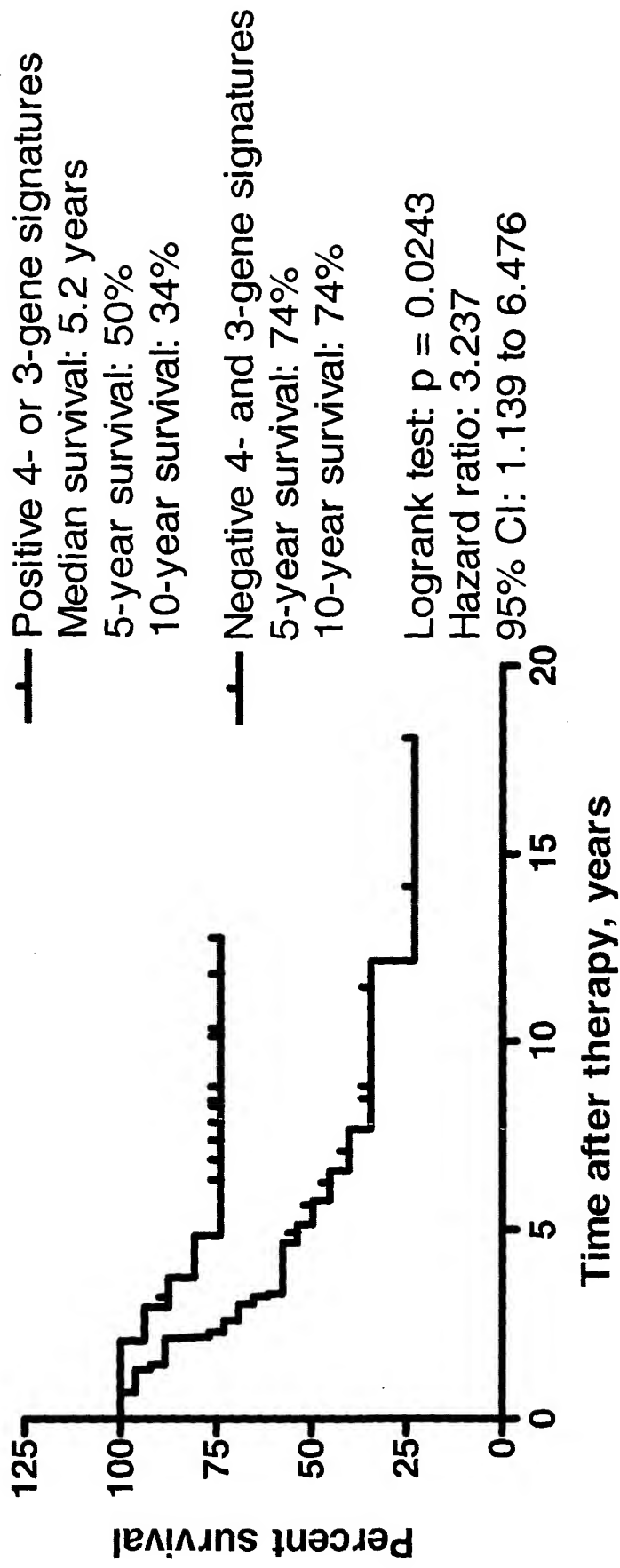
63B

Survival of 109 breast cancer patients with ER+ tumors and LN- disease



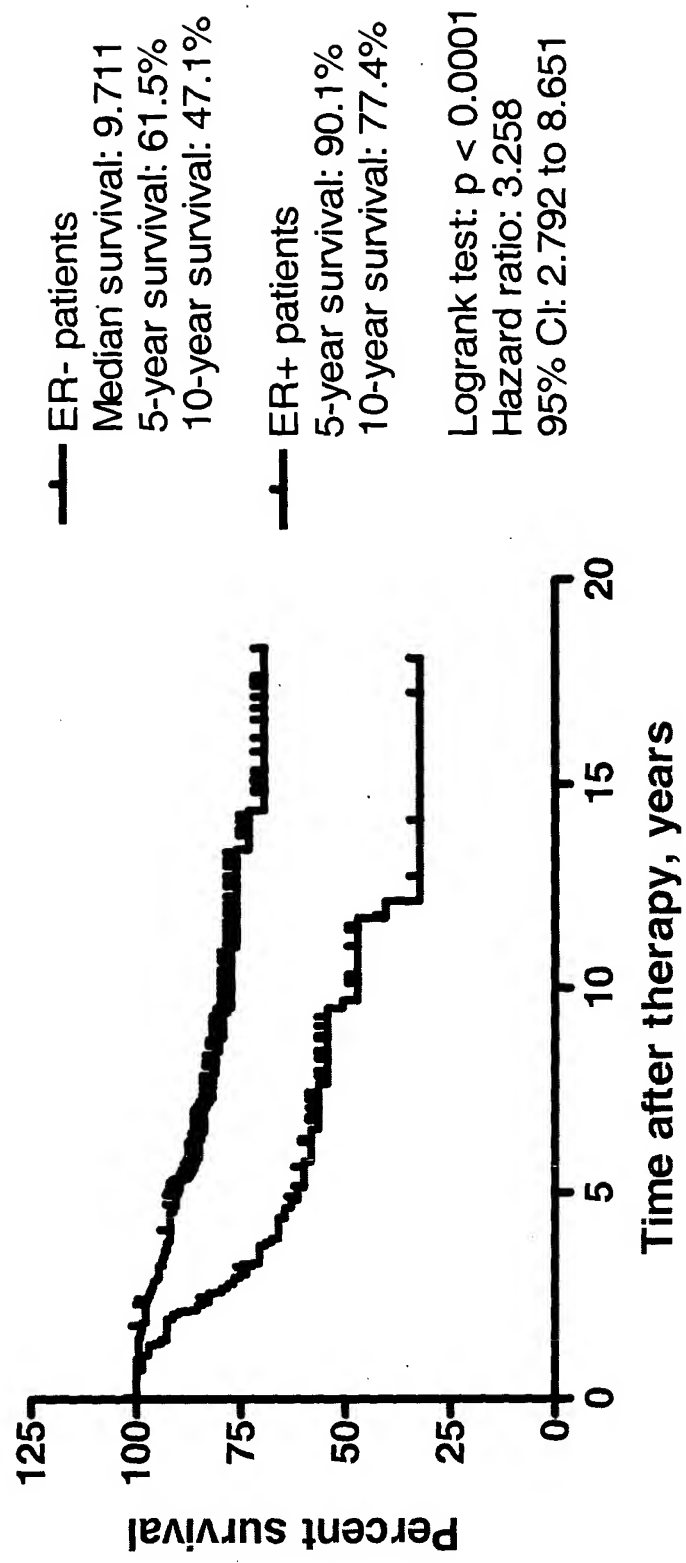
63C

Survival of 42 breast cancer patients with ER- tumors and LN- disease



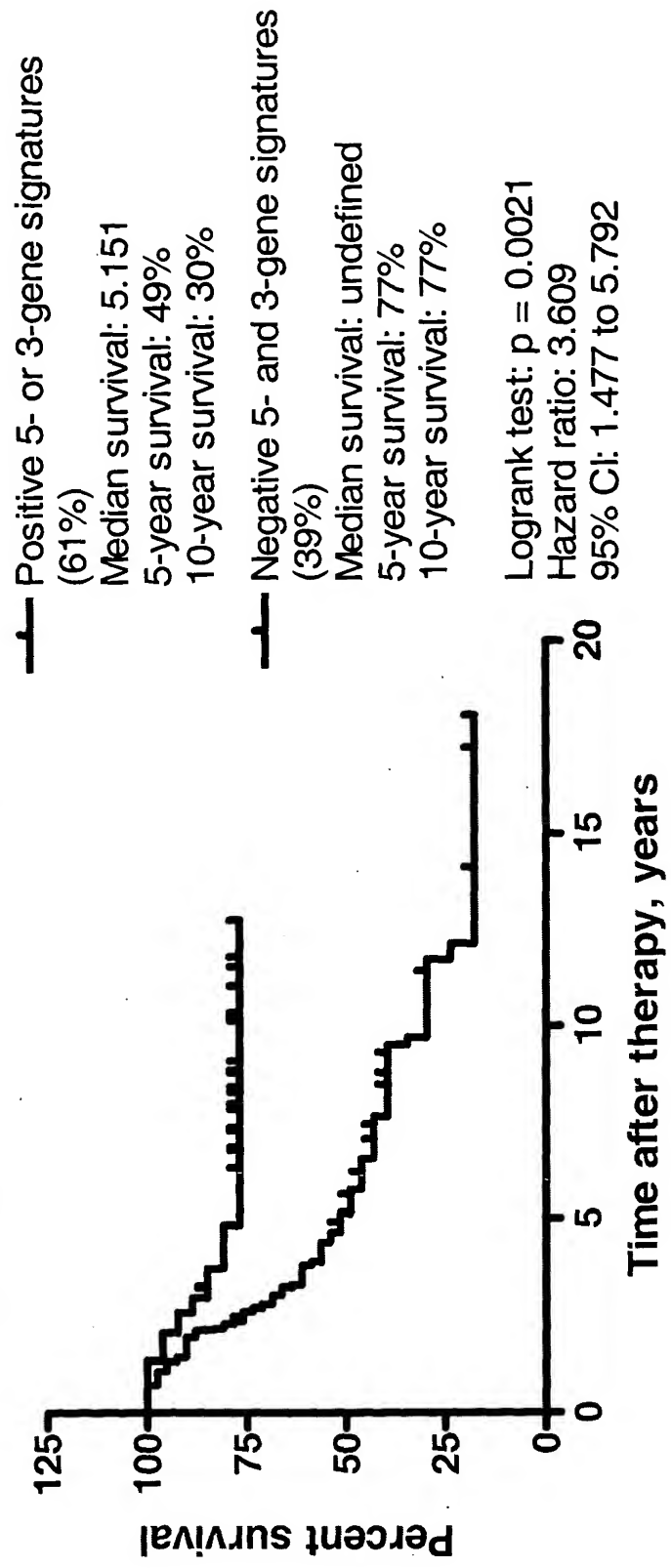
64A

Survival of breast cancer patients with ER+ and ER- tumors



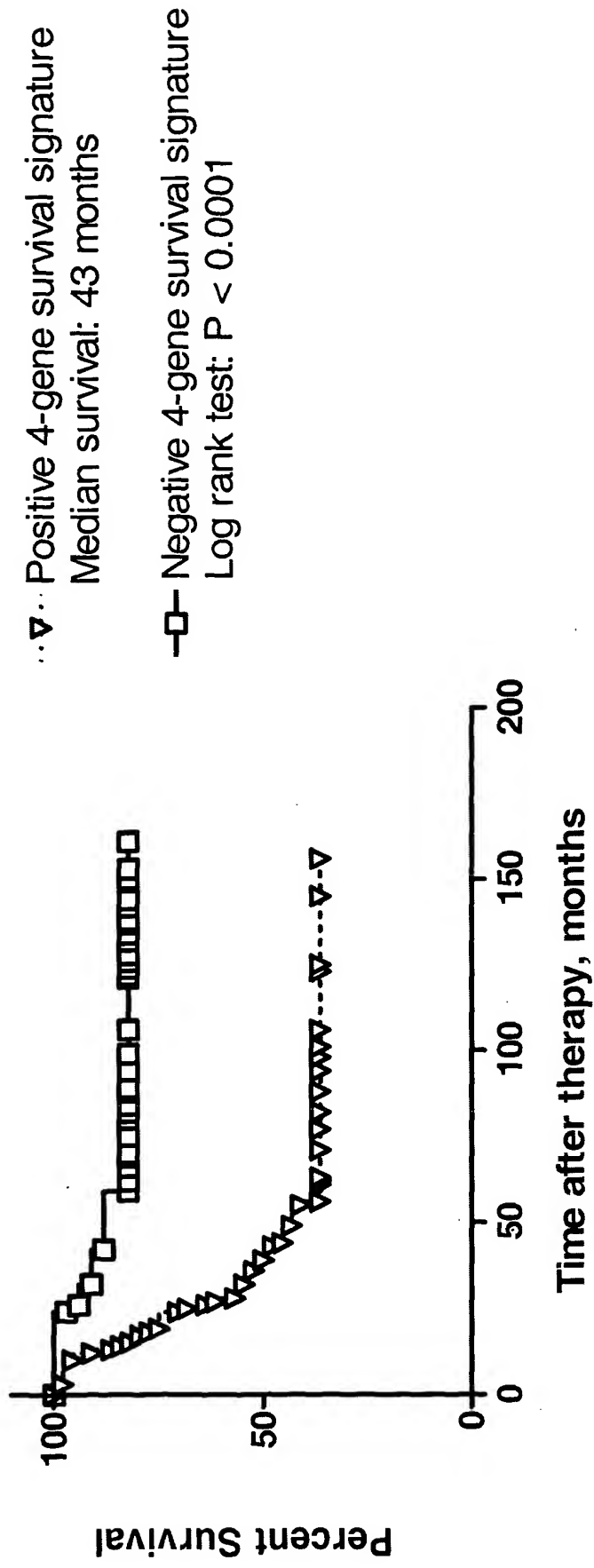
64B

Survival of 69 breast cancer patients with ER- tumors



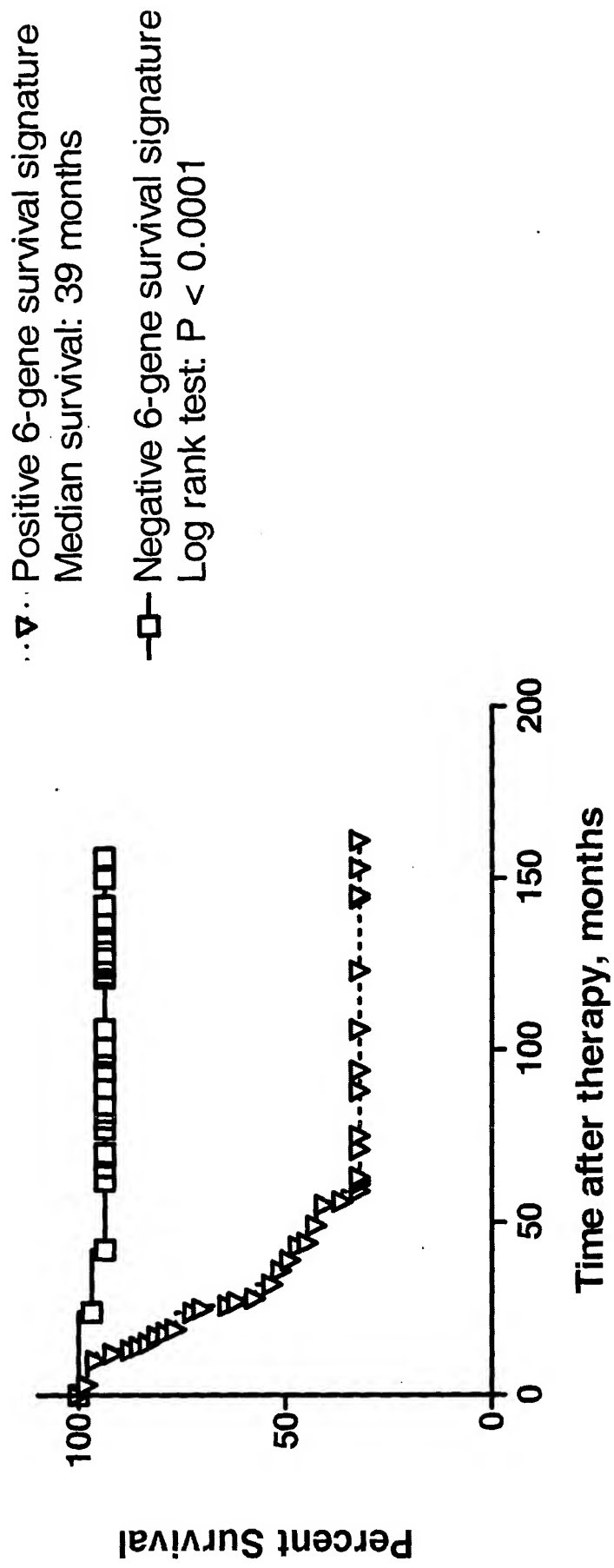
65A

**Metastasis-free survival
of 78 breast cancer patients**



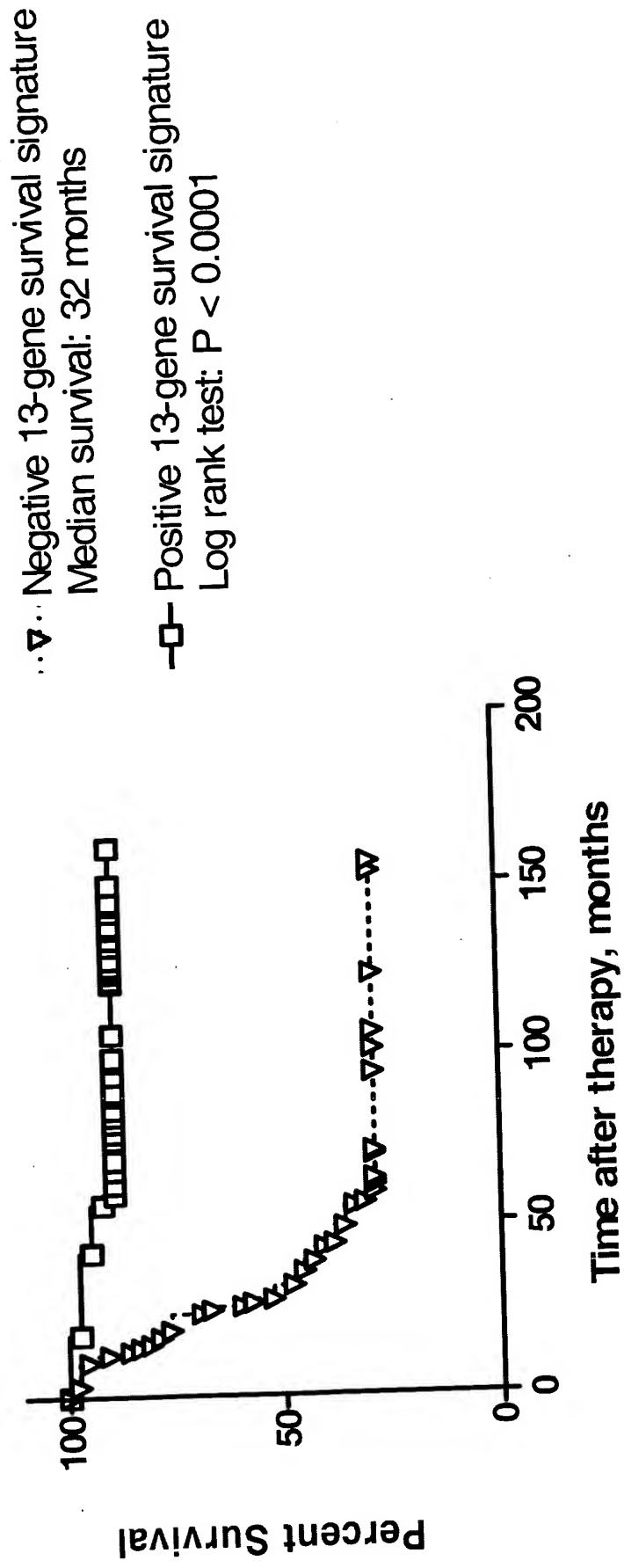
65B

Metastasis-free survival of 78 breast cancer patients



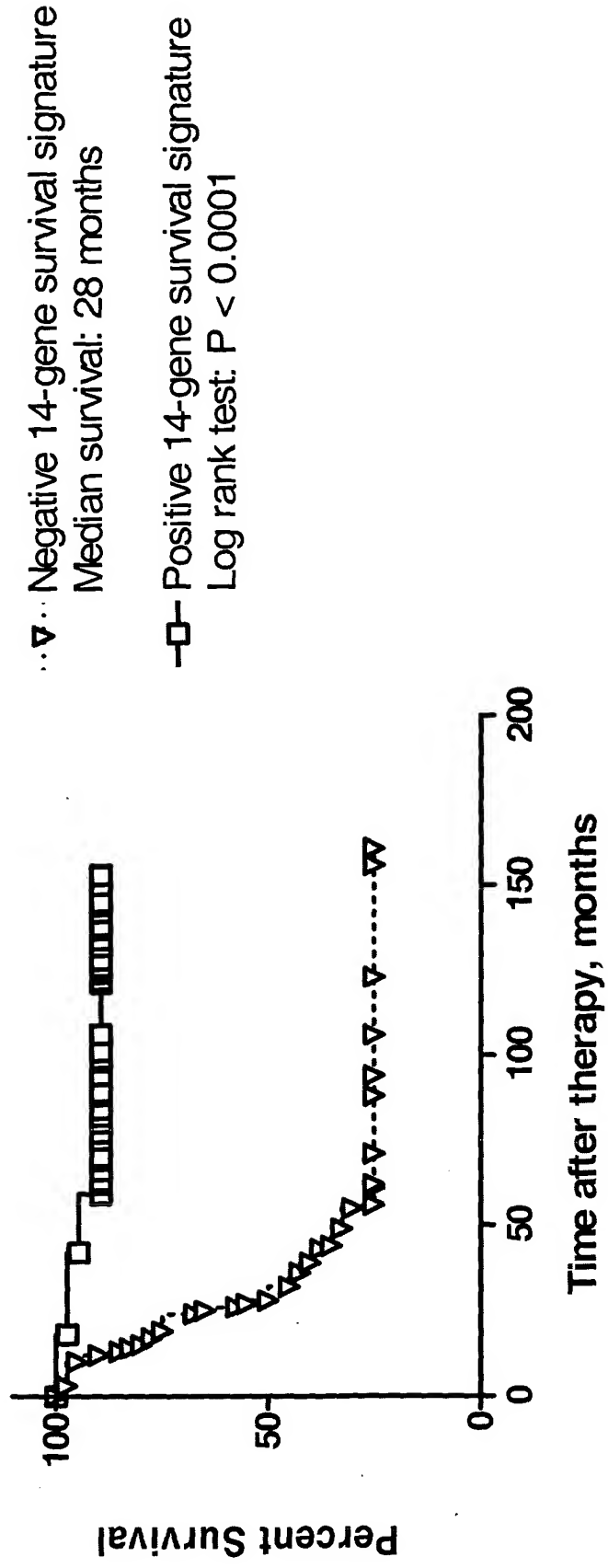
65C

Metastasis-free survival of 78 breast cancer patients



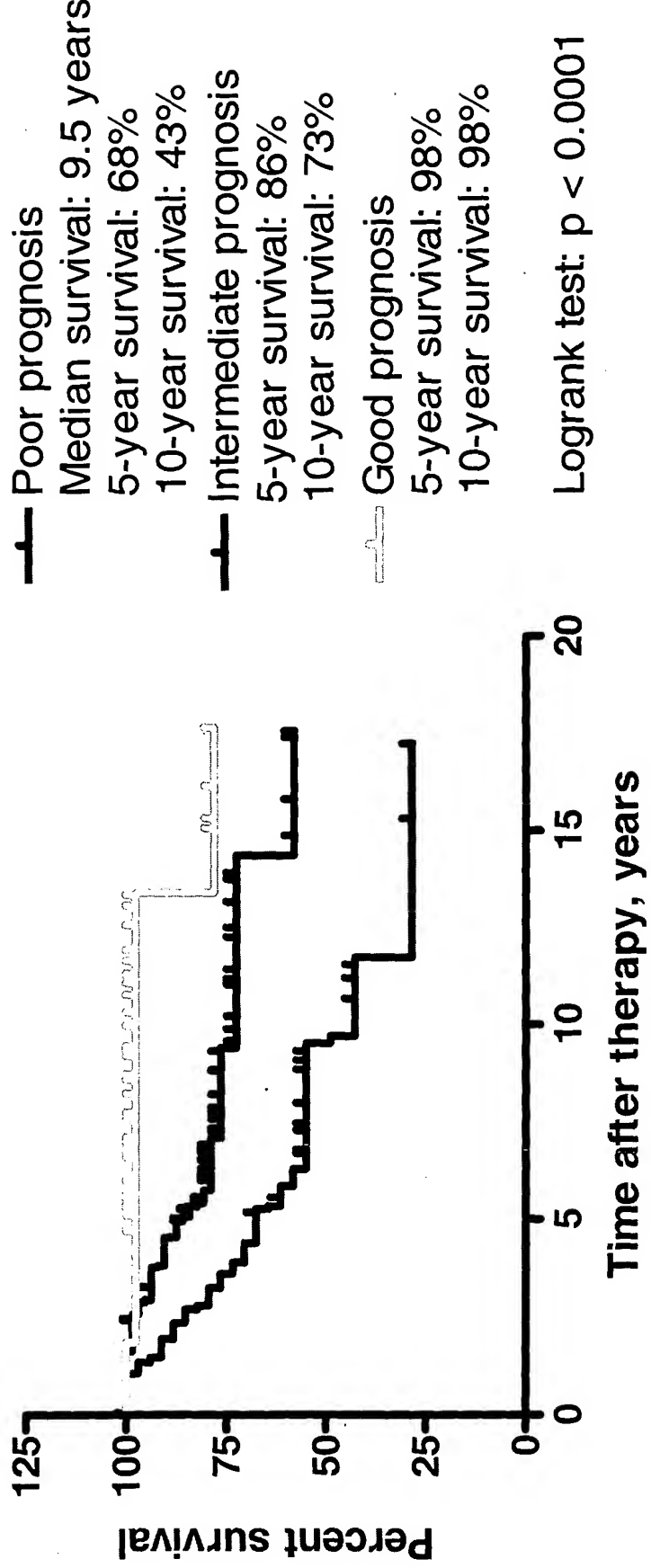
65D

Metastasis-free survival of 78 breast cancer patients



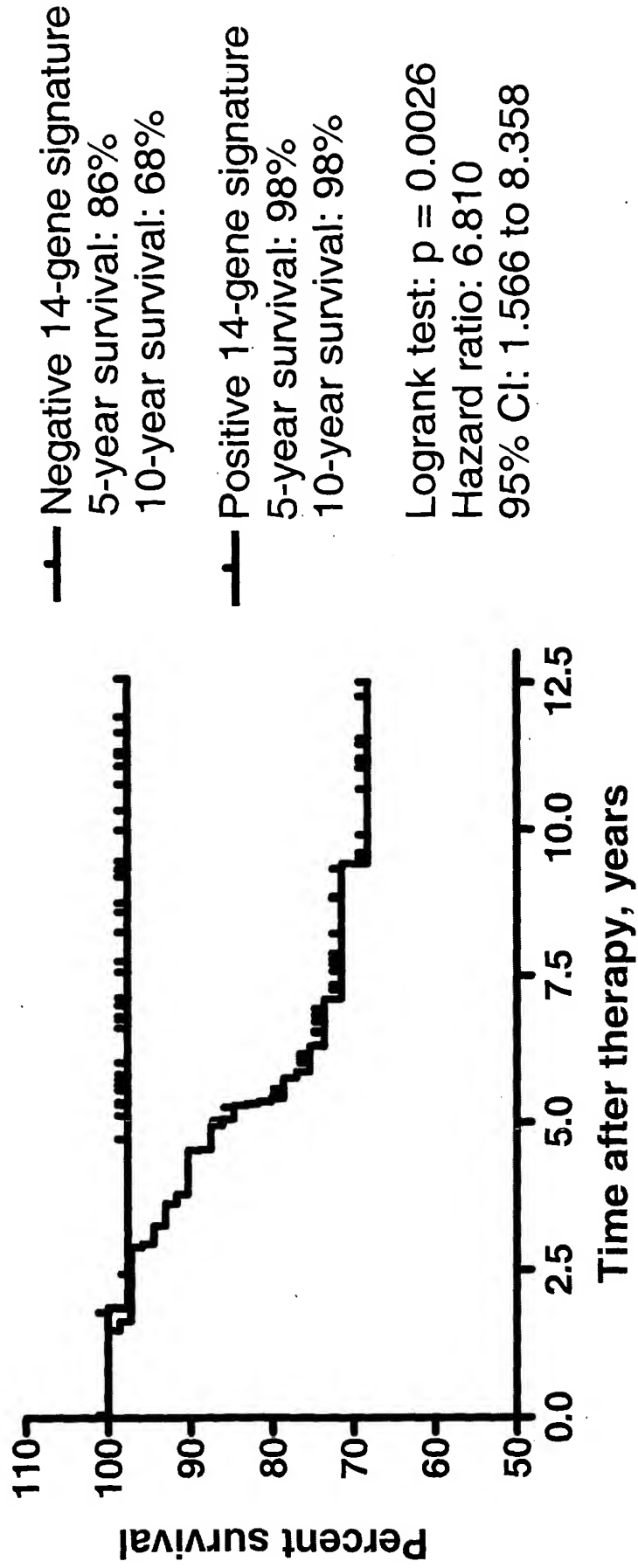
66A

Survival of 144 breast cancer patients with LN+ disease classified into sub-groups using the 14-gene survival predictor



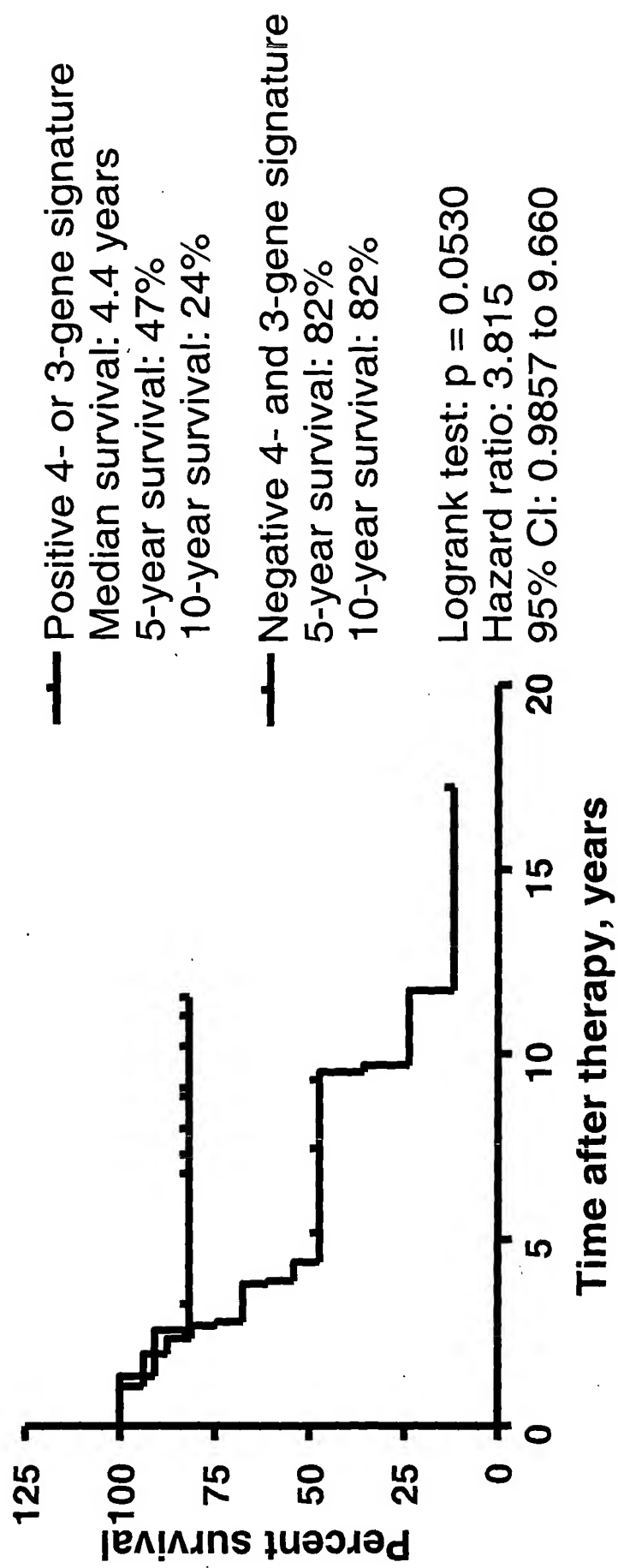
66B

Survival of 117 breast cancer patients with ER+ tumors and LN+ disease



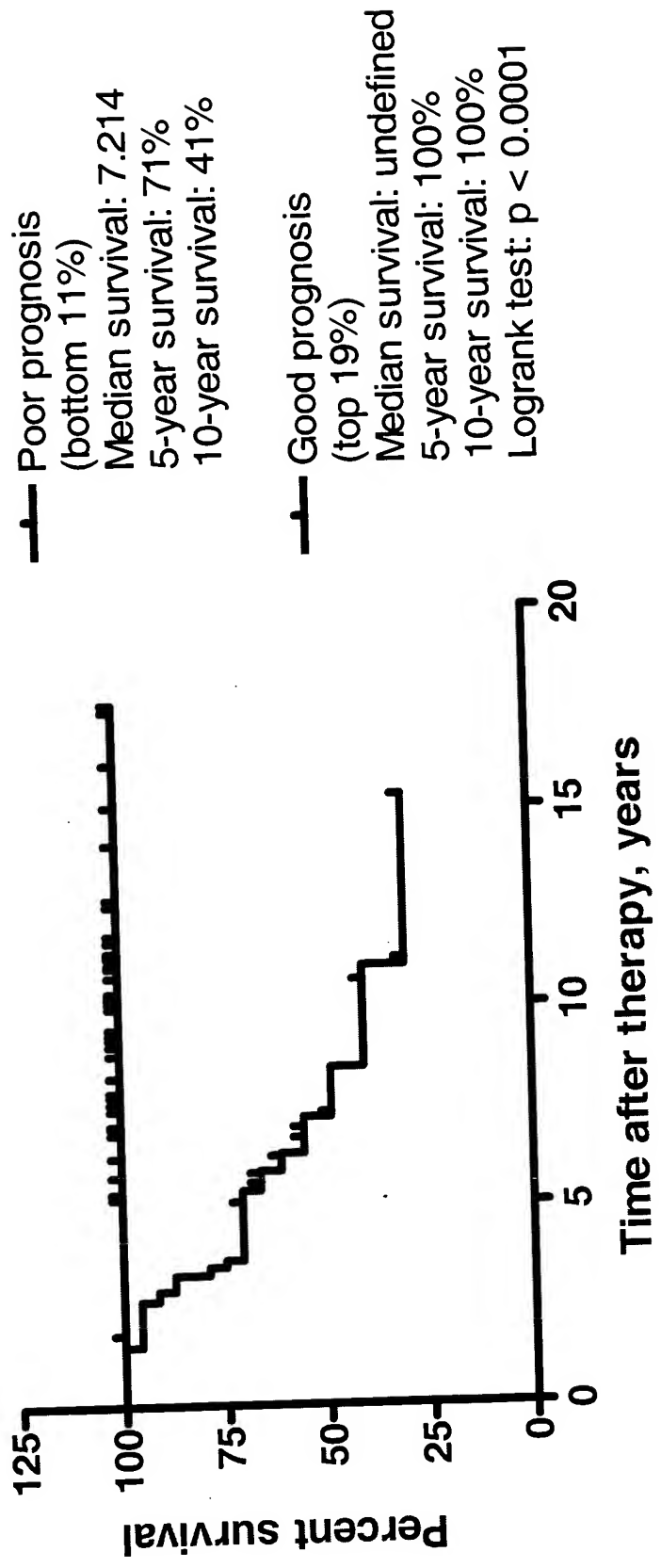
66C

Survival of 27 breast cancer patients with ER- tumors and LN+ disease



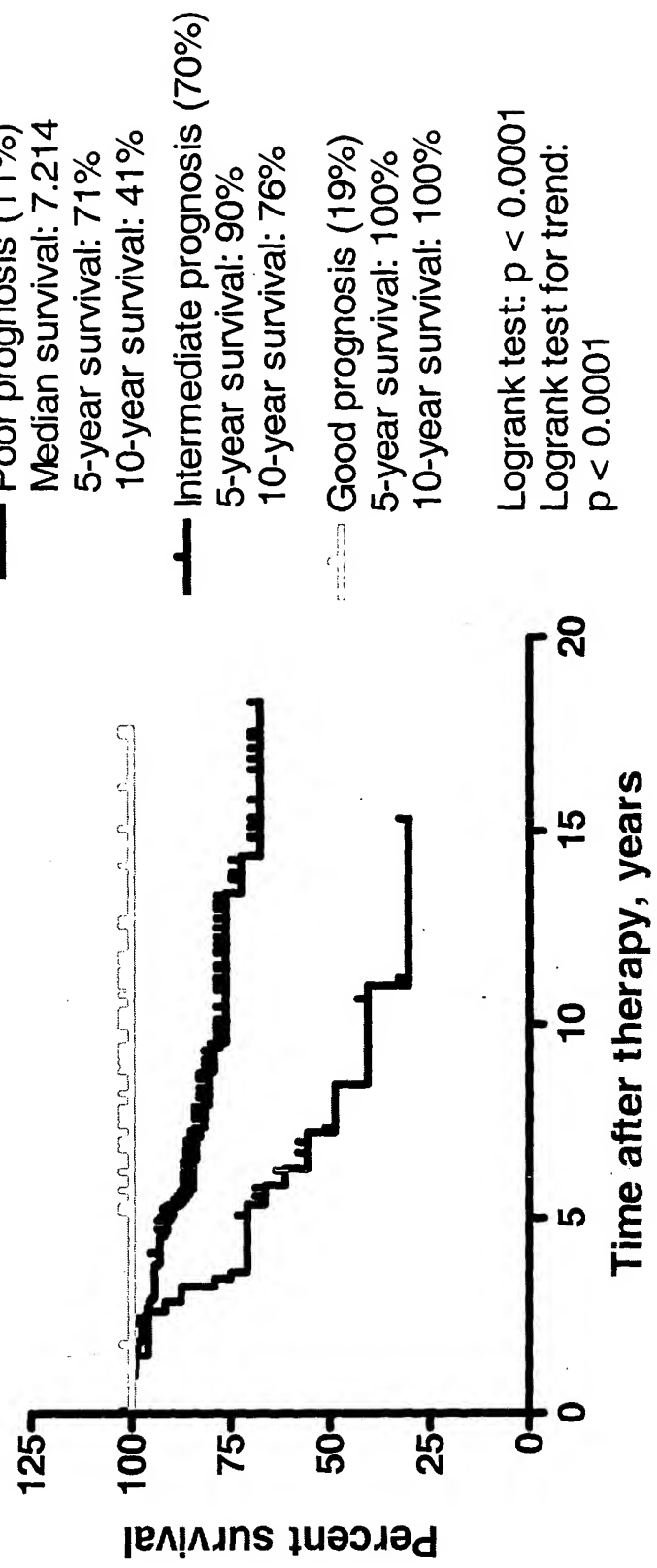
67A

Survival of ER+ breast cancer patients with positive and negative 14-gene signature



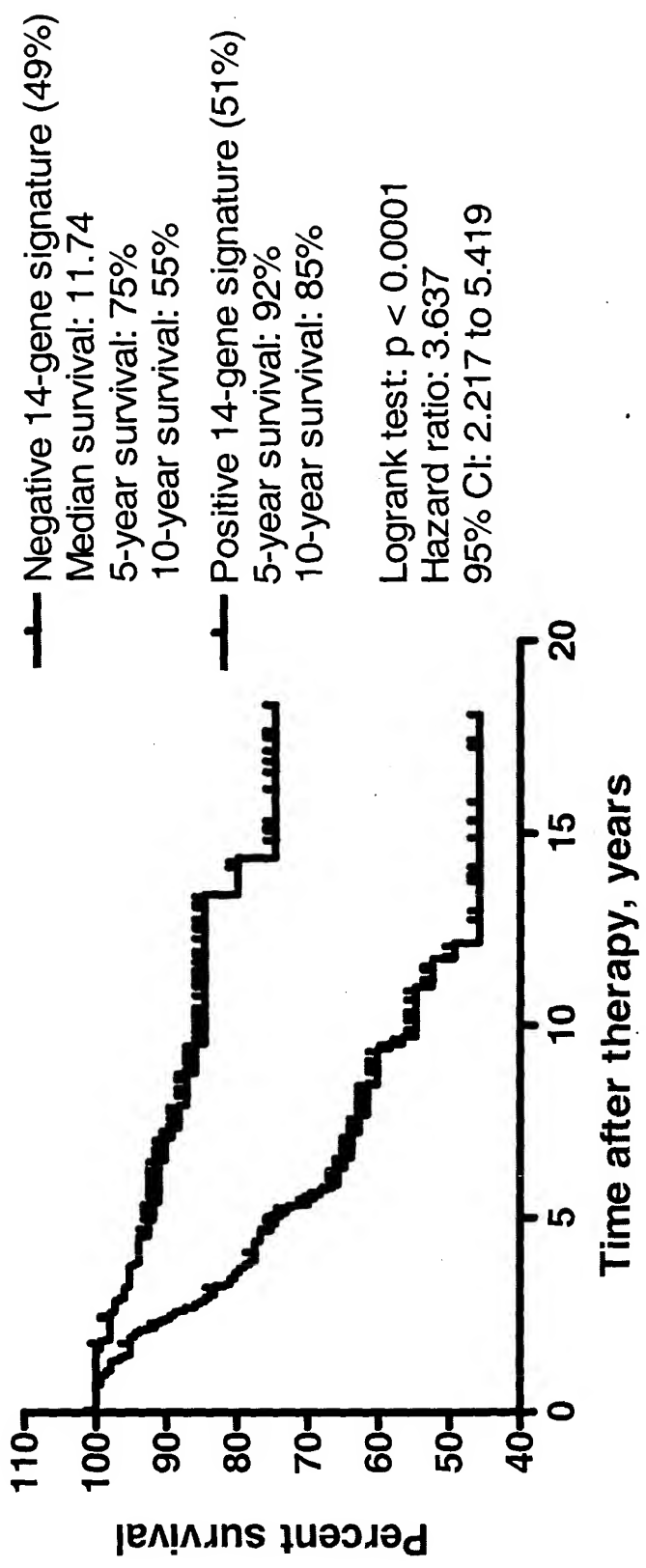
67B

**Survival of ER+ breast cancer patients
classified based on relative values
of the 14-gene signature**



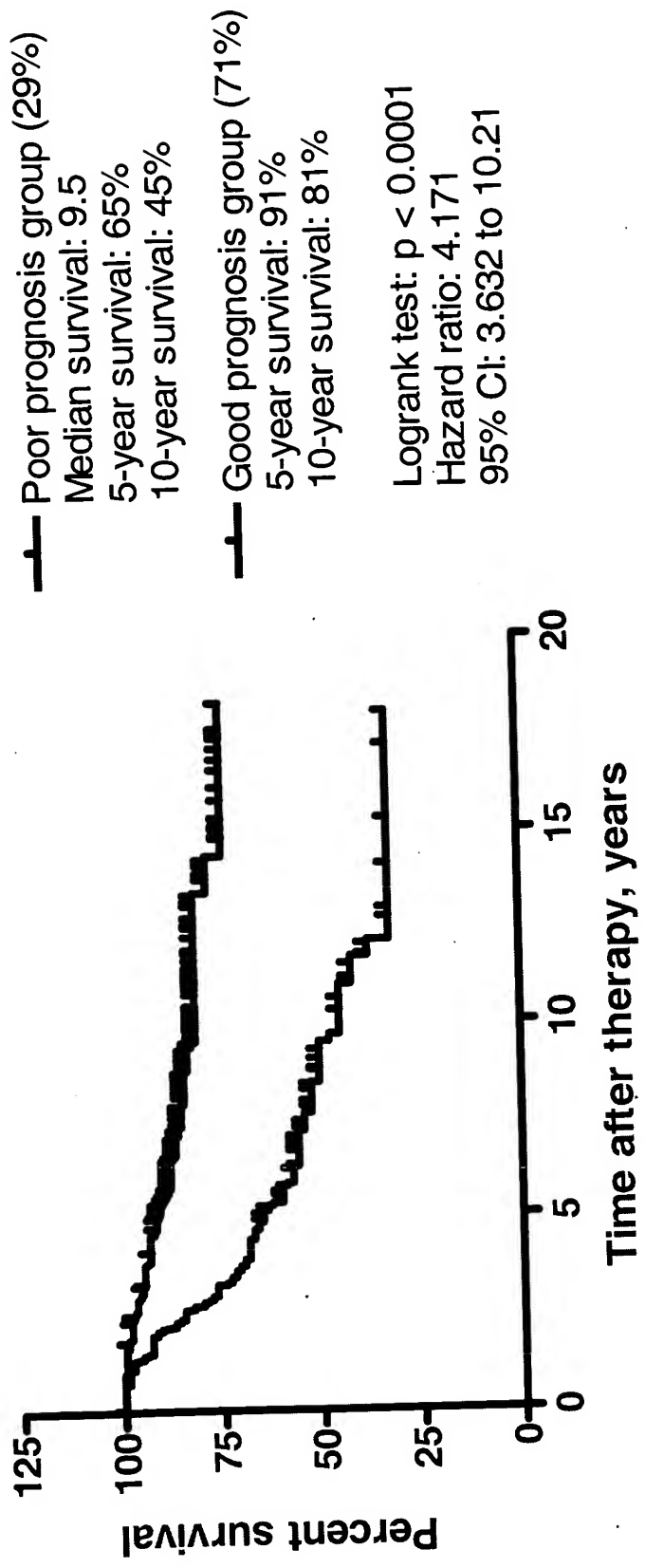
68A

**Survival of 295 breast cancer patients
with positive and negative
14-gene signature (0.00 cut off)**

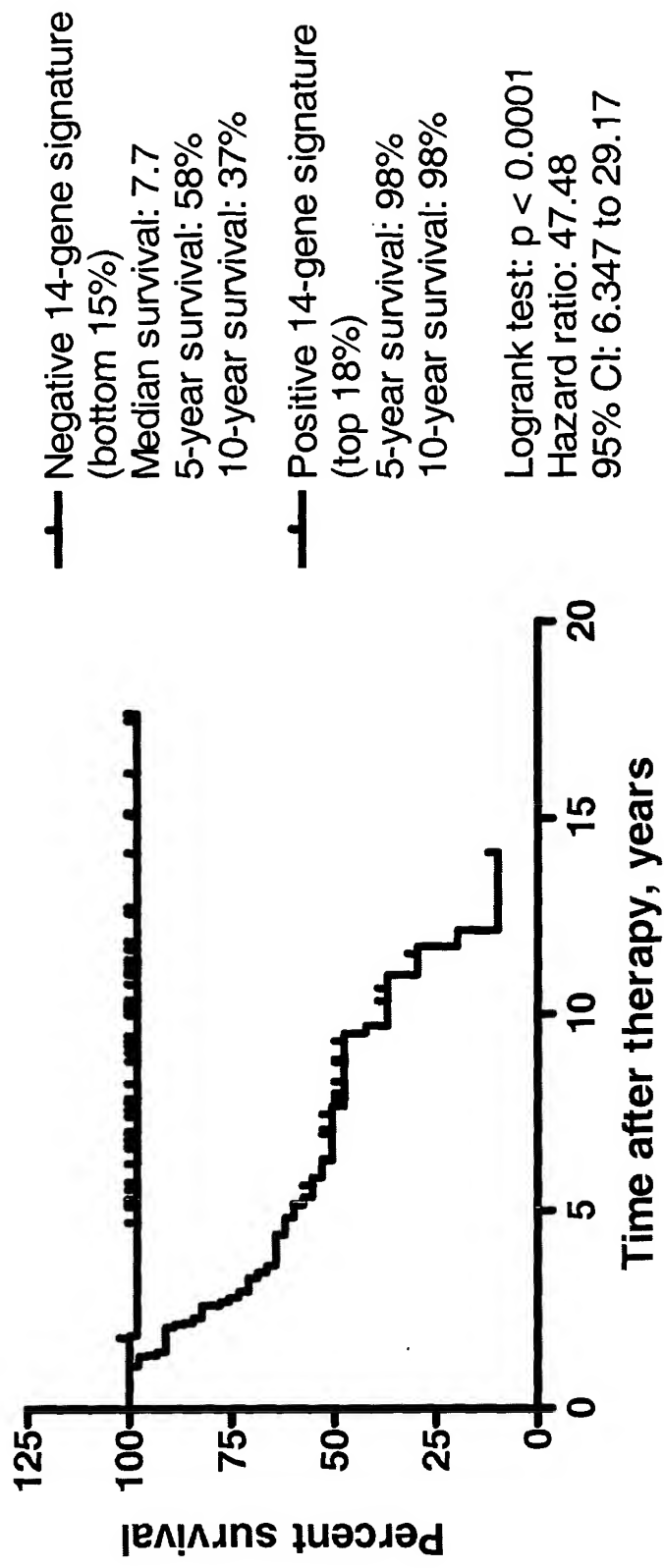


68B

**Survival of 295 breast cancer patients
with positive and negative
14-gene signature (-0.55 cut off)**

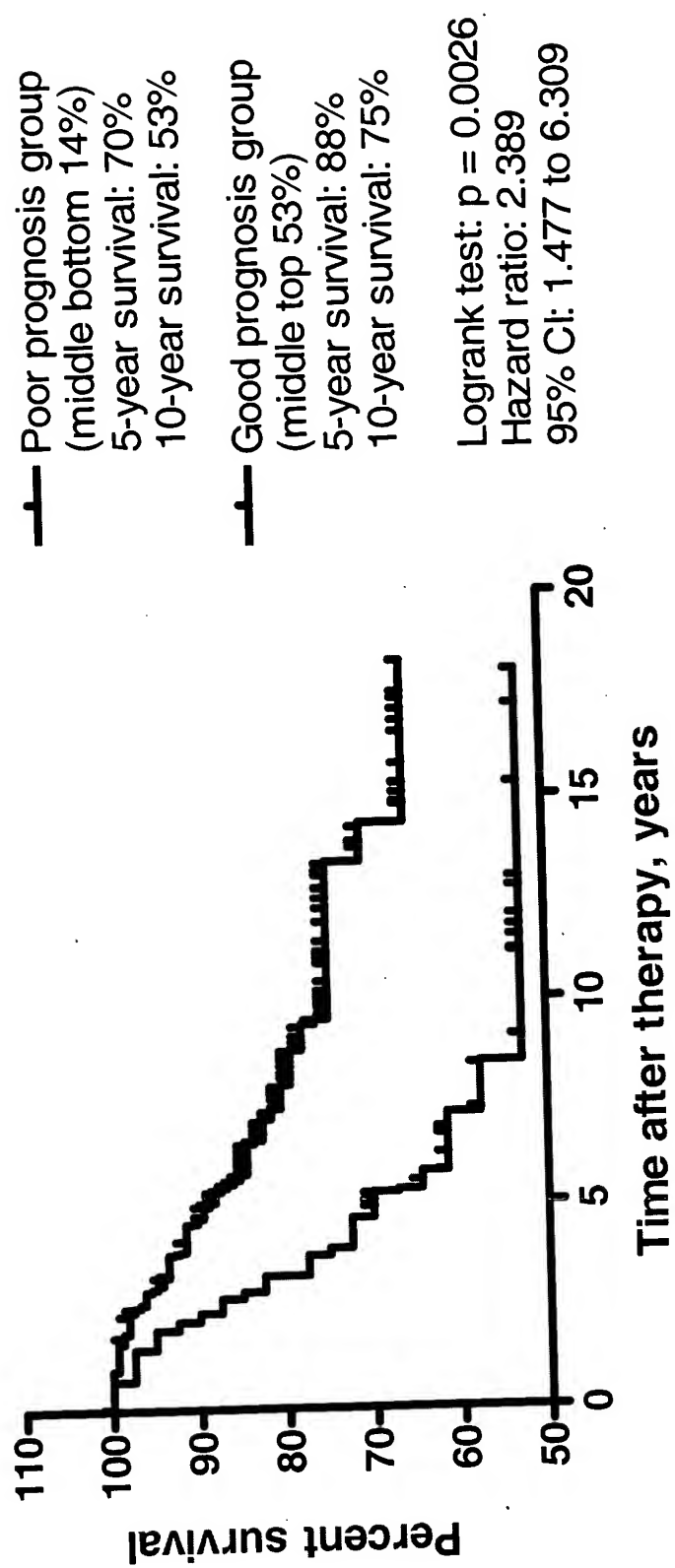


Survival of breast cancer patients with positive and negative 14-gene signature



68D

Survival of breast cancer patients with positive and negative 14-gene signature



Survival of breast cancer patients classified based on relative values of the 14-gene signature

